Timecourse of Haloperidol-Induced Midbrain Tyrosine Hydroxylase Downregulation and Interventions for Neuroprotection

TIMECOURSE OF HALOPERIDOL-INDUCED MIDBRAIN TYROSINE HYDROXYLASE DOWNREGULATION AND INTERVENTIONS FOR NEUROPROTECTION

BY

Lisa M. Lagrou, B.Sc.

A Thesis

Submitted to the School of Graduate Studies

in Partial Fulfillment of the Requirements

for the Degree

Master of Science

McMaster University

MASTER OF SCIENCE (2006) McMaster University

(Medical Science, Neuroscience & Behavioural Science) Hamilton, Ontario

TITLE: Timecourse of Haloperidol-Induced Midbrain Tyrosine Hydroxylase Downregulation and Interventions for Neuroprotection.

AUTHOR: Lisa M. Lagrou, B.Sc.
(University of Waterloo, Waterloo, Ontario, Canada)

SUPERVISOR: Dr. Michael F. Mazurek, M.D., FRCP (C), Professor of Medicine (Neurology)

NUMBER OF PAGES: xiii, 115

ACKNOWLEDGEMENTS

I would first and foremost wish to thank Dr. Mazurek, my supervisor, for providing the opportunity to experience both the joys and frustrations of research. Your support, counsel and guidance over the past year have been much appreciated. E.M. Forster said it best - "Spoon feeding in the long run teaches us nothing but the shape of the spoon." Thank you enabling my personal growth and independence through self-directed learning.

I would equally like to express my gratitude to my parents, Francis and Norma Lagrou, and my brother, Rob Lagrou. They have been incredible support in every way possible over the past several years. Mom, I'll do my best to make "Freedom 55" happen.

My lab mates, especially Lindsey MacGillivray and Mike Zettler, have seen me through many frustrations (caspase staining) and joys (microglia) of research. I would like to thank both of you for listening and encouraging me to carry forward. I would also like to acknowledge Beth Davies and Korosh Kianizad for their friendship and support over the past year. Your fun-spirited natures have put many smiles on my face and made the past year enjoyable.

Lastly, I would like to thank Sharon Facia for all her hard work, friendly chats and favours that have not gone unnoticed.

ABSTRACT

Schizophrenia is treated with haloperidol, an antipsychotic drug. Although highly effective in treating the positive symptoms of this disease, extrapyramidal side effects also accompany haloperidol treatment, including parkinsonism. Previous investigations revealed that dopamine receptor blockade by haloperidol was not temporally correlated with the appearance of parkinsonian side effects, which begin approximately 3 weeks after haloperidol treatment. In fact, by using tyrosine hydroxylase as a marker for dopamine, TH-immunoreactivity was significantly decreased 5 minutes after haloperidol administration and further downregulation was seen after 10 minutes. Microglial activation has also been implicated in Parkinson's disease models. Haloperidol also induces maximal microglial activation at 5 minutes after administration, with activation increasing by 2 minutes. In this respect, microglial activation may precede TH downregulation, thereby mediating the downregulation. In order to test this possibility, minocycline, a microglial inhibitor, was administered to Sprague-Dawley rats. Minocycline successfully inhibited microglial activation and showed partial protection over TH levels. Caffeine and nicotine have also been implicated as neuroprotective agents in Parkinson's disease. Epidemiological evidence has indicated that both caffeine and nicotine protect against Parkinson's disease. Therefore, caffeine and nicotine were independently tested and found to both prevent TH downregulation and inhibit microglial activation. Overall, microglial activation has been found to correlate with TH downregulation induced by haloperidol. Minocycline, nicotine and caffeine have all been found to inhibit microglial activation, preventing neurotoxicity associated with haloperidol administration.

TABLE OF CONTENTS

LIST OF ILLUSTRATIONS

LIST OF TABLES

LIST OF ABBREVIATIONS

3-MT	3-methoxytyramine
$A_{2A}R$	Adenosine class 2A receptor
AAADC	Aromatic amino acid decarboxylase
ABC	Avidin biotin complex
AC	Adenylyl cyclase
ACh	Acetylcholine
APC	Antigen presenting cell
APD	Antipsychotic drug
AMP	Adenosine monophosphate
ANOVA	Analysis of variance
ATP	Adenosine triphosphate
BH_2	Dihydrobiopterin
CNS	Central nervous system
COOH	Carboxyl terminal of a protein
COMT	Catechol-O-methyltransferase
COX-2	Cyclooxygenase-2
D2	Dopamine class 2 receptor
DA	Dopamine
DOPAC	3, 4-dihydrophenylacetic acid
E1-E3	Extracellular loops
EPS	Extrapyramidal side effects
GABA	Gamma-aminobutyric acid
GPe	External segment of the globus pallidus
GPi	Internal segment of the globus pallidus
HAL	Haloperidol
HVA	Homovanillic acid
I2-I3	Intracellular loops
IgG	Immunoglobulin G
IL	Interleukin
iNOS	Inducible nitric oxide synthase
L-DOPA	L-dihydroxyphenylalanine
LPS	Lipopolysaccharide
M1-M5	Muscarinic receptor class 1-Muscarinic receptor class 5
MAO	Monoamine oxidase
MAPK	Mitogen-activated protein kinase
MCP	Monocyte chemotactic protein
METH	Methamphetamine
MHC	Major histocompatibility complex
MIP	Macrophage inflammatory protein
MPTP	1-methyl-4-phenyl-1,2,3,6-tetrahydropyridine
mRNA	Messenger ribonucleic acid
nAChR	Nicotinic acetylcholine receptors
NGF	Nerve growth factor

NH_2	Amino terminal of a protein
NMDA	N-methyl-D-aspartic acid
P	Purine
PBS	Phosphate buffered saline
PGE_2	Prostaglandin-E_2
PNS	Peripheral nervous system
q-B_2	Quininoid-dihydrobiopterin
SEM	Standard error of the mean
SN	Substantia nigra
SNc	Substantia nigra pars compacta
STN	Subthalmic nucleus
TH	Tyrosine hydroxylase
TNF	Tumour necrosis factor
TNFR	Tumour necrosis factor receptor
VTA	Ventral tegmental area

EXPERIMENTAL RATIONALE

Haloperidol, administered to Schizophrenic patients, relieves psychotic symptoms by blocking dopamine receptors. The neurobiology of Schizophrenia is unknown, although it is thought to be caused by an overactive dopamine system. This reasoning is concluded from dopamine receptor antagonists, such as anti-psychotic drugs, ameliorating the psychotic episodes experienced by schizophrenic patients. Over time, treatment with haloperidol induces extrapyramidal side effects. One of the late-onset symptoms patients experience are parkinsonian symptoms. Parkinson's disease is characterized by akinesia, bradykinesia, muscle rigidity and a resting tremor. Causation of these motor symptoms is being investigated in this series of studies to follow.

Parkinsonism is a side effect that appears in patients approximately 3 weeks after haloperidol administration. This delay in symptomology suggests that the blockade of dopamine receptors by haloperidol is not the causative factor. Haloperidol, upon ingestion and absorption, blocks receptors immediately, and therefore, if the receptors were causing the side effects, they should be seen soon after drug administration. However, side effects do not appear until approximately 3 weeks following treatment. Our lab has investigated this phenomenon and we have found that treatment with haloperidol induces apoptosis in dopaminergic neurons of the substantia nigra pars compacta. Because haloperidol is administered to patients to control their psychotic episodes, interventions, which can be used to protect the dopamine neurons from degeneration, have been investigated here. As well, a timecourse of TH-downregulation by haloperidol has been studied in order to understand the involvement of microglia in the neurodegeneration process.

Objectives

1. To determine whether APD-induced TH downregulation is preceded by microglial activation.

2. To determine if minocycline can prevent microglial upregulation and prevent tyrosine hydroxylase downregulation following APD administration.

3. To determine if caffeine and nicotine can independently prevent tyrosine hydroxylase downregulation following antipsychotic drug (APD) administration.

4. To determine if APDs, caffeine and nicotine administration can affect microglial populations.

BACKGROUND LITERATURE

History of Schizophrenia & Haloperidol

Emil Kraepelin coined the term Schizophrenia in the 1880's (Jones, 2005). Before this time, mental disorders were not studied or diagnosed in reference to onset, progression, and outcome (Kandel, et al., 2000). Kraepelin began studying and classifying mental diseases in terms of symptoms and tracing these symptoms from disease onset forward (Kandel, et al., 2000). Since this time, many drugs have been discovered to reduce the symptoms of this disease, targeting both the negative and positive symptoms. Negative symptoms are those that are depressed from the normal state and include emotional flatness, social withdrawal, lack of initiative and self-care. Positive symptoms are those symptoms that are exaggerated from the natural state, including delusions and hallucinations.

One class of drugs targeted at relieving these symptoms are the neuroleptic medications. Neuroleptic drugs were discovered serendipitously in the 1950's when Rhone-Poulenc Laboratories were dedicated to discovering anti-histamine drugs (Kapur and Mamo, 2003). In discovering chlorpromazine, initially synthesized as an anti-histamine, physicians also noted that the drug produced calming effects on patients (Shen, 1999). This drug was then administered with success to patients with mental disorders. One clinical case described a 57-year-old labourer at Val de Grâce Hospital with erratic, uncontrollable behaviour (Shen, 1999). After treatment with chlorpromazine, he was reported to be calmer and more socially adept (Shen, 1999).

The development of chlorpromazine led to a mass search for other anti-psychotic agents. Haloperidol (HAL), see figure 1, was a neuroleptic drug introduced to the US market in 1958, shortly after chlorpromazine's introduction (Shen, 1999). HAL is a dopamine (DA) class 2 (D2) receptor antagonist (Hiroi, et al., 2002), rendering it effective in treating the positive symptoms of Schizophrenia, yet ineffective in the negative symptoms and neurocognitive deficits (Capuano, et al., 2002). As well, by blocking D2 receptors, HAL induces extrapyramidal side effects (EPS). EPS are defined by parkinsonian symptoms, including muscular rigidity and tremor, akathisia (motor restlessness resulting in an inability to sit still), dyskinesia (involuntary movements) and dystonia (prolonged muscle contraction and disordered muscle tone resulting in twisting body motions) (Capuano, et al., 2002). These symptoms are common to many early neuroleptics and are termed "typical" antipsychotic agents (Capuano et al., 2002).

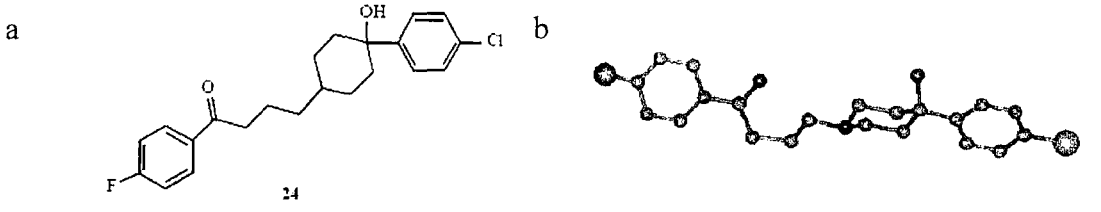

Figure 1 – Structures of haloperidol. (a) The chemical structure of haloperidol. (b) The x-ray crystal structure of haloperidol. (Kandel, et al., 2000).

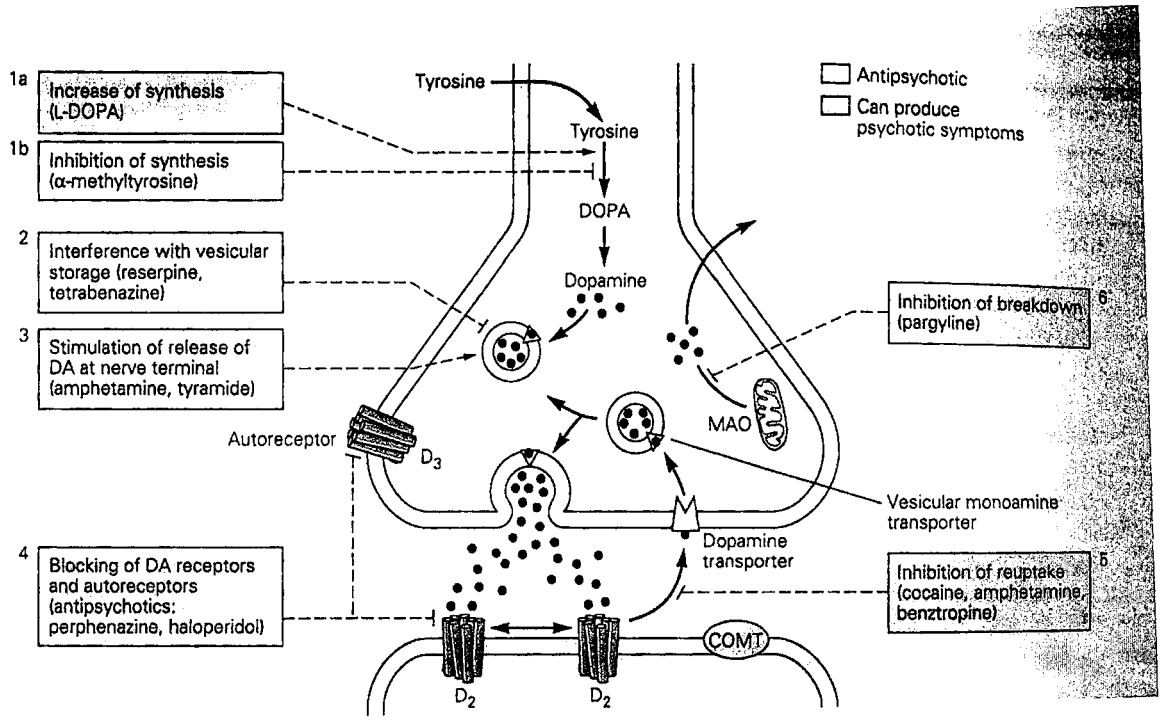

Figure 2 – The steps in dopamine synthesis and sites at which various drugs act. Haloperidol is depicted as blocking pre-synaptic autoreceptors and post-synaptic dopamine class 2 receptors in box 4. (Kandel, et al., 2000).

HAL-induced Parkinsonism has been recently investigated in our lab. Levinson, et al. (1998) found that HAL induces changes in brain structure, long after the drug has been cleared from the body. Specifically, chronic administration of HAL leads to a down-regulation of tyrosine hydroxylase (TH) immunoreactivity in the substantia nigra (SN). This characteristic loss of dopamine-producing neurons provides a model with which to study idiopathic Parkinson's disease.

Idiopathic Parkinson's disease has been shown to have genetic, environmental, inflammatory components, along with mitochondrial dysfunction (Lotharius and Brundin, 2002). Recently, the inflammatory perspective has been gaining increased attention and changing current thinking in Parkinson's theories (Orr, et al., 2002). Specifically, the role of microglia has become an

important issue. Microglia are thought to mediate the inflammation within the parkinsonian brain (Orr, et al., 2002).

Microglia

Microglia, resident macrophages of the brain, are normally present in a non-activated state (Orr, et al., 2002). Once a pathogen enters the brain, microglia are capable of up-regulating the expression of major histocompatibility complex (MHC) molecules, especially MHC class-II molecules in the SN pars compacta in Parkinson's disease (Teismann and Schulz, 2004). MHC class-II molecules are upregulated on cell's surfaces for presentation of antigens to other immune cells. As well, the β-2 microglobulin chain of the MHC class-I molecule is also upregulated during Parkinson's disease (Teismann and Schulz, 2004). Both of these molecules are involved with antigen presentation and therefore, activated microglia are inducible antigen-presenting cells (APCs), able to modulate the immune response. Microglia are one of three types of glia in the nervous system, but it has been noted that microglia are the most likely to function as APCs (Streit, 2002).

Microglia also have the ability to produce pro-inflammatory cytokines, thereby recruiting other innate immune cells (Teismann and Schulz, 2004). Human microglia have been found to express mRNAs of IL-1β, IL-6, IL-8, IL-10, IL-12, IL-15, TNF-α, macrophage inflammatory protein (MIP)-1α, MIP-1 β, and macrophage, monocyte chemotactic protein (MCP)-1 under non-stimulating conditions (Kim and de Vellis, 2005). Under stimulating conditions with lipopolysaccharide (LPS), microglia have been found to produce all cytokines (IL-1 to IL-13), except IL-15 (Kim and de Vellis, 2005). Human microglial cells express mRNA transcripts for

cytokine receptors IL-1RI, IL-1RII, IL-5R, IL-6R, IL-8R, IL-9R, IL-10R, IL-12R, IL-13R, IL-15R, TNFRI, and TNFRII (Kim and de Vellis, 2005). The expression of both the cytokine and its receptor is postulated to be a mechanism for propagation of inflammation in neurodegenerative diseases (Kim and de Vellis, 2005).

Microglia not only have receptors for other cytokines, but they also have receptors for neurotransmitters and neuropeptides. For example, a recent study demonstrated the presence of α7-nicotinic acetylcholine receptors (nAChR) on murine microglia *in vitro* and *in vivo* (Shytle, et al., 2004). Similarly, murine microglia have been found to also have adenosine receptors, specifically adenosine receptor type 2A ($A_{2A}R$) (Saura, et al., 2005).

Nicotine

Epidemiological evidence has shown that nicotine, a nAChR agonist, also protects against dopamine neuron loss in the SN (Shytle, et al., 2004). Studies have confirmed that there is a dose-response relationship between risk of developing Parkinson's disease and smoking: the more cigarettes that are smoked, the lower the risk of Parkinsonism (Morens, et al., 1995; Baron, 1996; Gorell, et al., 1999; Tanner, et al., 2002). Even though there are many chemicals found in cigarettes, nicotine is thought to be the active chemical in protecting against Parkinson's disease. In experimental models, nicotine has been reported to protect against neurotoxin-induced neuronal damage and stimulate dopamine release from the striatum (Quik, 2004).

Nicotine is the addictive substance naturally found in tobacco leaves, which are dried and used in cigarettes, cigars, chewing tobacco and snuff (Hukkanen, et al., 2005). Nicotine is found in 2

isomers, with 90% of the nicotine in cigarettes in the (S)-isomer and 10% in the (R)-isomer, with a plasma half-life of 2 hours (Hukkanen, et al., 2005). The pH of inhaled smoke in most cigarettes is approximately neutral, pH 6.0-7.0 (Pankow et al., 2003). After inhalation, the nicotine is rapidly absorbed through the alveoli of the lungs. The blood is sent to the left ventricle and then distributed systemically and to the brain (Hukkanen, et al., 2005). This is partially because the nicotine dissolves into the fluid in the lung of pH 7.4, allowing ease of transfer across biological membranes. At acidic pH, nicotine becomes ionized and does not cross membranes readily. Therefore, at a neutral or basic pH, nicotine is un-ionized and can more easily cross biological membranes (Hukkanen, et al., 2005). From inhalation, nicotine only takes 10-20 seconds in order for it to reach the brain, which activates the dopamine reward pathway, see figure 3 (Benowitz, 1990, 1996).

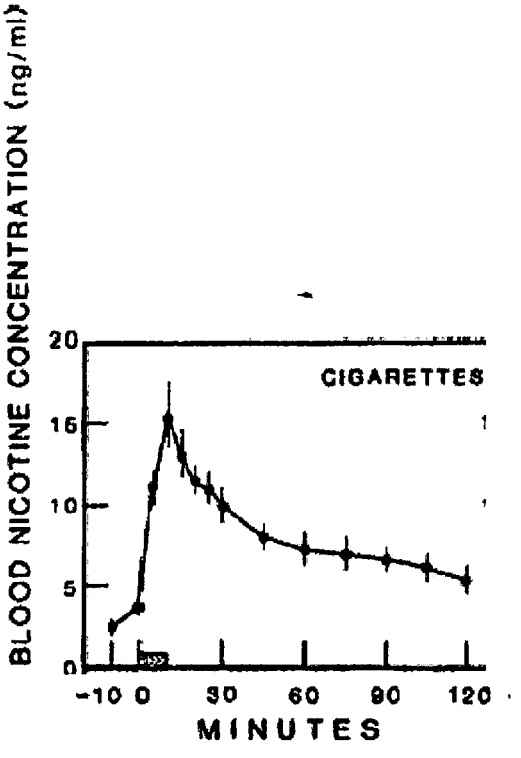

Figure 3 – Blood concentrations of nicotine during and after cigarette smoking for 9 minutes (shaded area on the graph). This is the average value reported for 10 subjects ± S.E.M. (Hukkanen, et al., 2005).

Brain nicotine levels are at least two times higher than in peripheral blood (Kemp, et al., 1997). This is due to a higher number of nicotinic acetylcholine receptors in the brain (Hukkanen, et al., 2005). Peripheral trough blood levels of nicotine range from 10 to 37 ng/mL in smokers, but at peak concentrations may elevate as high as 50 ng/mL (Schneider, et al., 2001).

Seventy to eighty percent of nicotine administered to the body is metabolized into cotinine (Hukkanen, et al., 2005). The first step in the metabolism of nicotine into cotinine is mediated by a cytochrome P450 system to produce nicotine-$\Delta^{1'(5')}$-iminium ion (Hukkanen, et al., 2005). This compound is then transformed into cotinine by a cytoplasmic aldehyde oxidase (Brandange and Lindblom, 1979; Gorrod and Hibberd, 1982).

The second most abundant metabolite of nicotine is nicotine N'-oxide by an enzyme called flavin-containing monoxygenase 3 (Hukkanen, et al., 2005). This compound is not further metabolized in the body, but instead is eliminated through the urine (Hukkanen, et al., 2005). In humans, approximately 4%-7% of nicotine taken into the body is metabolized by this pathway, but in rats cotinine and nicotine N'-oxide are formed in equal amounts (Hukkanen, et al., 2005).

Next, the body can methylate nicotine producing nicotine isomethonium ion (Hukkanen, et al., 2005). The enzyme amine N-methyl transferase catalyzes this reaction. Another metabolite of nicotine is formed through the process of glucuronidation. Although approximately 3% to 5% of nicotine is metabolized through this pathway in humans, this process has been undetectable in rat species (Hukkanen, et al., 2005). This produces (S)-nicotine-N-β-glucuronide, catalyzed by uridine diphosphate glucuronosyltransferase (Seaton, et al., 1993).

The last main pathway for nicotine degradation is through oxidative-N-methylation. This process converts nicotine into nornicotine. These findings are summarized in figure 4. As the nicotine becomes further metabolized, the end products of nicotine metabolism are excreted in the following concentrations, as seen in figure 5: cotinine (10 to 15% of nicotine in urine), *trans*-3'-hydroxycotinine (33–40%), cotinine glucuronide (12–17%), and *trans*-3'-hydroxycotinine glucuronide (7–9%). (Hukkanen, et al., 2005).

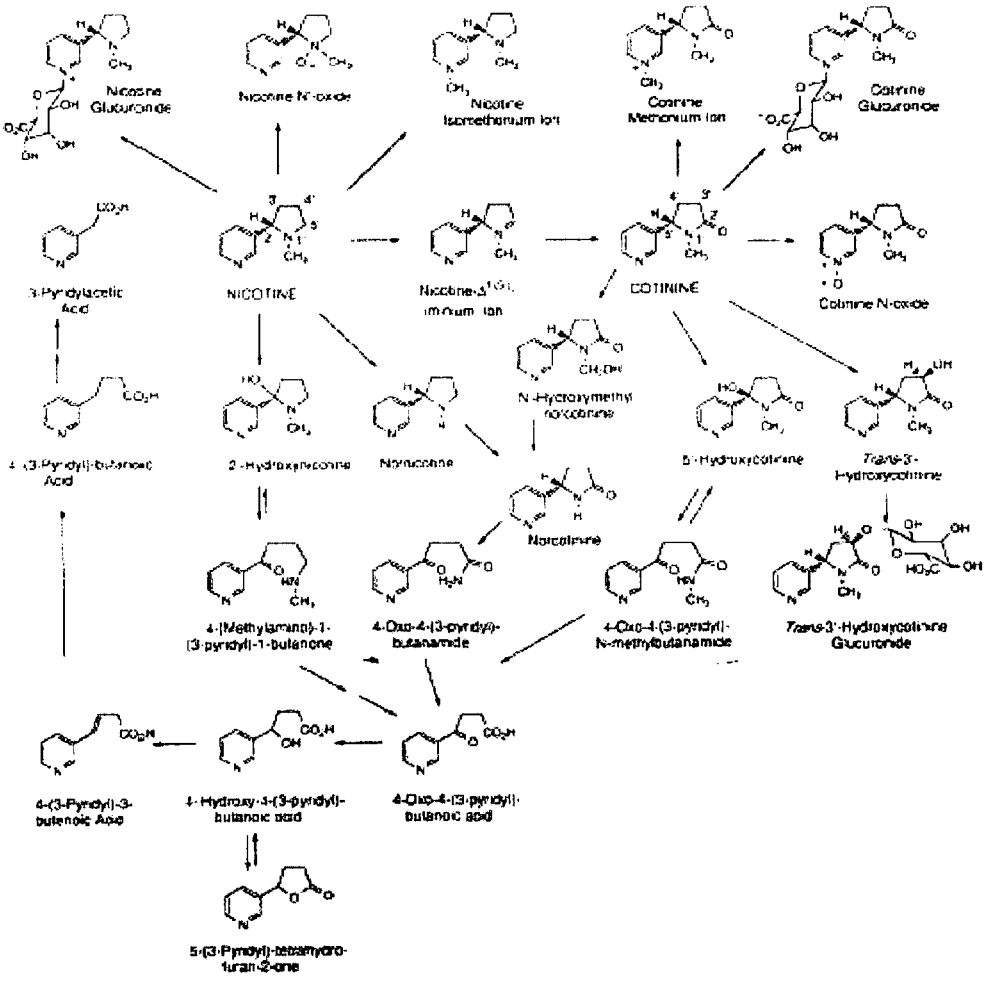

Figure 4 – Pathways of metabolism for nicotine. The six primary metabolites of nicotine are cotinine, nicotine N'-oxide, nicotine isomethonium ion, nicotine glucuronide, nornicotine and 2'-hydroxynicotine. (Hukkanen, et al., 2005).

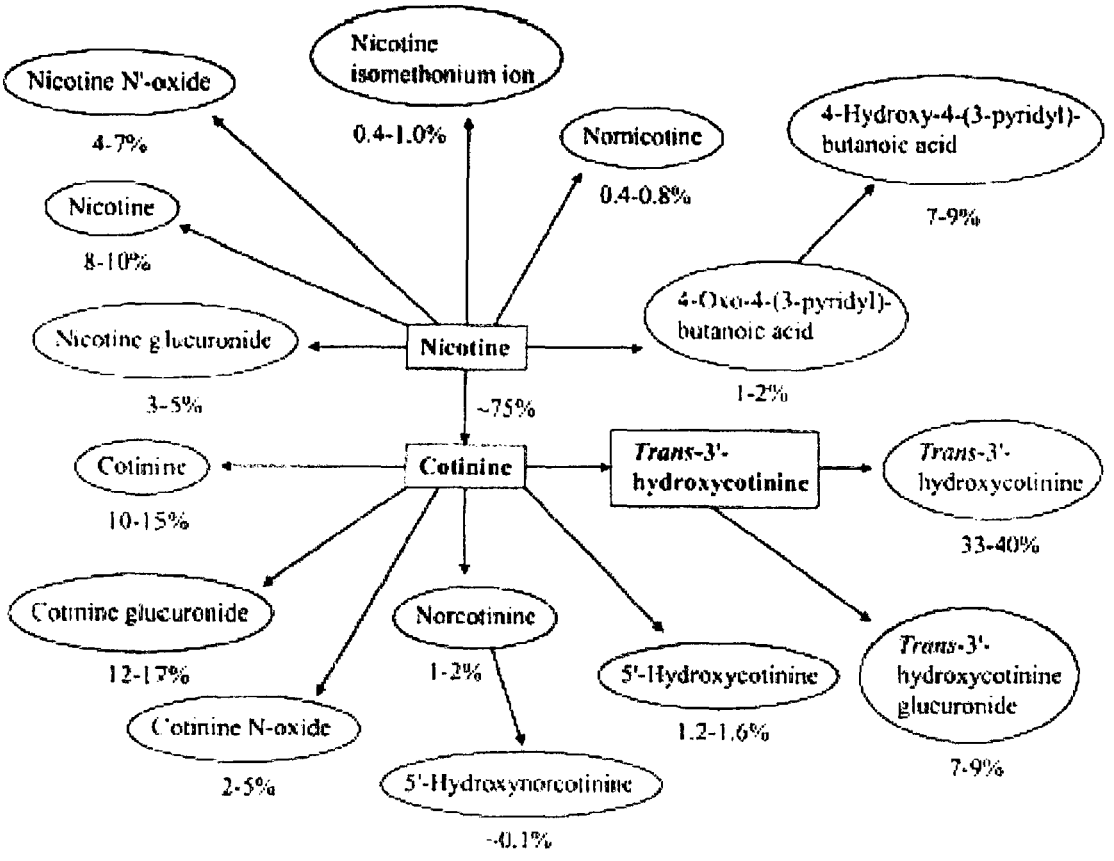

Figure 5 – Quantitative analysis of nicotine metabolism in humans. Nicotine is preferentially degraded by hepatic metabolism into many different compounds. Most nicotine is degraded into cotinine (75%). (Hukkanen, et al., 2005).

Acetylcholine

Acetylcholine is a small-molecule neurotransmitter that is present in the PNS and the CNS (Kandel, et al., 2000). There are 6 major ACh subsystems, including the magnocellular basal complex. This is the largest subset of cholinergic neurons, mainly providing input to the hippocampus and cortex (Gotti and Clementi, 2004). The other subsets of cholinergic neurons are peduncolopontine-laterodorsal tegmental complex, striatum, lower brain stem, habenula–interpeduncular system, and the autonomic nervous system (Gotti and Clementi, 2004).

Acetylcholine, the natural system that nicotine exploits, can bind to either nicotinic acetylcholine receptors or muscarinic ACh receptors (van Koppen and Kaiser, 2003). Muscarinic receptors mediate most of ACh's effects and are present in the central nervous system, peripheral nervous system and in the end organs of the parasympathetic nerves (van Koppen and Kaiser, 2003). They are members of the superfamily of seven transmembrane receptors and subsequently activate signal transduction pathways through heterotrimeric guanine nucleotide binding regulatory proteins (G proteins) (van Koppen and Kaiser, 2003). They are also present in the neuromuscular junction, which mediates muscle contractions. The muscarinic receptors are classified into 5 subtypes M1-M5, depending on their signal transduction pathway (van Koppen and Kaiser, 2003). For example, M1, M3 and M5 are G-protein pertussis-toxin insensitive receptors and lead to the activation of phospholipase C and phospholipase D (Caulfield, 1993; Rumenapp, et al., 2001). On the other hand, M2 and M4 couple to pertussis-toxin sensitive g-proteins (Caulfield, 1993; Rumenapp, et al., 2001).

Although muscarinic receptors are present, nicotine binds to and agonizes nicotinic ACh receptors (nAChR's). nAChR's are present in the nervous system, peripherally and centrally (Gotti and Clementi, 2004). In the peripheral nervous system, they are present in ganglia, and in the CNS. They are also present in the CNS in such centres involved in sleep, pain, hunger and various cognitive functions (Gotti and Clementi, 2004). Unlike the muscarinic receptors, the nAChR's are a member of the gene superfamily of ligand-gated ion channels (Karlin, 2002). This structure is seen in figure 6.

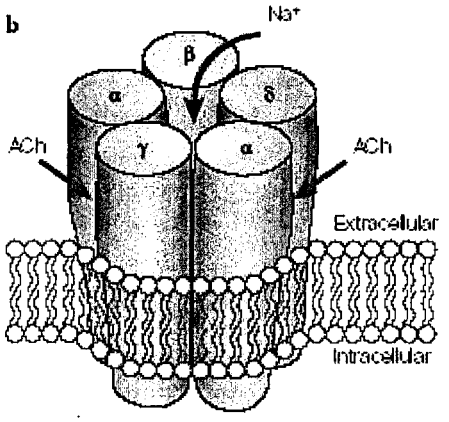

Figure 6 – The structure of the nicotinic acetylcholine receptor. The ion channel is depicted in the centre of the receptor. Also, the ACh binding sites are shown, which are between the α and γ subunits and the α and δ subunits (Karlin, 2002).

The structure of the receptor varies with the subunits that compose it. In neurons, there are 12 subunits that can be combined to form a functional receptor (Karlin, 2002). These subunits range between α2-α10 and β2- β4 (Karlin, 2002). There are functional differences between these subunits. For example, α7, α8, and α9 can form homopentamers, but α2- α6 and α10 can combine with β subunits or other α subunits (Karlin, 2002).

Focusing on the dopamine-releasing cells of the mesostiatal system, α6, α4 and some α3 subunits have been discovered aiding in dopamine release in the striatum as well as β2 subunits (Gotti and Clementi, 2004). α4β2 receptors compose 70% of receptors in the striatum and α6β2 compose

another 20% (Gotti and Clementi, 2004). It is thought that α4β2 receptors are the most abundant receptor subtype across the entire brain, including in the SN.

Caffeine

Epidemiological evidence has also shown that drinking caffeine, an adenosine receptor antagonist, reduces the risk of developing Parkinson's disease (Saura, et al., 2005). In the early 90's, many studies were designed to test the validity of the caffeine neuroprotection theory (Jimenez-Jimenez, et al., 1992; Grandinetti, et al., 1994; Morano, et al., 1994; Hellenbrand, et al., 1996; Fall, et al., 1999). The first studies conducted by Jimenez-Jimenez and Morano found that a lowered risk of Parkinson's disease was found with administration of caffeine, but their data did not reach significance. This was suggested to be due to confounding factors with cigarette smoking. As further larger studies emerged, caffeine was found to significantly decrease the risk of developing Parkinson's disease (Hellenbrand, et al., 1996; Fall, et al., 1999; Benedetti, et al., 2000). These results reported a dose-dependent relationship between smoking and protection from Parkinson's disease.

Caffeine (1,3,7-trimethylxanthine) is naturally found in tea leaves, cocoa beans, cola nuts and coffee beans (Nawrot, et al., 2003). In the United States, the average coffee drinker intakes a mean of 2-4 cups of coffee/day, which relates to approximately 4 mg of caffeine/kg/day (Mandel, 2002). Heavy coffee drinkers may intake 5-7 mg/kg/day, with an upper limit seen of 15 mg/kg/day (Mandel, 2002).

After caffeine is taken into the body, it is essentially all absorbed into the bloodstream from the gastrointestinal tract (Nawrot, et al., 2003). The caffeine is distributed to all body tissues, and is

able to cross the blood-brain barrier (Nawrot, et al., 2003). It is demethylated to dimethylxanthine compounds (Benowitz, et al., 1995). The serum half-life of caffeine is on average 4 hours, but can vary between 2 and 7 hours, depending on age, sex, use of oral contraceptives, pregnancy, and smoking (Xu, et al., 2005; Nawrot, et al., 2003). 80% of caffeine is then metabolized to paraxanthine (1, 7-dimethylxanthine), with smaller percentages metabolized to theobromine (3, 7-dimethylxanthine) and theophylline (1, 3-dimethylxanthine), see figure 7 (Benowitz, et al., 1995; Xu, et al., 2005). Only 1-5% of caffeine consumed is excreted in the urine unchanged or metabolized (Nawrot, et al., 2003).

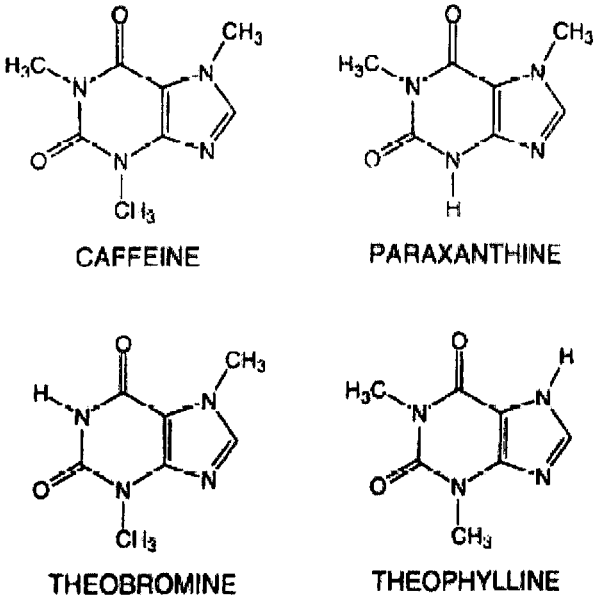

Figure 7 – Chemical structures of caffeine and its primary metabolites. (Benowitz, et al., 1995).

Theophylline and paraxanthine, nonspecific adenosine receptor antagonists, at low micromolar concentrations were also reported to attenuate MPTP toxicity in mice in a preliminary study (Xu, et al., 2005).

Adenosine

Caffeine exploits the body's natural adenosine systems. Adenosine is a purine nucleoside present in the CNS (Hasko, et al., 2005). Adenosine binds to adenosine receptors of 4 subtypes: A_1, A_{2A}, A_{2B} and A_3 (Hasko, et al., 2005). Like dopamine and muscarinic receptors, adenosine receptors are members of the gene superfamily of seven transmembrane receptors and subsequently activate signal transduction pathways through heterotrimeric G proteins (Ribeiro, et al., 2003). The structure of these receptors is shown in figure 8. ATP, the main energy for all cells, is metabolized into adenosine. Adenosine is present in all cells, including neurons and glia (Ribeiro, et al., 2003). Adenosine is not considered a "classical" neurotransmitter because it is not stored in vesicles. Instead, it is released into the extracellular space through a nucleoside transporter, which also re-uptakes the adenosine after its release (Ribeiro, et al., 2003).

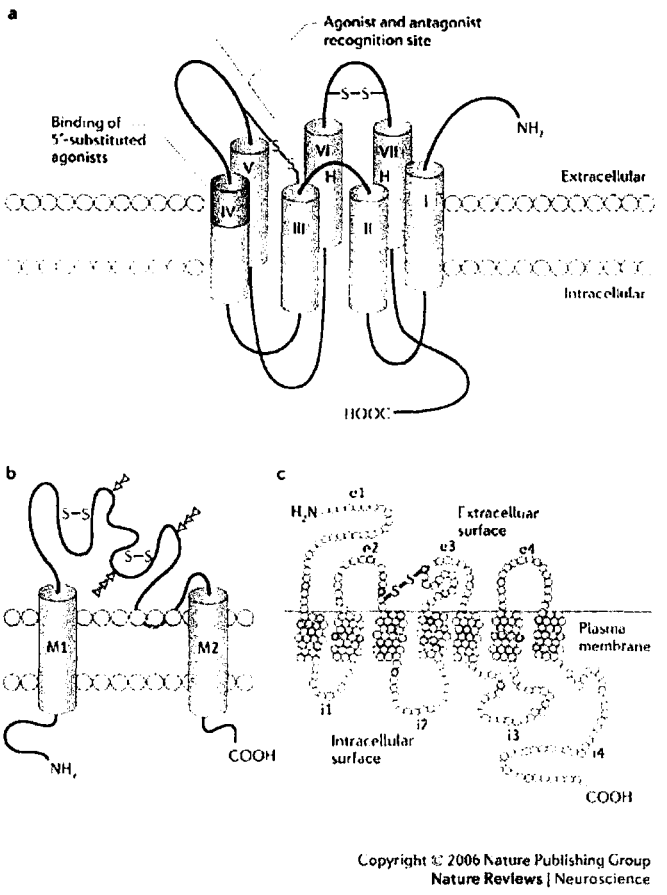

Figure 8 – The purine 1 (P1) family of receptors for extracellular adenosine are G-protein-coupled receptors that signal by inhibiting or activating adenylate cyclase (a). The P2 family of receptors binds extracellular ATP or ADP, and are comprised of two types of receptors (P2X and P2Y). The P2X family of receptors are ligand-gated ion channels (b) and the P2Y family are G-protein-coupled receptors (c). S–S, disulphide bond; e1–e4, extracellular domain loops 1–4; i1–i4, intracellular domain loops 1–4. (Fields and Burnstock, 2006)

Adenosine receptors are either high affinity (A_1 and A_{2A}) or low affinity (A_{2B} and A_3) (Ribeiro, et al., 2003). Not only are there functional differences in these receptors, but they are also distributed differently within the CNS. The A_1 receptor is preferentially found in the brain cortex, cerebellum, hippocampus, and dorsal horn of spinal cord. A_{2A} receptors are highly expressed in the striato-pallidal GABAergic neurons and olfactory bulb; they are also expressed in lower levels in other brain regions. A_{2B} has a relatively low level of expression in the brain

(Dixon et al., 1996), whereas A3 has intermediate levels of expression in the human cerebellum and hippocampus and low levels elsewhere in the brain (Fredholm, et al., 2001). This distribution pattern can be seen in figure 9.

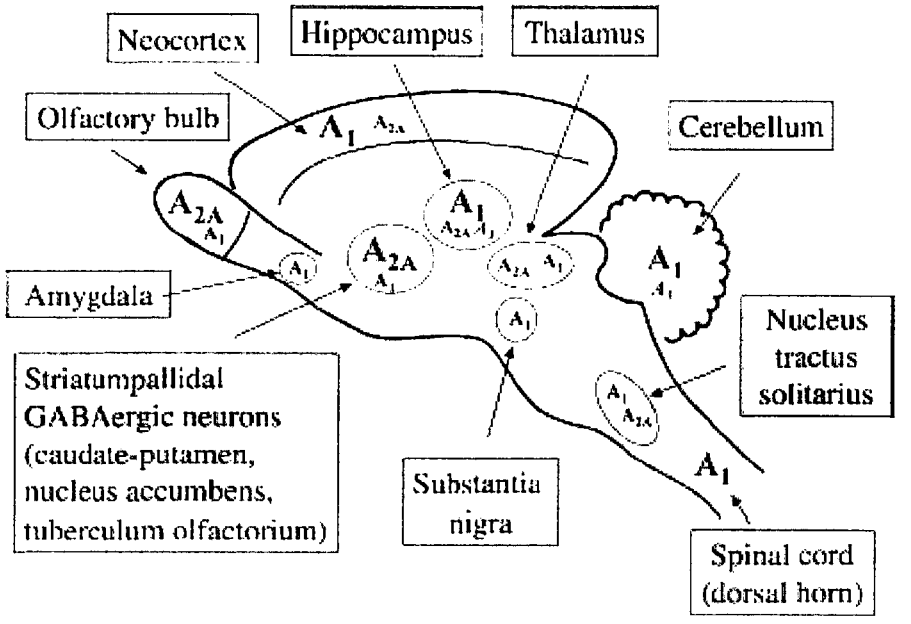

Figure 9 – Distribution of adenosine receptors in the brain. Density levels are shown by the size of the letters in each of the brain areas. (Ribeiro, et al., 2003).

Although adenosine receptors all are coupled to G proteins, there are differences in the types of g-proteins they are linked with. A_1 and A_3 receptors couple with inhibitory g-proteins, such as G_i and G_o, whereas A_{2A} and A_{2B} usually couple with stimulatory g-proteins, such as G_s (Linden, 2001). A_{2A} receptors, like D2 receptors, stimulate adenylyl cyclase (AC), thus producing a response in the cell. On the other hand, A_1 receptors inhibit AC. In the striatum, A_{2A} receptors are mainly coupled to G_{olf}, a G-protein abundant in this brain area that also activates adenylyl cyclase (Ribeiro, et al., 2003).

Adenosine is uptaken into cells from the extracellular fluid. It is dependant upon concentration gradients and therefore displays facilitated diffusion (Ribeiro, et al., 2003). The extracellular

fluid has 2 sources of adenosine: facilitated diffusion movement from the cell to the exterior and the conversion of adenine nucleotides to adenosine by through a series of ectoenzymes. (Zimmermann and Braun, 1999; Ribeiro, et al., 2003).

Intracellular levels of adenosine depend on cytosolic 5'-nucleotidase, an enzyme converting AMP into adenosine, and adenosine kinase, an enzyme that converts adenosine into AMP (Ribeiro, et al., 2003). Because transport of adenosine depends on facilitated diffusion, the movement of adenosine depends upon intracellular and extracellular concentrations.

Dopamine

Pathways

The neurobiology of Parkinson's disease is found in the nigrostriatal dopamine system. These dopaminergic neurons originate in cell groups A8, A9, and A10 of the midbrain. Cell group A9, otherwise known as the substantia nigra, projects to the striatum forming the nigrostriatal pathway. These projections are involved in motor responses. Cell group A8, known as the retrorubral field, projects rostrally to the frontotemporal cortex along with cell group A10, known as the ventral tegmental area. These projections form the mesocorticolimbic dopamine system, forming the pathways for emotion, thought, memory storage and reward.

There is a separate group of dopaminergic cells, A11 and A13, which have cell bodies in the dorsal hypothalamus and project to the spinal cord. These pathways regulate the activity of sympathetic preganglionic neurons. The last group of dopaminergic neurons, A12 and A14, with cell bodies in the arcuate nucleus of the hypothalamus, are aligned along the wall of the third ventricle and project to the pituitary stalk. Their projections form the pathways for the

tuberoinfundibular hypothalamic neuroendocrine system. The four major dopaminergic pathways are outlined below in figure 10.

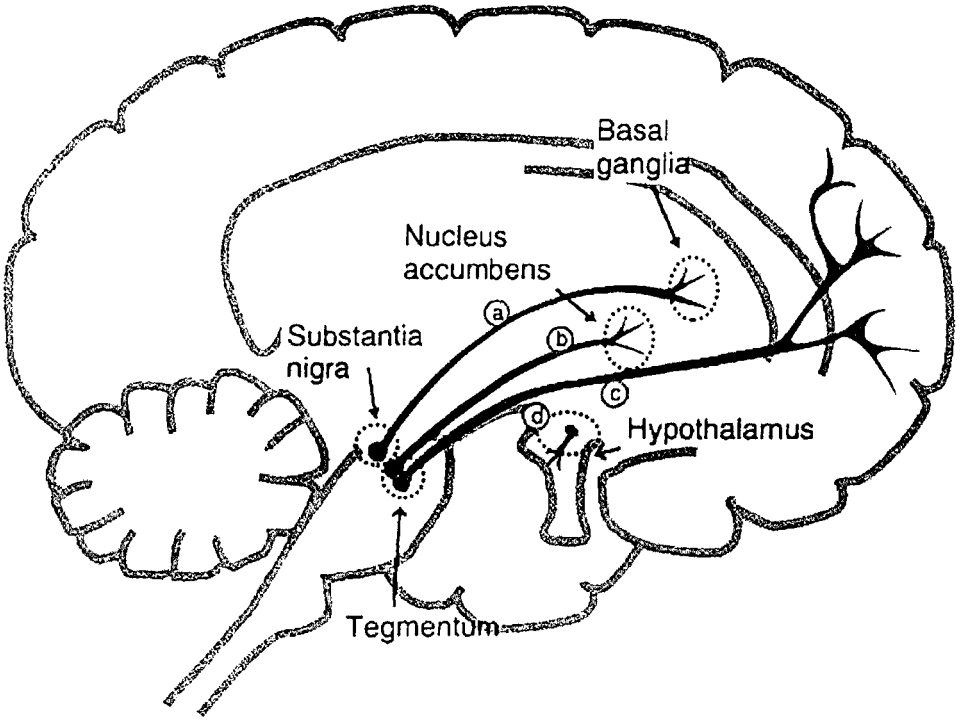

Figure 10 – The four major dopaminergic tracts of the brain. (a) The nigrostriatal system extends from the substantia nigra to the striatum. (b) The mesolimbic system originates in the ventral tegmental area and projects to the limbic system. (c) The mesocortical system projects from the ventral tegmental area to the neocortex, such as the prefrontal cortex. (d) The tuberoinfundibular system originates in the arcuate nucleus of the hypothalamus and projects to the pituitary stalk.

The substantia nigra is a part of the basal ganglia circuit in the midbrain. There are 4 components to this circuit, including the striatum, the globus pallidus, the substantia nigra, and the subthalmic nucleus. Eighty percent of the dopamine found in the brain is in the basal ganglia. This circuit receives input from the cerebral cortex, and then relays information to the thalamus, where the signals are then sent to the brainstem, prefrontal, premotor and motor cortices. The basal ganglia circuit plays a role in voluntary motor movement. Therefore, when a nucleus within this circuit is not functioning properly, one of three motor symptoms occurs.

These motor symptoms include tremor or involuntary movements, muscular rigidity, and finally slowness of movement. These symptoms were thought to be controlled independently of pyramidal motor system and therefore are termed extrapyramidal disorders. This is now known to be untrue; the extrapyramidal motor system is extensively interconnected with the pyramidal motor system. Figure 11 describes the neurobiology of the basal ganglia circuit in the normal and parkinsonian brain.

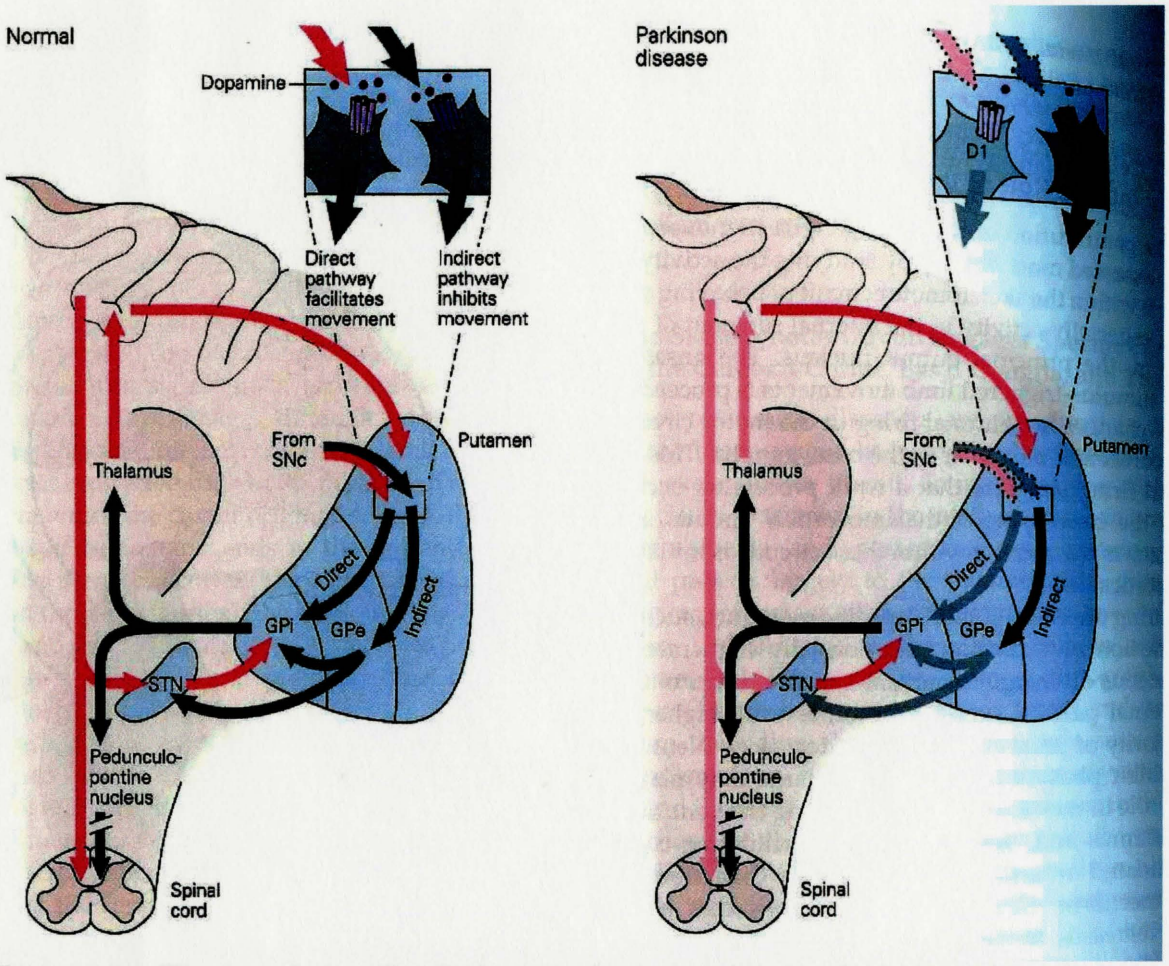

Figure 11 – The basal ganglia-thalmocortical circuitry under normal conditions (left) and in Parkinson's disease (right). Inhibitory connections are shown in grey and black arrows; excitatory connections are shown in red and pink arrows. Degeneration of the nigrostriatal system in Parkinson's disease leads to differential changes in activity in the two striatopallidal projections, indicated by changes in the darkness of connecting arrows. For example, in Parkinson's disease there is greater basal ganglia output to the thalamus. This causes further inhibition on the cortex, producing a paucity of movements. GPe = external

Synthesis

The synthesis of dopamine begins with the amino acid tyrosine (Kandel, et al., 2000). Tyrosine is taken into the body through dietary sources and absorbed into the blood stream. Eventually, the tyrosine is shuttled across the blood-brain-barrier by a low-affinity amino acid transporter. From the cerebrospinal fluid, the tyrosine is taken into dopaminergic neurons by specific amino acid transporters. Tyrosine is then oxidized by tyrosine hydroxylase to L-dihydroxyphenylalanine (L-DOPA). Because this conversion is the slowest of dopamine synthesis, this is the rate-limiting step (Kandel, et al., 2000). Tyrosine hydroxylase requires a co-factor, reduced pteridine, to carry out its reaction. This donates hydrogen to tyrosine, in order to fully catalyze the conversion to dopamine. L-DOPA is then decarboxylated by L-DOPA decarboxylase to dopamine. This process is shown in figure 12.

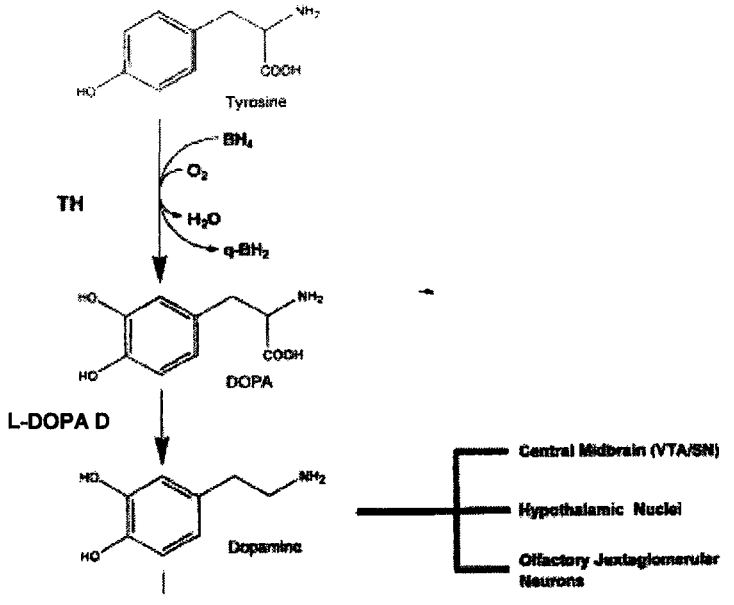

Figure 12 – Biosythetic pathway of dopamine. The first step in dopamine synthesis is the conversion of dopamine to 3, 4-dihydroxyphenylalanine (DOPA) by tyrosine hydroxylase. The subsequent step converts DOPA to dopamine and is catalyzed by L-DOPA decarboxylase (L-DOPA D). The TH reaction utilizes tyrosine, molecular oxygen (0_2), and BH_4 as cosubstrates in the formation of DOPA and the byproducts H_20 and quininoid-dihydrobiopterin ($q\text{-}B_2$). (adapted from Kumer and Vrana, 1996).

Once dopamine is synthesized, it is stored in vesicles within the neuron. In these vesicles, the dopamine is concentrated to 0.1M, which is 10-1000 times higher than in the cytosol. Dopamine is stored in these vesicles until an action potential stimulates the neuron and the vesicles move to the axon terminal.

Receptors

The dopamine receptors of the brain are classified into five subtypes: D1, D2, D3, D4 and D5 (Smythies, 2005). Chronologically, the D1 and D2 receptors were discovered first using dopamine receptor antagonists and monitoring the downstream effects. The D1 receptor was found to stimulate the adenylyl cyclase pathway, whereas the D2 receptor was found to inhibit this pathway (Missale, et al., 1998). With the advent of cloning techniques, the other dopamine receptors were found (D3, D4, and D5). After structural, pharmacological, and biochemical studies, it was reported that these receptors all fall under the 2 initial classifications of receptors (Missale, et al., 1998). The D1 and D5 receptors share high similarity in the functionality and their transmembrane domains. D2, D3, and D4 receptors also share similarity in their functionality and transmembrane domains (Missale, et al., 1998). This is shown in figure 13.

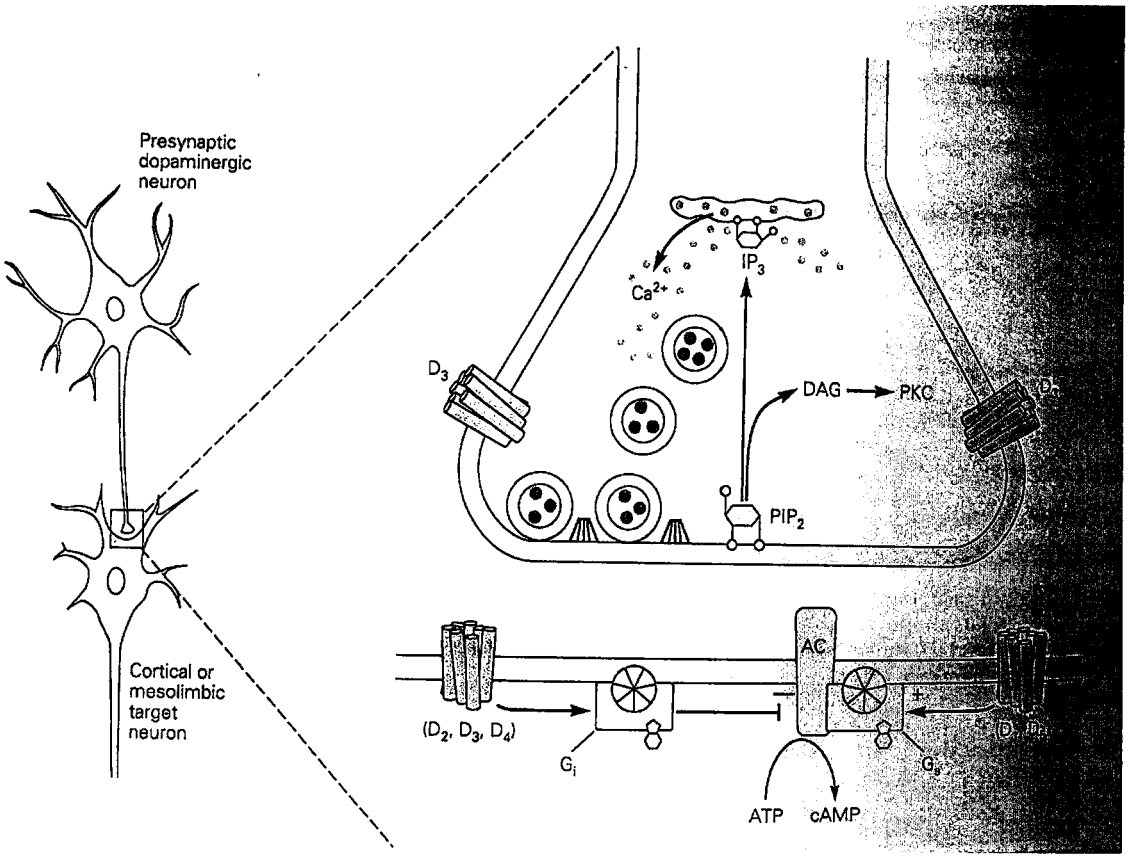

Figure 13 – Four types of dopamine receptors. D3 receptors are present on the pre- and post-synaptic membranes. D1, D2, and D4 receptors are present on the post-synaptic membrane. D2, D3, and D4 are functionally similar and inhibit adenylyl cyclase activity. D1 and D5 receptors are also functionally similar and stimulate adenylyl cyclase activity. (Kandel, et al., 2000).

All dopamine receptors are metabotrophic, meaning they are coupled to G-proteins. They are members of the seven transmembrane domain G-coupled receptor family. The structure of the D1-like receptor is seen in figure 14.

The dopamine receptor can be split into an NH_2 terminus, a COOH terminus and a transmembrane domain. The NH_2 terminal has a similar amount of amino acids between all receptor subtypes, but the N-glycosylation sites are variable (Missale, et al., 1998). In the D1 receptor family, only 2 glycosylation sites exist. The D2 receptor family has variable numbers of

glycosylation sites. For example, the D2 receptor has 4, the D3 receptor has 3 and the D4 receptor has only one (Missale, et al., 1998).

The structure of the COOH terminal is much more variable within dopamine receptors than the NH_2 terminal. For example, the D1-like receptors have a 7 times longer COOH terminal than D2-like receptors. There is also a signature cysteine residue within every dopamine receptor, although the position of the cysteine varies depending on the receptor subtype. The D2-like receptor has a cysteine residue located at the end of the COOH terminal, whereas the D1-like receptor has the comparable cysteine residue near the beginning of the COOH terminal (Missale, et al., 1998). The D2-like receptors also have a much longer third intracellular loop and interact with G_i proteins to inhibit adenylyl cyclase, whereas the D1 receptors have a shorter third intracellular loop and use G_s protein in order to activate adenylyl cyclase (Missale, et al., 1998).

The differences within the intracellular loops convey the specificity of the receptor. For example, dopamine displays a 20-times higher affinity for the D2 receptor than the D3 receptor. In a study conducted by Robinson, et al., (1994), it is shown that variances in the intracellular domain can partially account for this difference.

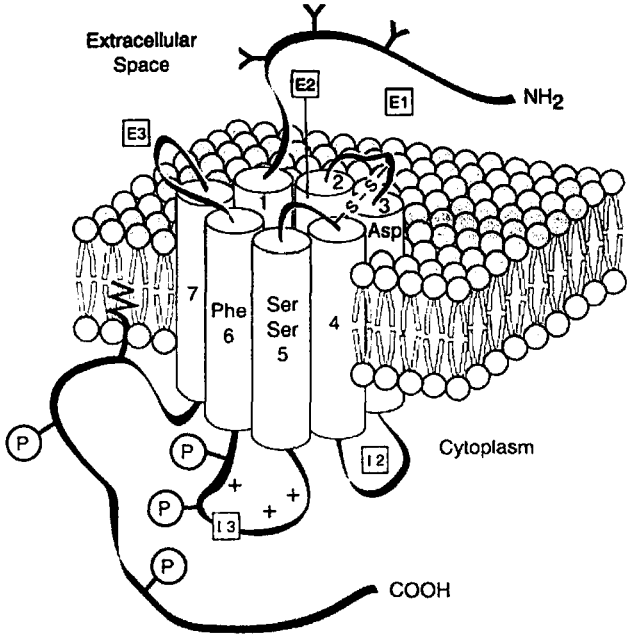

Figure 14 – The structure of a D1-like receptor. At the NH_2 terminal, the three potential glycosylation sites are shown. The signature cysteine residue is shown at the COOH terminal. As well, transmembrane domains are shown, and labelled 1-7. Potential phosphorylation sites are indicated by P. E1-E3 represent the extracellular loops, where is I2-I3 represent the intracellular loops. (Missale, et al., 1998).

Degradation

Dopamine is metabolized by actions of the enzymes monoamine oxidase (MAO) and catechol-O-methyltransferase (COMT). Dopamine can be equally degraded by either MAO A or B. The primary metabolite of MAO dopamine degradation is 3, 4-dihydrophenylacetic acid (DOPAC). DOPAC can be processed by COMT to further metabolize the compound into homovanillic acid (HVA). Oxidative by-products are produced by MAO dopamine metabolism (Youdim and Riederer, et al., 2004). MAO-A is present in peripheral and central adrenergic systems, whereas MAO-B is densely located in the basal ganglia and glial cells (Levitt, et al., 1982; Westlund, et al., 1985). Both MAO-A and MAO-B have approximately equal abilities to oxidize dopamine, and are present on the outer membrane of the mitochondrion (Youdim, et al., 2006). In the rat

brain, MAO-A and MAO-B concentrations are approximately equal in dopaminergic neurons (Youdim and Riederer, et al., 2004). See figure 16.

COMT also degrades dopamine, both in the peripheral nervous system as well as the central nervous system. COMT catalyzes the transfer of methyl groups to substrates containing a catechol group. It is present in the rat brain, with no specific regional distribution (Broch and Fonnum, 1972). It is present in the cytoplasm of cells, either free or loosely bound to membranes within the cell cytoplasm (Axelrod and Tomchick, 1958). COMT degrades dopamine to produce 3-methoxytyramine (3-MT), which then undergoes another enzymatic reaction with MAO to produce HVA (figure 16). Levels of (3-MT) are considered a marker for extraneuronal dopamine metabolism.

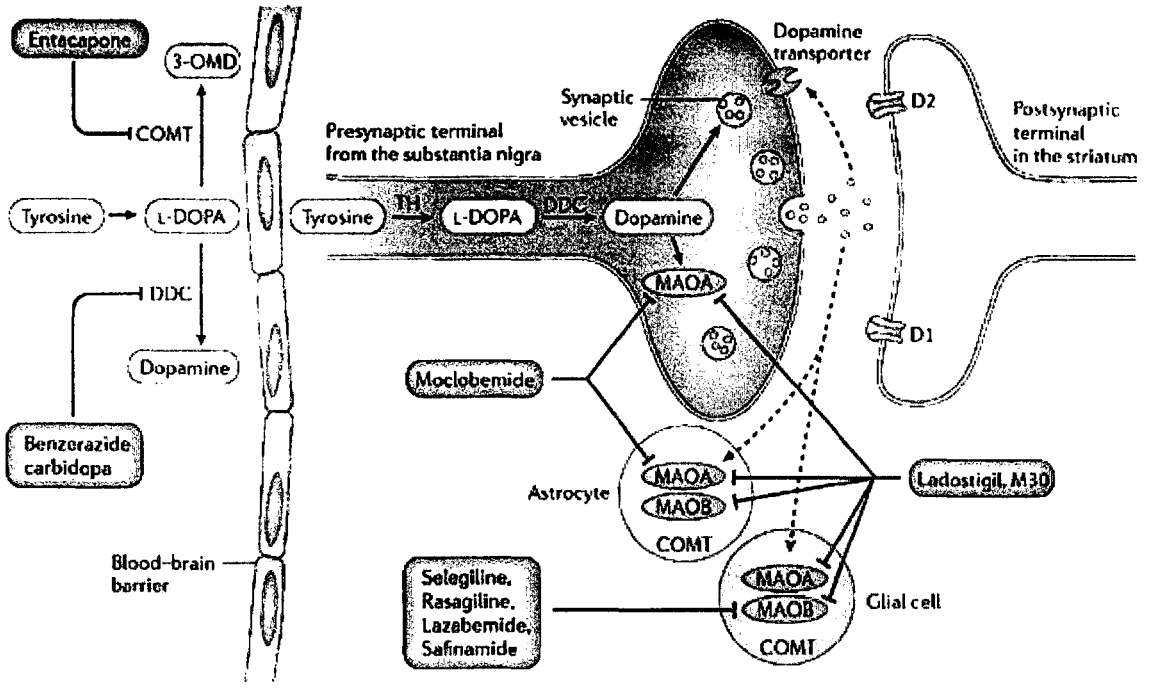

Figure 15 – The pathway of dopamine synthesis proceeds from tyrosine via tyrosine hydroxylase (TH) catalysis to levodopa (L-DOPA), and subsequent decarboxylation by dopa decarboxylase (DDC) to dopamine. Dopamine is metabolized by intraneuronal monoamine oxidase A (MAO-A), and by glial and astrocyte MAO-A, MAOB and COMT. There are many selective and non-selective MAO inhibitors, which are shown interacting with the neuron, astrocytes and glial cells. (Youdim, et al., 2006).

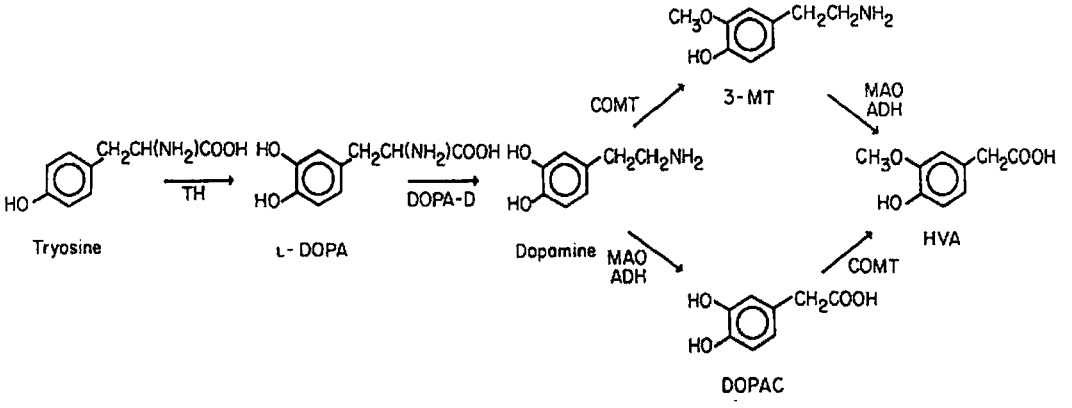

Figure 16 – Synthesis and degradation of dopamine by the action of MAO and COMT.

1. TIMECOURSE OF HALOPERIDOL – INDUCED MIDBRAIN DOPAMINE NEURON DOWNREGULATION

INTRODUCTION

Antipsychotic drugs are the mainstay treatment for Schizophrenia. Haloperidol, an APD, is a dopamine receptor antagonist, which prevents dopamine release from the substantia nigra to the striatum. Because of the lack of dopamine release, extrapyramidal side effects are seen with haloperidol administration. Although minutes after HAL administration dopamine receptors are blocked, the extrapyramidal side effects do not manifest themselves until approximately 3 weeks after treatment. The late-onset side effects therefore do not correlate with the receptor blockade. Therefore, a simple receptor blockade cannot solely be the causative factor.

Loss of dopaminergic neurons in the substantia nigra is the neurobiology of Parkinson's disease. Previous findings in our lab have shown that HAL administration caused a downregulation of tyrosine hydroxylase, the rate-limiting enzyme for dopamine biosynthesis. Upon further investigation, 10 minutes after HAL treatment TH is downregulated in dopaminergic neurons of the substantia nigra. In this study, we looked at the ultra-short timecourse of HAL-induced TH downregulation in midbrain dopamine neurons to pinpoint the time of TH downregulation.

METHODS

Subjects

Forty-five male Sprague-Dawley rats (Charles River, PQ), weighing 200-225 g, were singly housed with free access to food and water, on a 12 hour:12 hour light:dark cycle. Animals were habituated to their new environment for 7 days prior to treatments. Weights were recorded bi-weekly to ensure animal health. All efforts were made to follow McMaster University Central Animal Facility Guidelines and Canadian Council on Animal Care.

Drugs

Haloperidol was obtained from Sabex Inc. (QC, Canada).

Treatment Regimen

Rats were randomly assigned to one of five different treatment groups. Groups of rats were injected with HAL (2 mg/kg) 1 minute (n=9), 2 minutes (n=9), 5 minutes (n=9), or 10 minutes (n=9), prior to decapitation. A control group (n=9) were injected with saline (0.9%) 10 minutes prior to decapitation.

Animal Sacrifice Procedure

Rats were decapitated and brains were immediately removed. Brains were placed in ice cold 4% paraformaldehyde (pH=7.2) and refrigerated for 1 week prior to sectioning.

Tissue Sectioning

Twenty-four hours prior to sectioning, brains were placed in a 15% sucrose solution for cryoprotection. Consecutive coronal sections (40μm) were taken at -18°C on a cryostat (Leica CM 1900, Heidelberg, Germany) and placed 3 sections per well in 0.1 M phosphate buffered saline (PBS) in a 24-well plate from caudal to rostral.

Immunohistochemistry

Sections of SN were selected for each animal at bregma -5.3 mm to -5.8 mm. Bregma -5.3 mm corresponds to an area with a thick portion of the third cranial nerve, which provides an anatomical landmark and demarcation between the SNc (substantia nigra pars compacta) and the ventral tegmental area (VTA). Bregma -5.8 mm corresponds to an area where accessory tracts of the third nerve cross between the SNc and VTA. These landmarks were used to select appropriate tissue for immunohistochemistry.

Sections were then processed for TH immunohistochemistry. Sections were placed in 0.3% hydrogen peroxide in methanol for 30 minutes and then washed in PBS for 10 minutes. Tissues then entered a solution of 5% normal goat serum for 1 hour to prevent non-specific primary antibody binding. Tissues were subsequently incubated in rabbit anti-TH antibody (1:1500; Chemicon, CA, USA) for 2 hours at room temperature and 70 hours at 4°C. Tissues were washed for 10 minutes in PBS, three more times and incubated in biotinylated goat anti-rabbit IgG secondary antibody (1:400; Vector Laboratories, CA, USA). Tissues were washed three more times in PBS for 10 minutes each, and incubated in ABC for 1 hour to form an avidin/biotin complex. All sections were rinsed three more times in PBS for 10 minutes each and placed into the chromagen, 3, 3-diaminobenzidine tetrachloride (D-5637; Sigma, MO, USA).

The sections were then mounted onto (3-aminopropyl)triethoxysilane-coated slides and covered slipped with D.P.X., neutral mounting medium (317616; Aldrich, WI, USA).

A second set of sections were also processed for TH and CD11b (OX-42), a microglial marker, for fluorescent immunohistochemistry. Sections were placed in 0.3% hydrogen peroxide dissolved in methanol for 30 minutes to destroy endogenous peroxidases present in red blood cells. Tissues were then washed in PBS for 10 minutes. Sections then entered a solution of 10% normal donkey serum for 1 hour to prevent non-specific primary antibody binding. Tissues were then placed in mouse anti-CD11b antibody (1:500; Serotec, NC, USA) for 1 hour at room temperature and 24 hours at 4°C. Tissues were washed for 10 minutes three more times and incubated for 1 hour at room temperature in donkey anti-mouse IgG secondary antibody conjugated to Cy5 (1:800; Chemicon, CA, USA). Sections were kept in the dark for the remaining of the procedure. Tissues were washed three more times for 10 minutes each in PBS and then re-entered a 1 hour incubation in 10% normal donkey serum. Sections were then placed in rabbit anti-TH antibody (1:500; Chemicon, CA, USA) for 1 hour at room temperature and 24 hours at 4°C. Tissues were rinsed in PBS for three 10 minute PBS washes and subsequently incubated in donkey anti-rabbit IgG, conjugated to Cy3 (1:800; Chemicon, CA, USA) for 1 hour at room temperature. The sections were then rinsed three more times for 10 minutes each and mounted onto (3-aminopropyl)triethoxysilane-coated slides and covered slipped with Vectashield mounting medium for fluorescence (Vector Laboratories, CA, USA).

Quantitative Morphometry

Slides were coded and the treatment regimen was blinded to the person quantifying the section. Tissues were manually counted for TH- and OX-42-immunoreactive cells at 20x magnification for both the left and right hemispheres. Due to the high magnification, the entire SN could not be seen in the field of the microscope. SN was divided into three areas (lateral, central and medial) for counting. When the cell counting was completed, slides were decoded and arranged due to treatment group. The cell counts were then averaged within groups and a mean ± standard error of the mean (SEM) was calculated. Cell diameters for TH-immunoreactive cells were also measured in both the x and y directions, with the aid of MetaMorph software.

Statistical Analysis

The cell count data and the cell diameter data were analyzed separately using a one-way analysis of variance (ANOVA), followed by *post-hoc* Tukey test. Significance was determined at the $p < 0.05$ level. All statistics were performed using SPSS version 13.0.

RESULTS

TH counts

SN

Analysis of cell counts revealed a highly significant HAL-induced TH downregulation, $F(4,35) = 18.33$, $p < 0.001$. HAL produced a significant ($p < 0.05$) 15% reduction of TH-immunoreactive cell counts within 5 minutes of administration, decreasing by a 28% by 10 minutes ($p<0.001$), compared to saline-injected animals. The 10 minute HAL-treated animal cell counts were significantly different from every other group ($p < 0.05$). Most important, a significant difference was seen between the 5 minute and 10 minute HAL-treated groups ($p = 0.041$). No significant changes were observed in the animals which had received HAL 1 or 2 minutes prior to sacrifice. Cell counts were adjusted for cell sizes by the Abercrombie formula, as seen in Appendix I.

Cell counts for SN processed for TH-immunohistochemistry

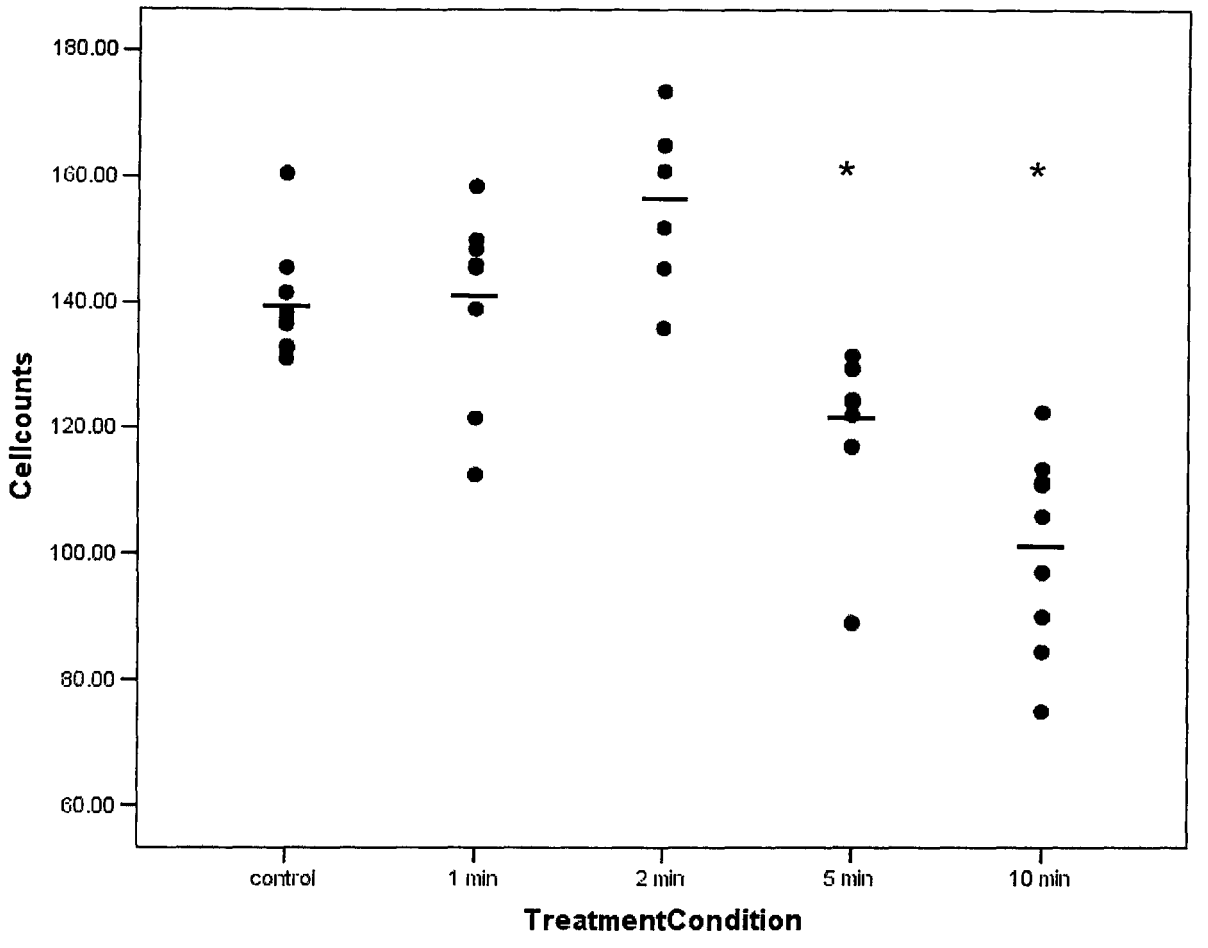

Figure 17 – Scatter plot of TH-positive cells in the substantia nigra per 40 μm hemi section. Each dot represents the mean number of TH-positive cell counts for one animal, with the horizontal line representing the group mean. TH-positive cell counts were significantly decreased in the SN of HAL-treated animals by 15% ($p < 0.05$) at 5 minutes and by 28% ($p < 0.001$) at 10 minutes.

Treatment Regimen	Control	1 min + HAL	2 min + HAL	5 min + HAL	10 min HAL
Mean ± S.E.M.	139.6 ± 3.0	140.2 ± 5.5	155.5 ± 5.6	120.9 ± 4.8	101.2 ± 5.2

Table 1 – Mean cell counts ± S.E.M. for TH-positive cells in the SN.

Photomicrographs (20x magnification) of SN processed for TH-immunohistochemistry

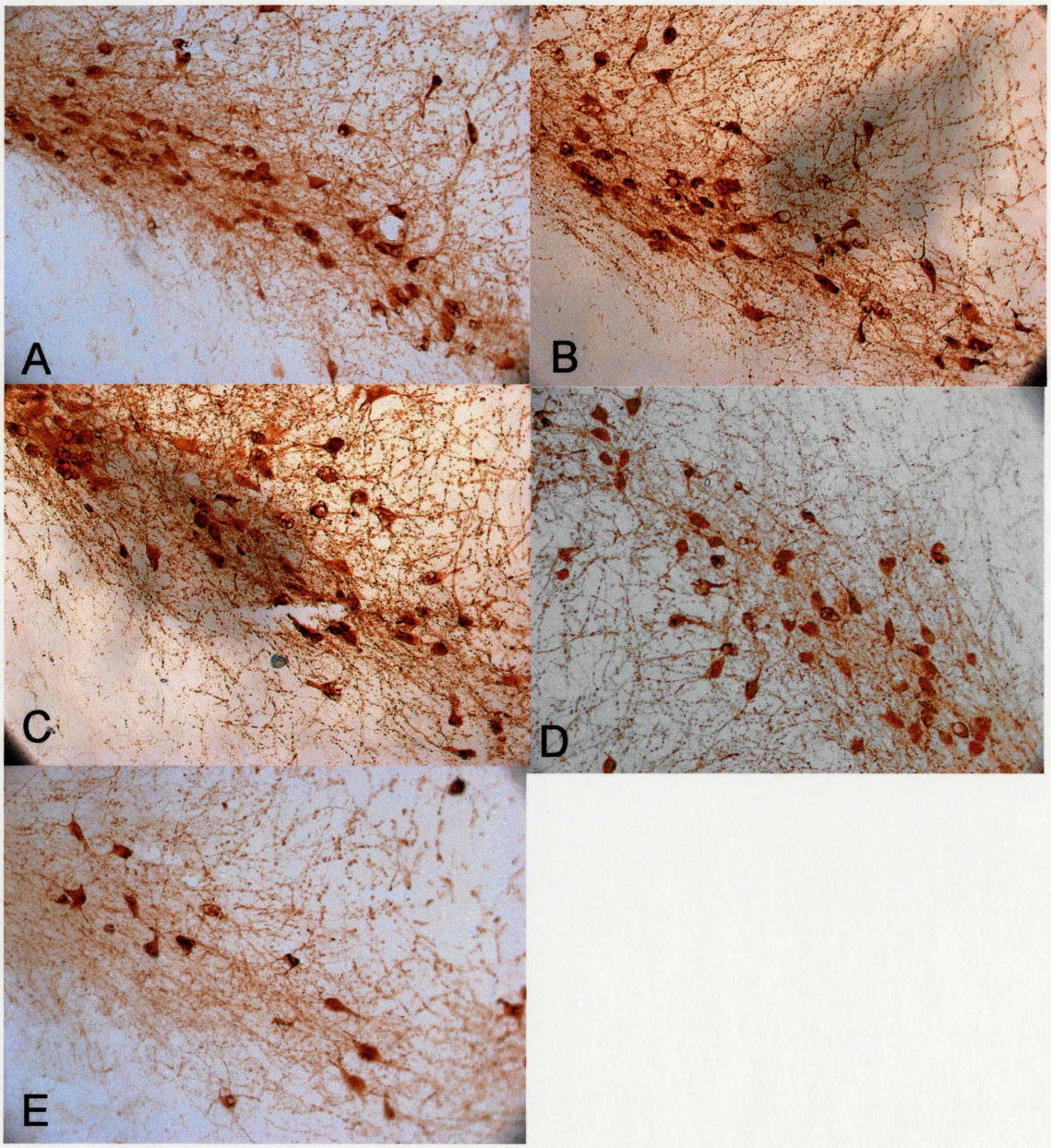

Figure 18 – Photomicrographs (20x magnification) of TH-positive immunoreactivity in the SN for each group taken at bregma -5.3mm. There was a significant decrease in TH-positive cell counts at 5 minutes and 10 minutes in the HAL-treated groups.
A: Control
B: 1 min HAL
C: 2 min HAL
D: 5 min HAL
E: 10 min HAL

VTA

Analysis of cell counts revealed no significant change in TH-immunoreactivity between any groups, $F(4,37) = 1.98$, $p = 0.12$. HAL produced no significant reduction in TH-positive cell counts compared to saline-injected animals, although the 10 minute HAL-treated animals tended toward a decrease in TH-positive cells. A non-significant 5% reduction in TH-immunoreactive cells was seen in the 10 minute HAL-treated animals compared to saline-injected controls.

Cell counts in Ventral Tegmental Area processed for TH-immunohistochemistry

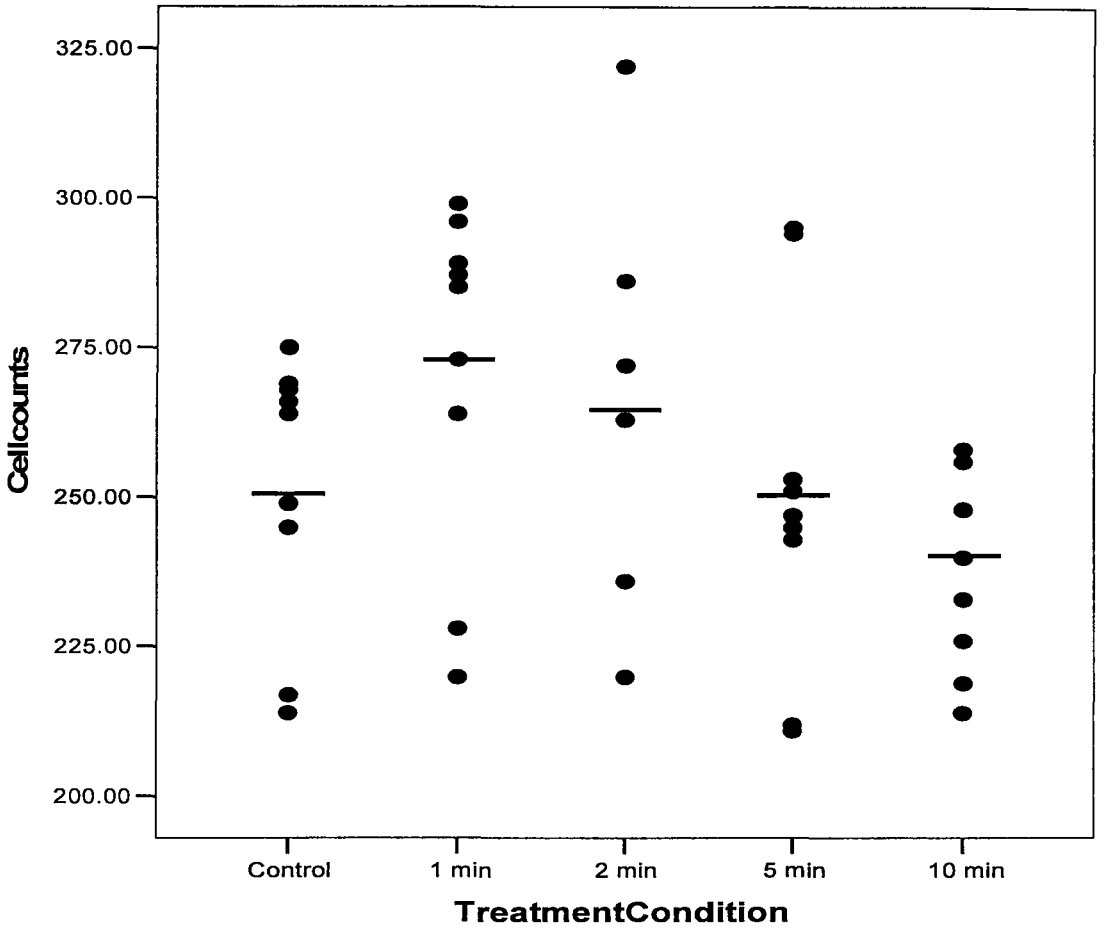

Figure 19 – Number of TH-positive cells in the ventral tegmental area per 40 μm hemi section. Each dot represents the mean number of TH-positive cell counts for one animal, with the horizontal line representing the group mean. TH-positive cell counts were not significantly decreased in the VTA of HAL-treated rats, although a decreasing trend was seen in the 5 and 10 minute HAL-treated animals.

Treatment Regimen	Control	1 min + HAL	2 min + HAL	5 min + HAL	10 min HAL
Mean ± S.E.M.	251.9 ± 7.6	271.2 ± 9.6	266.5 ± 14.8	250.1 ± 9.9	239.1 ± 5.7

Table 2 - Mean cell counts ± S.E.M. for TH-positive cells in the VTA.

Photomicrographs (20x magnification) of SN processed for TH-immunohistochemistry

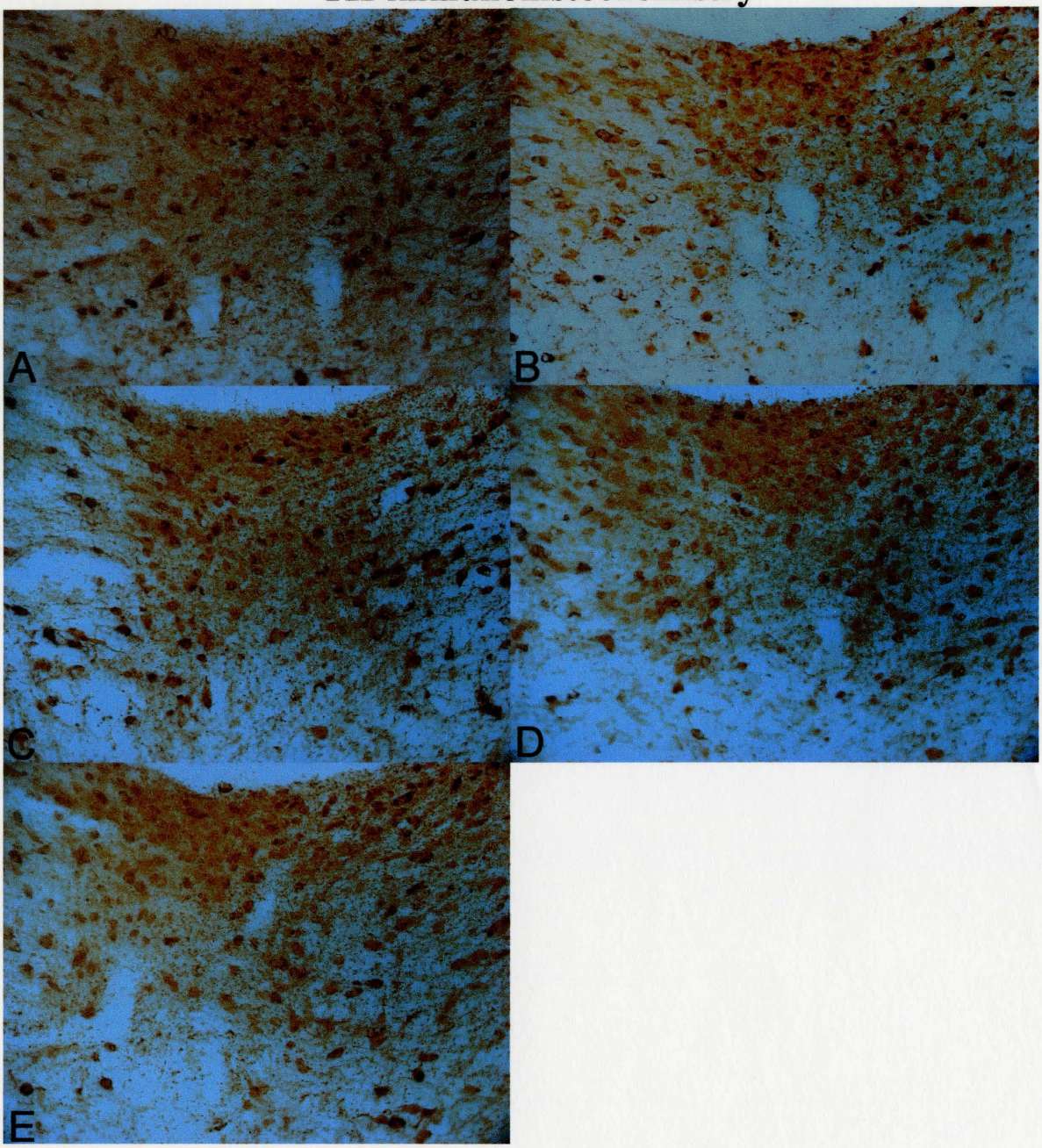

Figure 20 – Photomicrographs (20x magnification) of TH-positive immunoreactivity in the VTA for each group taken at bregma -5.3mm. There were no significant changes in TH-positive cell counts.
A: Control
B: 1 minute HAL
C: 2 minute HAL
D: 5 minute HAL
E: 10 minute HAL

TH & OX-42 Double Label

SN

TH counts

Analysis of cell counts revealed that a significant difference was seen with HAL treatment, $F(4,37) = 5.1$, $p = 0.002$. The 10 minute HAL treatment produced a significant 21% reduction in TH-positive cell counts compared to sham-treated animals ($p < 0.02$). A significant 19% reduction was also seen with 5 minute treatment of HAL compared to controls ($p < 0.04$). HAL treatment for both 1 minute and 2 minute prior to decapitation showed no significant difference from sham-treated animals.

Cell counts for Substantia Nigra processed for TH-immunofluorescence

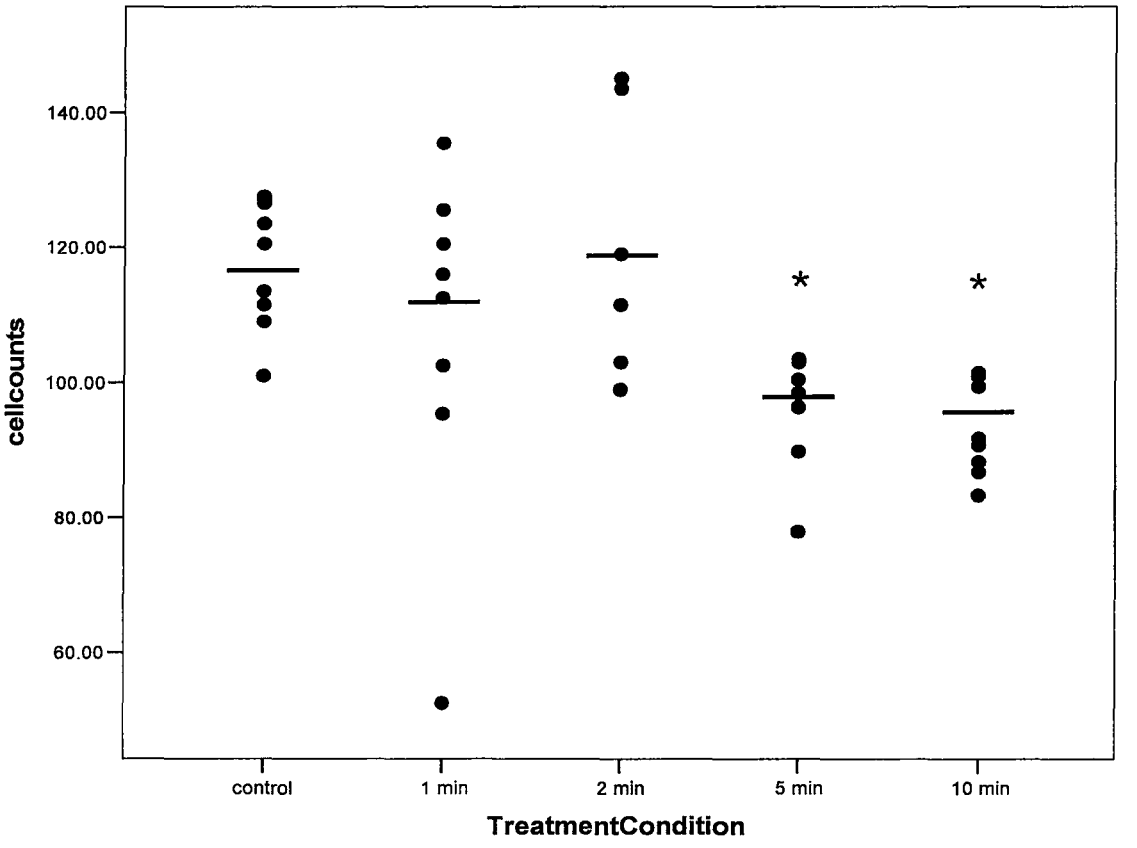

Figure 21 – Scatter plot of TH-positive cells in the substantia nigra per 40 μm hemi section. Each dot represents the mean number of TH-positive cell counts for one animal, with the horizontal line representing the group mean. TH-positive cell counts were significantly decreased in the SN of HAL-treated animals by 19% ($p < 0.04$) at 5 minutes and by 21% ($p < 0.02$) at 10 minutes.

Treatment Regimen	Control	1 min + HAL	2 min + HAL	5 min + HAL	10 min HAL
Mean ± S.E.M.	117.8 ± 3.2	110.7 ± 8.5	120.2 ± 8.1	95.9 ± 2.8	93.7 ± 2.3

Table 3 – Mean cell counts ± S.E.M. for TH-positive cells in the SN.

Confocal images (20x magnification) of SN processed for TH-immunofluorescence

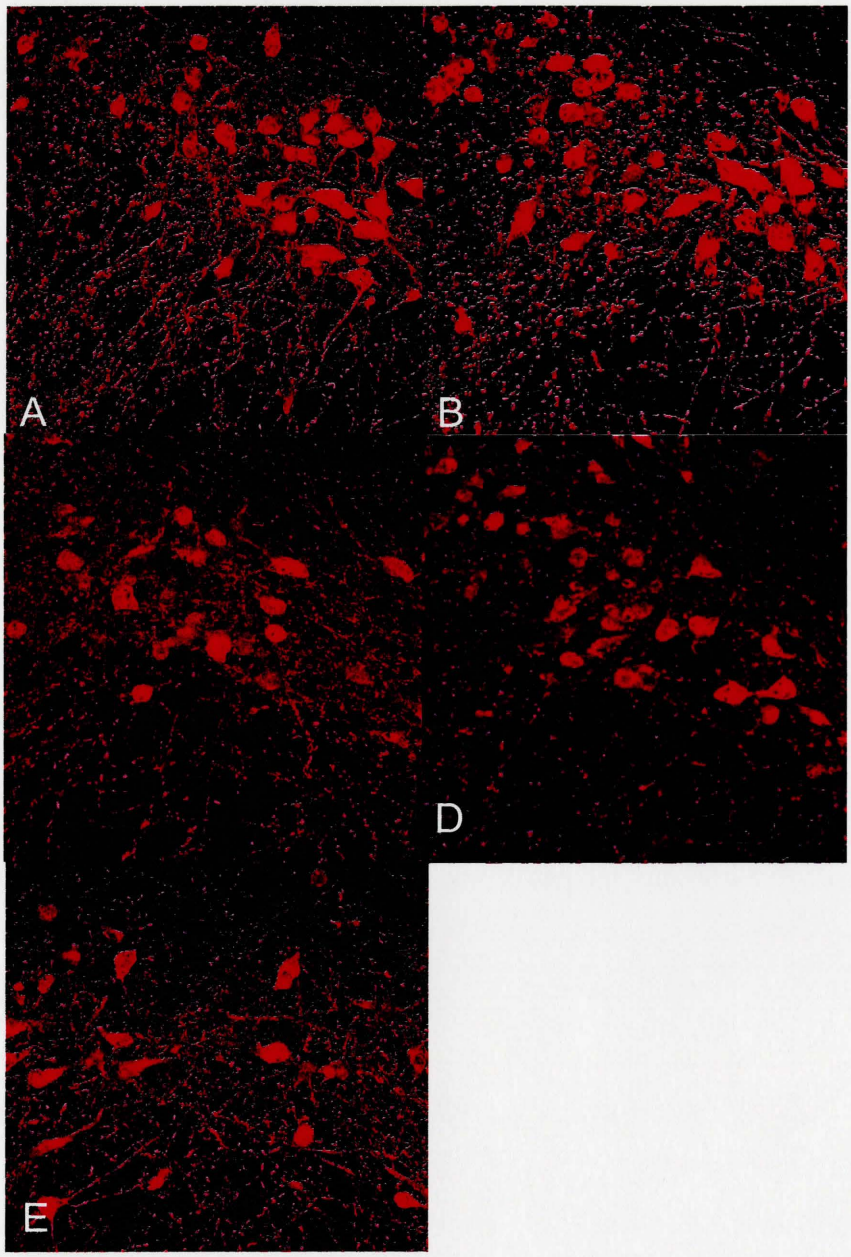

Figure 22 – Fluorescent images of TH-labelled cells of the SN taken per drug treatment group as visualized on the confocal microscope at 20x magnification. A significant decrease was seen at 5 minutes and 10 minutes in HAL-treated animals.
A: Control
B: 1 minute HAL
C: 2 minute HAL
D: 5 minute HAL
E: 10 minute HAL

OX-42 counts

Analysis of cell counts revealed a highly significant HAL-induced change in OX-42 immunoreactivity, $F(4,37) = 10.8$, $p < 0.001$. Animals treated with HAL 10 minutes prior to decapitation showed a 33% increase in activated microglia ($p = 0.01$). Similarly, a significant ($p < 0.001$) 37% increase in OX-42 positive cells was seen in the animals treated with HAL 5 minutes prior to sacrifice. There was no significant difference seen in the 1 minute or 2 minute HAL-treated groups, although there was a non-significant 22% increase in the 2 minute HAL group.

Activated microglial cell counts for Substantia Nigra processed for OX-42-immunofluorescence

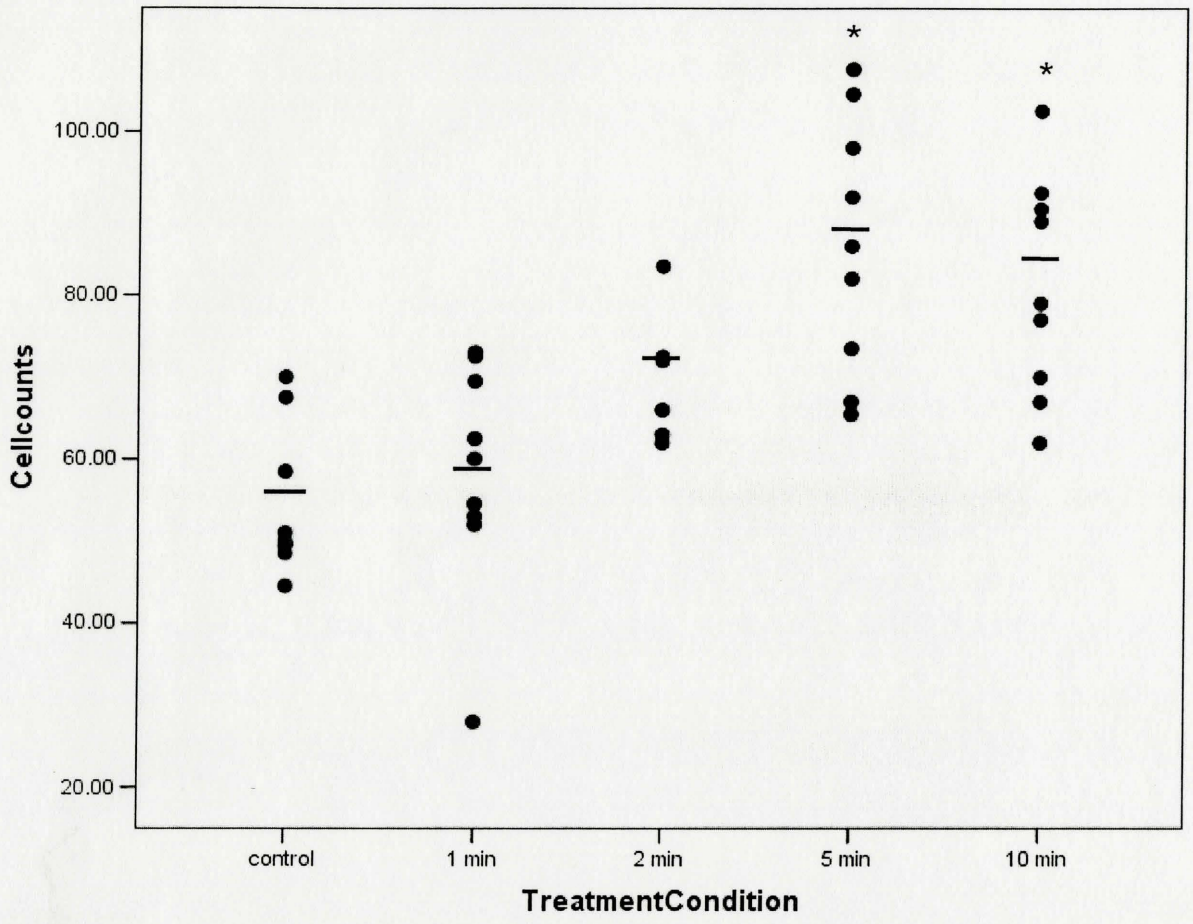

Figure 23 – Scatter plot of OX42-positive cells in the substantia nigra per 40 μm hemi section. Each dot represents the mean number of OX-42-positive cell counts for one animal, with the horizontal line representing the group mean. OX-42-positive cell counts were significantly increased in the SN of HAL-treated animals by 37% ($p < 0.001$) at 5 minutes and by 33% at 10 minutes ($p = 0.01$). There was also a non-significant 22% increase in OX-42 immunoreactivity seen at 2 minutes.

Treatment Regimen	Control	1 min. HAL	2 min. HAL	5 min. HAL	10 min. HAL
Mean ± S.E.M.	54.3 ± 3.0	58.3 ± 4.7	69.8 ± 3.3	86.2 ± 5.2	81.1 ± 4.5

Table 4 – Mean cell counts ± S.E.M. for OX-42-positive cells in the SN.

Confocal images (20x magnification) of SN processed for TH-immunofluorescence

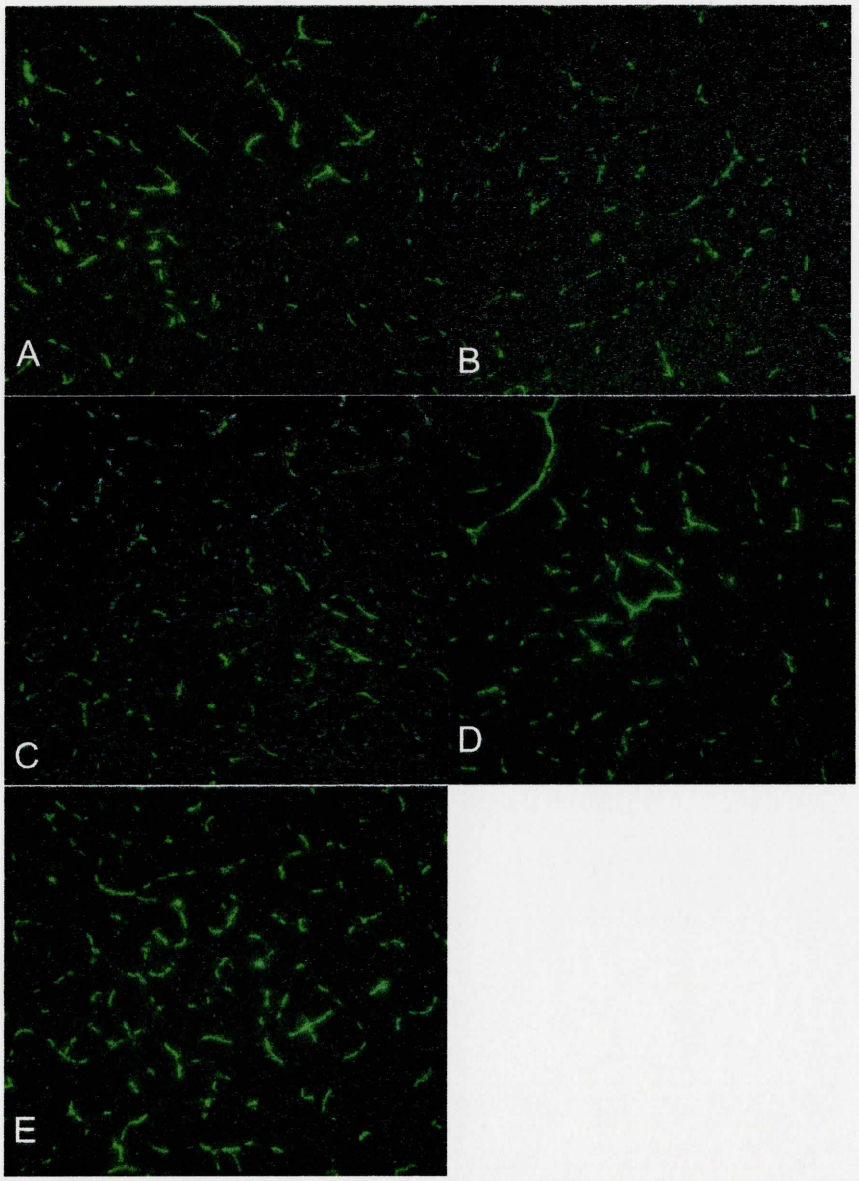

Figure 24 – Fluorescent images of OX-42-labelled cells of the SN taken per drug treatment group as visualized on the confocal microscope at 20x magnification. A significant increase was seen at 5 minutes and 10 minutes in HAL-treated animals. A non-significant increase was also seen at 2 minutes in HAL-treated animals.
A: Control
B: 1 minute HAL
C: 2 minute HAL
D: 5 minute HAL
E: 10 minute HAL

TH cell diameter

SN

A significant difference in cell sizes was seen between groups, $F(4,36) = 3.55$, $p = 0.015$. 10 minute HAL-treated animals had a significantly higher cell size compared to control animals ($p = 0.017$). No other groups showed any significant difference compared to control animals. See figure 18.

Mean cell diameters in the Substantia Nigra processed for TH-immunohistochemistry

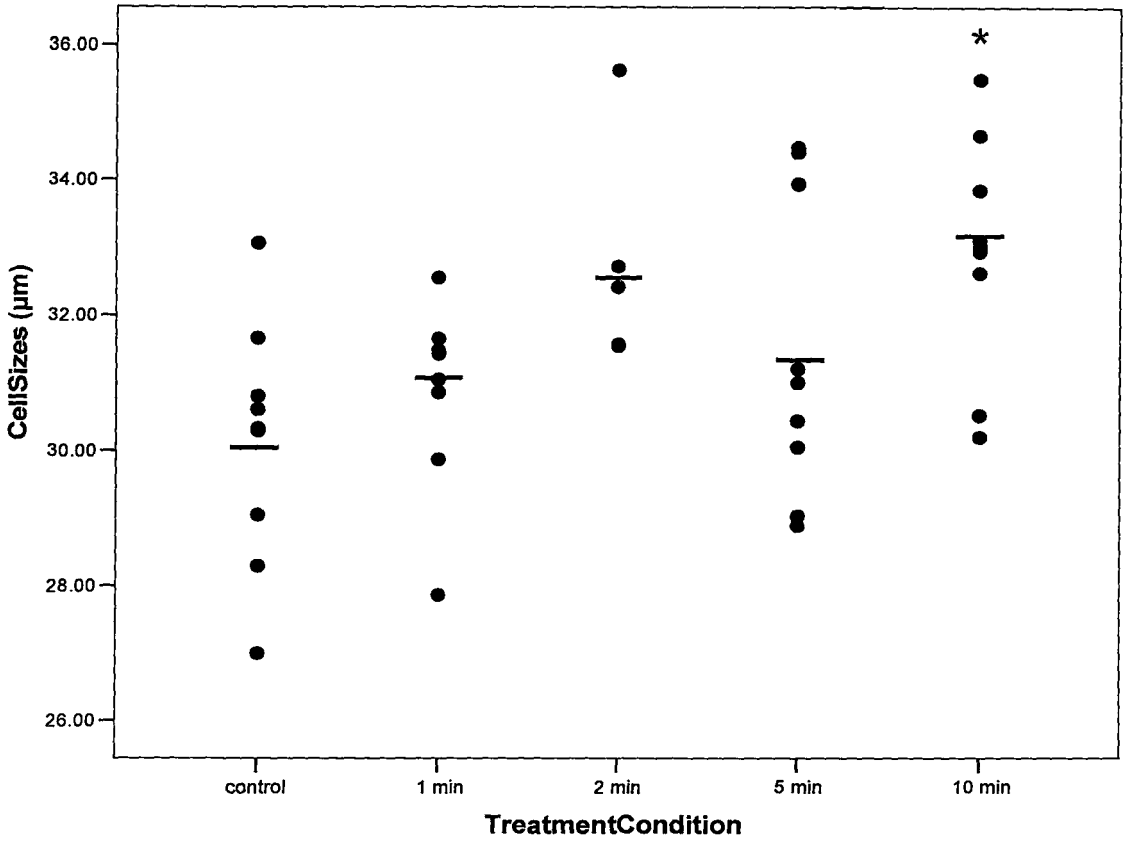

Figure 25 – Mean cell diameter (µm) of TH-positive cells of the substantia nigra per 40 µm hemi section. Each dot represents the mean diameter of 10 TH-positive cells for one animal of, with the horizontal line representing the group mean. There was a significant difference seen between the control and 10 minute HAL-treated groups ($p = 0.017$).

Treatment Regimen	Control	1 min. HAL	2 min. HAL	5 min. HAL	10 min. HAL
Mean ± S.E.M.	30.1 ± 0.60	30.8 ± 0.50	32.6 ± 0.65	31.5 ± 0.74	32.9 ± 0.57

Table 5 – Mean cell diameter ± S.E.M. for TH-positive cells in the SN.

DISCUSSION

These results indicate that HAL induces significant TH downregulation by 5 minutes post-exposure, with further downregulation seen after 10 minutes. Significant microglial activation is also seen 5 minutes after HAL administration, although activation is increasing by 2 minutes. This suggests that microglial activation may precede TH downregulation. Activated microglia have been implicated in Parkinson's disease models and have been shown to cluster around dopaminergic neurons. Toxic mediators of inflammation, such as TNF, iNOS, and COX-2 are produced by activated microglia (Liu and Hong, 2003). These products can bind to and stimulate receptors of other microglia, consequently propagating cytotoxicity. COX-2 can also bind to dopaminergic neurons, initiating cellular stress responses and cellular death pathways.

This theory has been tested with the MPTP model of Parkinson's disease. Vijitruth, et al. 2006 tested the ability of COX-2 to activate microglia, inducing secondary dopaminergic cell death in the substantia nigra. They found that by either administration of valdecoxib, a COX-2 inhibitor, or by knocking out the COX-2 gene, there was decreased dopaminergic cell death and decreased microglial activation. Therefore, they concluded that COX-2 was a perpetuator of neuroinflammation. The activated microglia were proposed to release toxic mediators of inflammation in response to the increased levels of COX-2, including reactive oxygen species and TNF-α. This culminated in dopaminergic cell death as seen in Parkinson's disease, see figure 26 below.

Similar experiments have also concluded that microglial activation precedes damage to dopaminergic neurons. In LaVoie, et al. 2004, methamphetamine (METH) at neurotoxic doses

was administered to rats. METH neurotoxicity is thought to be associated with dopamine and is also used as a model for Parkinson's disease, like haloperidol. METH was found to induce microglial activation prior to dopamine terminal pathology. They found that at 1 day post-administration of METH, TH-immunoreactive fibres in the striatum were not significantly different from controls, yet microglial activation was significantly increased from control animals (LaVoie, et al., 2004). At day 2, the TH-immunoreactive fibres had swollen and correlated with maximal microglial response. This result supports the result found in this study, where microglia were found to activate prior to TH-downregulation. Although we found that microglial activation is increasing at 2 minutes, which is significantly faster than 1 day, we used a drug that would immediately block dopamine receptors. In the case of METH, it would have to enter into the monoaminergic terminals. Subsequently, it would interact with vesicular monoaminergic transporters, enter into monoaminergic vesicles and displace monoamines into the cytoplasm of the terminals. Monoamines would then be released into the synaptic cleft, by means of reverse transport through DAT (Cadet, et al., 2003). This process would take a much longer period of time compared to a receptor blockade by haloperidol. Therefore, microglial activation prior to TH-downregulation would correlate with other findings in Parkinson's disease models of neurotoxicity. All together, these findings suggest that microglia may mediate APD-induced toxicity in the substantia nigra through release of toxic inflammatory mediators.

The ventral tegmental area cell counts were not significantly decreased with HAL-treatment compared to controls, which contrasts the SN result. This finding is not surprising once the distribution of microglia in the brain is noted. Microglia, in mouse brain, are densely populated in the hippocampus, olfactory telencephalon, basal ganglia and substantia nigra (Lawson, et al.,

1990). Outside of these areas, the microglial populations are less dense. Therefore, activated microglia in densely populated areas would release an abundance of toxic inflammatory mediators creating a toxic environment for neurons to survive in. Another study also noted that microglia differentially express mRNA of inflammatory mediators. For example, microglia in the hippocampus express significantly higher mRNA levels of TNF-α compared to cerebellum and cortex microglia (Ren, et al., 1999). Therefore, it is possible that the production levels of TNF-α and other cytokines by microglia could vary between the VTA and the substantia nigra. This would induce differing microenvironments for the dopamine neurons, causing specific dopaminergic damage to neurons in the substantia nigra.

In this study, haloperidol also induced an increase in cell size in the substantia nigra. This increase in cell size has been noted in melanin-containing neurons of the substantia nigra of aged human brain tissue (Cabello, et al., 2002). This result has also been reported in a study performed by Cruz-Sanchez, et al. 1997, who performed a detailed Golgi stain and measured cell size of melanin-producing neurons in the substantia nigra. He too reported a swelling and beading of dendritic branches and distorted cell body shape. The increased cell size has been postulated to be due to an inherent loss of dopaminergic neurons. The loss of dopaminergic cells would lead to a decrease in dopamine production. Therefore, the remaining cells might try to compensate for the lack of dopamine and begin overproducing the neurotransmitter, causing the cell to swell. Haloperidol has been known to induce apoptosis in dopaminergic neurons (previous lab. finding). The apoptotic cells would have dysregulated protein functions, including protein synthesis and metabolism. Excess dopamine would not be properly released and

metabolized, thereby causing cellular swelling. There would also be increased vacuoles inside the cells, since the cell is undergoing a cell death process.

Andersson, et al. 2002 also found that either a 4-month or an 8-month administration HAL increased rat striatal volumes compared to control animals. It is proposed that long term dopamine receptor blockade induces hypertrophy, regeneration, activation and change in the number of striatal synapses (Muller and Seeman, 1977; Benes, et al., 1983; Meshul, et al., 1994; Roberts, et al., 1995). Since striatal synapses originate from cell bodies in the SN, we can propose that there may also be alterations in the dopamine cell bodies. In Benes, et al., 1983, no change in cell size was found in the SN, although animals were treated with chronic HAL. In our study, animals were only treated with HAL for 10 minutes. In a long term treatment, cells could adjust to receptor blockade by altering synapses, for example, as found in the Benes study. In an acute treatment of HAL, few cellular alterations would be completed. Therefore, the cells may swell upon acute treatment of HAL and adjust to receptor blockade upon chronic administration by altering synapses.

Overall, these results suggest that microglial activation may precede TH-downregulation in dopaminergic neurons of the substantia nigra. This suggests that treatment interventions such as minocycline might be an intervention to be used to prevent this change.

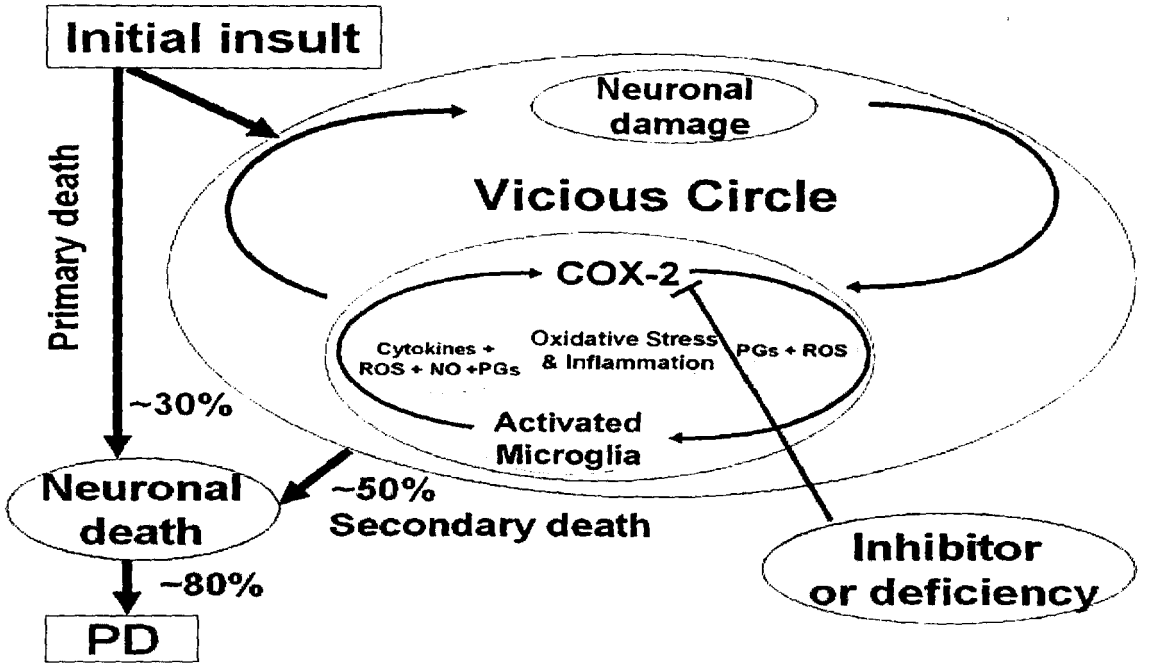

Figure 26 – Schematic flow chart depicting the role of the vicious circle in dopaminergic neurotoxicity. In Vijitruth, et al. 2006, the initial insult MPP+ exerts direct dopaminergic neurodegeneration (~30% of the original numbers). This initial decrease of TH-immunoreactivity in the substantia nigra is also seen with HAL administration. Neuronal damage initiates the vicious circle with COX-2 and microglia as the key components feeding oxidative and inflammatory damage to the neurons, which in turn progresses to the secondary damage/death which is coupled to the release of factors that initiate another cycle of oxidative and inflammatory insults. The positive feed back loop may continue until the additional neuronal death (~50% of the remaining of the initial death) combined with the initial loss exceed the amount needed for normal motor control (~80% total loss); thus the PD symptoms, such as postural instability or hypokinesia, occur. This vicious circle helps explain the chronic and prolong nature of PD progression. It is hypothesized that the blockade of COX-2 activity by selective COX-2 inhibitors or deficiency of COX-2 would attenuate the vicious circle and alleviate dopaminergic neurotoxicity by directly reducing COX-2 free radical production as well as by indirectly decreasing microglial activation and subsequent microglia-mediated damage. (Vijitruth, et al.., 2006)

2. HALOPERIDOL – INDUCED ACTIVATION OF MICROGLIA IS ATTENUATED BY TREATMENT WITH MINOCYCLINE

INTRODUCTION

Microglia are resident macrophages in the CNS that become activated upon brain injury. Microglia have been increasingly implicated in dopaminergic neurodegeneration in Parkinson's disease (Francis, et al., 1995; Czlonkowska, et al., 1996; Langston, et al., 1999). Upon activation, microglia release pro-inflammatory mediators into the surrounding environment causing increased inflammation and neural damage. Activated microglia release all cytokines (IL-1 to IL-13), except IL-15 and other inflammatory mediators including nitric oxide and COX-2 (Kim and de Vellis, 2005). Microglia also produce neurotrophic factors, such as NGF, and other molecules required for cellular growth and repair. Depending on the environment and degree of insult, microglia can respond in either a neurotoxic or neuroprotective role. Factors that influence the role played by microglia include cell density, distribution, and the morphological and functional state of these cells in differing brain regions (Lawson, et al., 1990; Ren, et al., 1999).

Haloperidol is known to block dopamine receptors on dopaminergic neurons. Previous findings in our lab have shown that blockade of these receptors leads to induction of apoptosis and upregulation of microglia. In order to prevent the neurotoxicity associated with microglial-induced inflammation, attempts at blocking microglial activation have been made.

Minocycline is a broad-spectrum semisynthetic tetracycline derivative with anti-inflammatory properties that are distinct from its antimicrobial actions (Yrjanheikki, et al., 1999; Wu et al., 2002; Sriram, et al., 2006). Along with its anti-biotic actions, minocycline has been recently found to inhibit microglial activation (Sriram, et al., 2006). Minocycline treatment has been used to ameliorate brain injury in a variety of models, including brain ischemia (Yrjanheikki, et al., 1998, 1999), excitotoxicity (Tikka and Koistinaho, 2001; Tikka, et al., 2001), β-amyloid neurotoxicity (Ryu, et al., 2004), spinal cord injury (Stirling, et al., 2004). Minocycline has also been found to delay onset of amyotrophic lateral sclerosis in a murine model (Kriz, et al., 2002; Van Den Bosch, et al., 2002). Similarly, minocycline has been reported to be neuroprotective against dopaminergic neurotoxicity caused by 6-hydroxydopamine and 1-methyl-4-phenyl-1,2,3,6-tetrahydropyridine (MPTP) (Du, et al., 2001; He, et al., 2001; Wu, et al., 2002). In this study, we have examined the effects of haloperidol and minocycline co-administration on midbrain dopamine neurons.

METHODS

Subjects

Twenty-seven male Sprague-Dawley rats (Charles River, PQ), weighing 200-225 g, were singly housed with free access to food and water, on a 12 hour:12 hour light:dark cycle. Animals were habituated to their new environment for 7 days prior to treatments. Weights were recorded bi-weekly to ensure animal health. All efforts were made to follow McMaster University Central Animal Facility Guidelines and Canadian Council on Animal Care.

Drugs

Haloperidol was obtained from Sabex Inc. (QC, Canada). Minocycline (M-9511) was purchased from Sigma-Aldrich, MO, USA.

Treatment Regimen

Rats were randomly assigned to one of three different treatment groups. Two groups of rats were injected with HAL (2 mg/kg) 10 minutes (n=9 each), prior to decapitation. One of these HAL-treated groups received subcutaneous minocycline (10 mg/kg) injections twice daily at 8am and 8 pm for a total of 20 mg/kg/day. Minocycline was reported to have a 12-hour half life. A control group (n=9) was injected with saline (0.9%) 10 minutes prior to decapitation.

Animal Sacrifice Procedure

After the series of injections, animals were anaesthetized with 40 mg of sodium pentobarbital i.p.. Rats were decapitated and brains were immediately removed. Brains were placed in ice cold 4% paraformaldehyde (pH=7.2) and refrigerated for 1 week prior to sectioning.

Tissue Sectioning

Twenty-four hours prior to sectioning, brains were placed in a 15% sucrose solution for cryoprotection. Consecutive coronal sections (40 μm) were taken at -18°C on a cryostat (Leica CM 1900, Heidelberg, Germany) and placed 3 sections per well in 0.1 M phosphate buffered saline (PBS) in a 24-well plate from caudal to rostral.

Immunohistochemistry

Sections of SN were selected for each animal at bregma -5.3 mm to -5.8 mm. Bregma -5.3 mm corresponds to an area with a thick portion of the third cranial nerve, which provides an anatomical landmark and demarcation between the SNc (Substantia nigra, pars compacta) and the ventral tegmental area (VTA). Bregma -5.8 mm corresponds to an area where accessory tracts of the third nerve cross between the SNc and VTA. These landmarks were used to select appropriate tissue for immunohistochemistry.

Sections were then processed for TH immunohistochemistry. Sections were placed in 0.3% hydrogen peroxide in methanol for 30 minutes and then washed in PBS for 10 minutes. Tissues then entered a solution of 5% normal goat serum for 1 hour to prevent non-specific primary antibody binding. Tissues were subsequently incubated in rabbit anti-TH antibody (1:1500; Chemicon, CA, USA) for 2 hours at room temperature and 70 hours at 4°C. Tissues were washed for 10 minutes in PBS, three more times and incubated in biotinylated goat anti-rabbit IgG secondary antibody (1:400; Vector Laboratories, CA, USA). Tissues were washed three more times in PBS for 10 minutes each, and incubated in ABC for 1 hour to form an avidin/biotin complex. All sections were rinsed three more times in PBS for 10 minutes each and placed into the chromagen, 3, 3-diaminobenzidine tetrachloride (D-5637; Sigma, MO, USA).

The sections were then mounted onto (3-aminopropyl)triethoxysilane-coated slides and covered slipped with D.P.X., neutral mounting medium (317616; Aldrich, WI, USA).

A second set of sections were also processed for TH and CD11b (OX-42), a microglial marker, for fluorescent immunohistochemistry. Sections were placed in 0.3% hydrogen peroxide dissolved in methanol for 30 minutes to destroy endogenous peroxidases present in red blood cells. Tissues were then washed in PBS for 10 minutes. Sections then entered a solution of 10% normal donkey serum for 1 hour to prevent non-specific primary antibody binding. Tissues were then placed in mouse anti-CD11b antibody (1:500; Serotec, NC, USA) for 1 hour at room temperature and 24 hours at 4°C. Tissues were washed for 10 minutes three more times and incubated for 1 hour at room temperature in donkey anti-mouse IgG secondary antibody conjugated to Cy5 (1:800; Chemicon, CA, USA). Sections were kept in the dark for the remaining of the procedure. Tissues were washed three more times for 10 minutes each in PBS and then re-entered a 1 hour incubation in 10% normal donkey serum. Sections were then placed in rabbit anti-TH antibody (1:500; Chemicon, CA, USA) for 1 hour at room temperature and 24 hours at 4°C. Tissues were rinsed in PBS for three 10 minute PBS washes and subsequently incubated in donkey anti-rabbit IgG, conjugated to Cy3 (1:800; Chemicon, CA, USA) for 1 hour at room temperature. The sections were then rinsed three more times for 10 minutes each and mounted onto (3-aminopropyl)triethoxysilane-coated slides and covered slipped with Vectashield mounting medium for fluorescence (Vector Laboratories, CA, USA).

Quantitative Morphometry

Slides were coded and the treatment regimen was blinded to the person quantifying the section. Tissues were manually counted for TH- and OX-42-immunoreactive cells at 20x magnification for both the left and right hemispheres. Due to the high magnification, the entire SN could not be seen in the field of the microscope. SN was divided into three areas (lateral, central and medial) for counting. When the cell counting was completed, slides were decoded and arranged due to treatment group. The cell counts were then averaged within groups and a mean ± standard error of the mean (SEM) was calculated. Cell diameters of TH-immunoreactive cells were measured in both the x and y directions, with the aid of MetaMorph software.

Statistical Analysis

The cell count data and the cell diameter data were analyzed using a one-way analysis of variance (ANOVA), followed by post-hoc Tukey test. Significance was determined at the $p < 0.05$ level. All statistics were performed using SPSS version 13.0.

RESULTS

SN

Analysis of cell counts revealed HAL induced a decrease in TH-immunoreactivity, $F(2,25) = 25.3$, $p < 0.001$. HAL produced a significant 28% decrease of TH-immunoreactive neurons 10 minutes post-injection ($p < 0.001$) compared to saline-injected animals. Minocycline partially protected against HAL-induced TH neuron downregulation. There was a significant difference seen between sham-injected animals and minocycline treated animals ($p = 0.025$) and a significance level less than $p = 0.001$ was seen between the 10 minute HAL treated animals and minocycline and HAL-treated animals. Cell counts were adjusted for cell sizes by the Abercrombie formula, as seen in Appendix I.

Cell Counts for Substantia Nigra processed for TH-immunohistochemistry

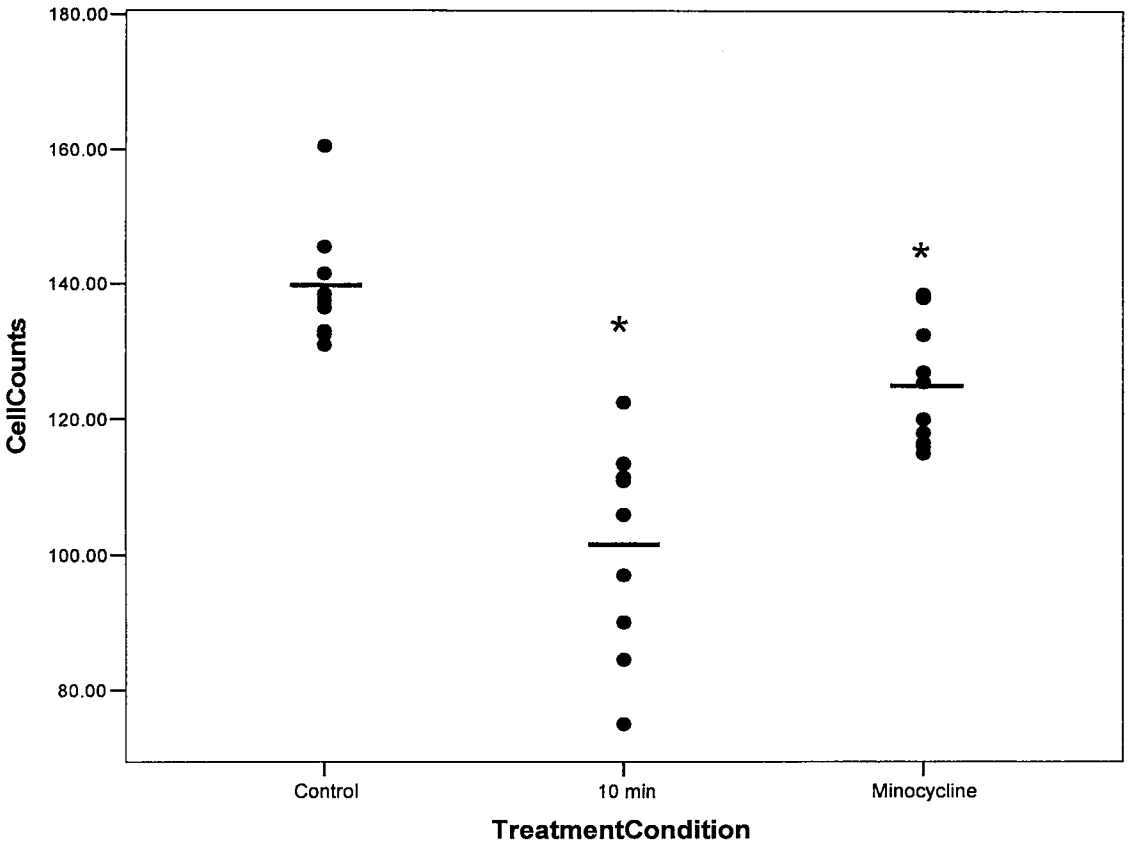

Figure 27 – Scatter plot of TH-positive cells in the substantia nigra per 40 μm hemi section. Each dot represents the mean number of TH-positive cell counts for one animal, with the horizontal line representing the group mean. TH-positive cell counts were significantly decreased in the SN of 10 min. HAL treated animals by 28% ($p < 0.01$).

Treatment Regimen	Control	10 min HAL	Minocycline + 10 min HAL
Mean ± S.E.M.	139.6 ± 3.0	101.2 ± 5.2	124.7 ± 2.9

Table 6 – Mean cell counts ± S.E.M. for TH-positive cells in the SN.

Photomicrographs (20x magnification) of SN processed for TH-immunohistochemistry

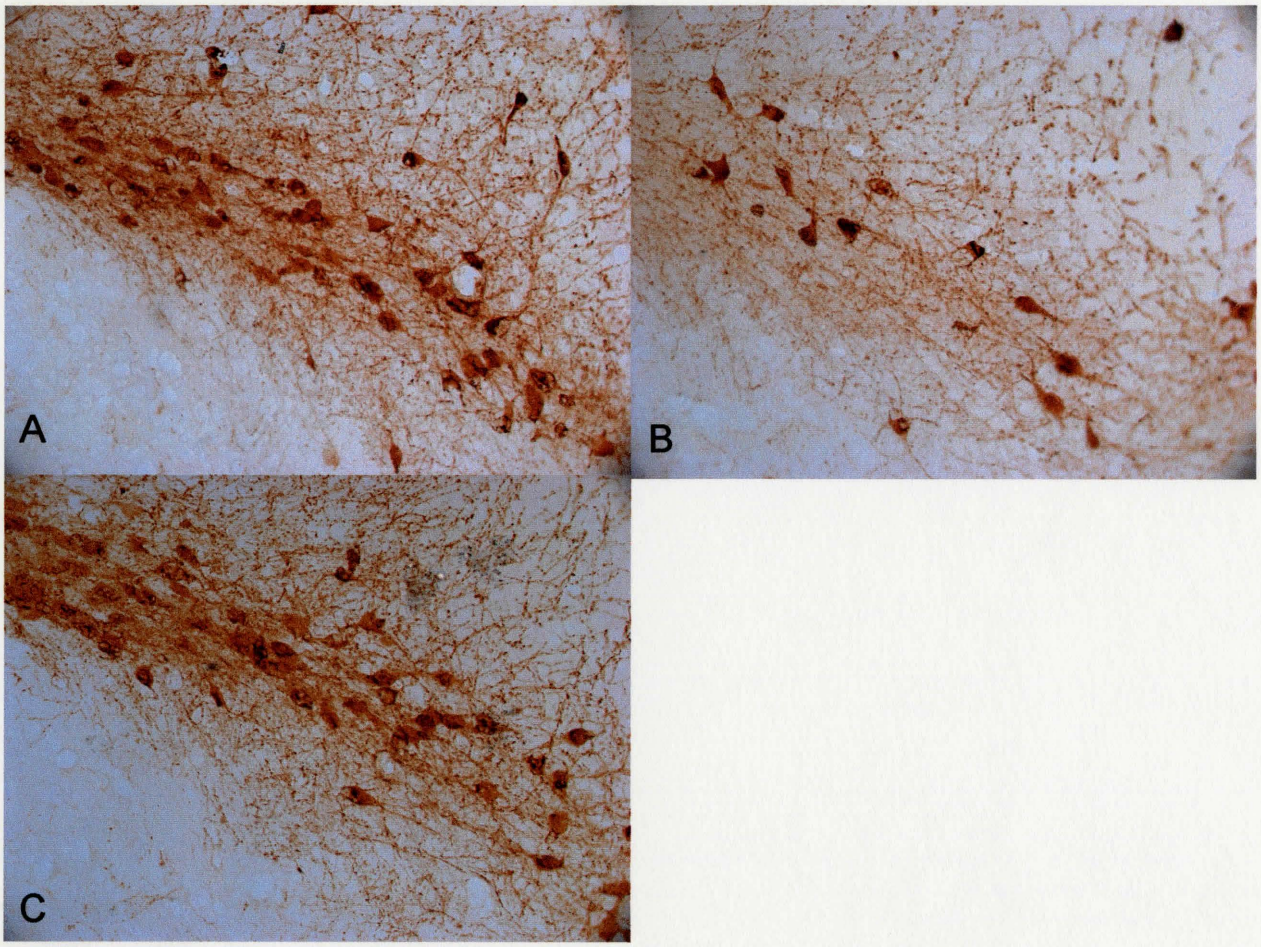

Figure 28 – Photomicrographs (20x magnification) of TH-positive immunoreactivity in the SN for each group taken at bregma -5.3mm. There was a significant decrease in TH-positive cell counts in the 10 min. HAL-treated group.
A: Control
B: 10 min. HAL
C: Minocycline + 10 min. HAL

VTA

Analysis of cell counts revealed that HAL induced no significant changes in TH-immunoreactivity, $F(2,25) = 3.10$, $p = 0.063$. HAL produced no significant reduction in TH-positive cell counts compared to saline-injected animals, although the HAL-treated animals tended toward a decrease. A non-significant 5% reduction in TH-immunoreactive cells was seen in the HAL-treated animals compared to saline-injected controls. There was a non-significant 11% increase seen in TH-immunoreactive cells with minocycline and HAL treatment co-administration when compared to the HAL treated animals.

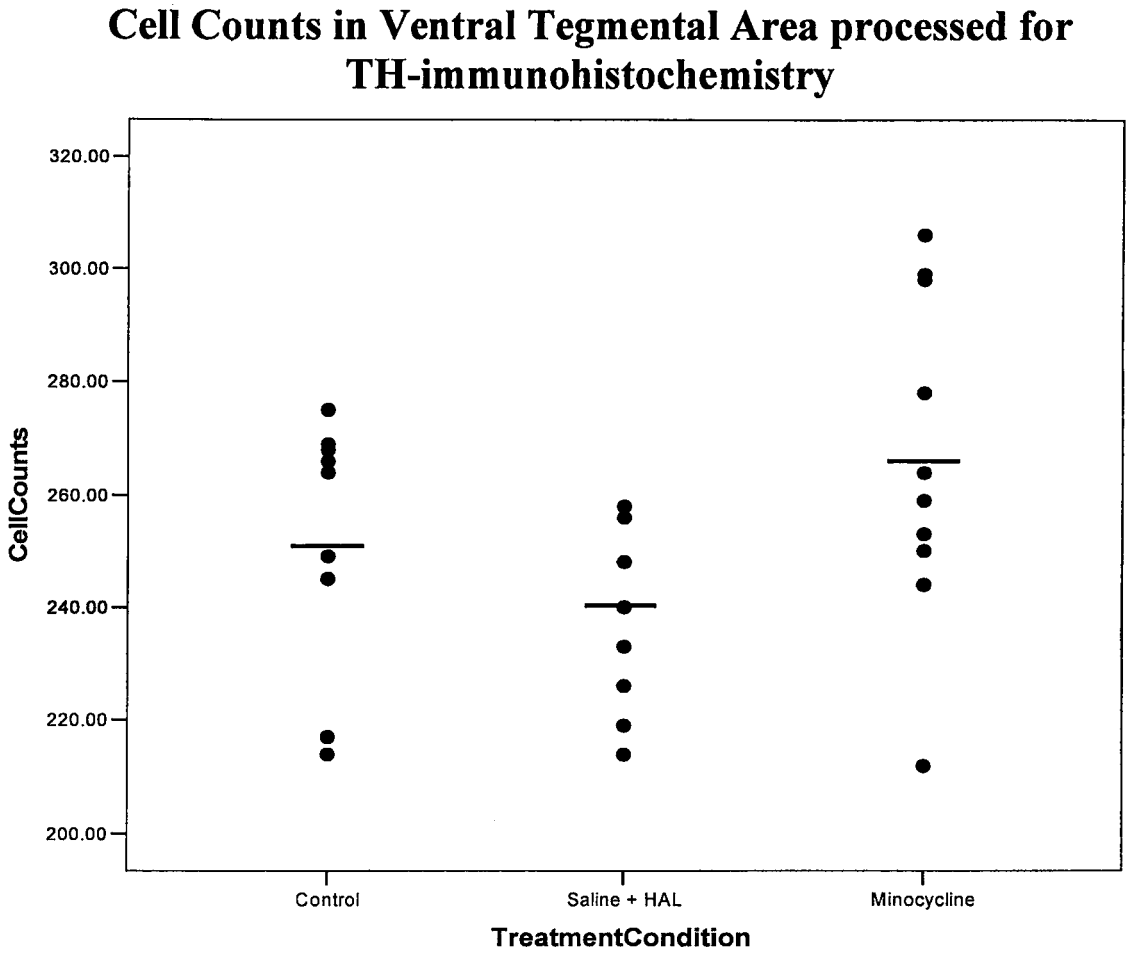

Figure 29 – Number of TH-positive cells in the ventral tegmental area per 40 μm hemi section. Each dot represents the mean number of TH-positive cell counts for one animal, with the horizontal line representing the group mean. TH-positive cell counts were not significantly decreased in the VTA of HAL-treated rats.

Treatment Regimen	Control	10 min. HAL	Minocycline + 10 min. HAL
Mean ± S.E.M.	251.9 ± 7.6	239.1 ± 5.7	266.3 ± 9.3

Table 7 – Mean cell counts ± S.E.M. for TH-positive cells in the VTA.

Photomicrographs (20x magnification) of SN processed for TH-immunohistochemistry

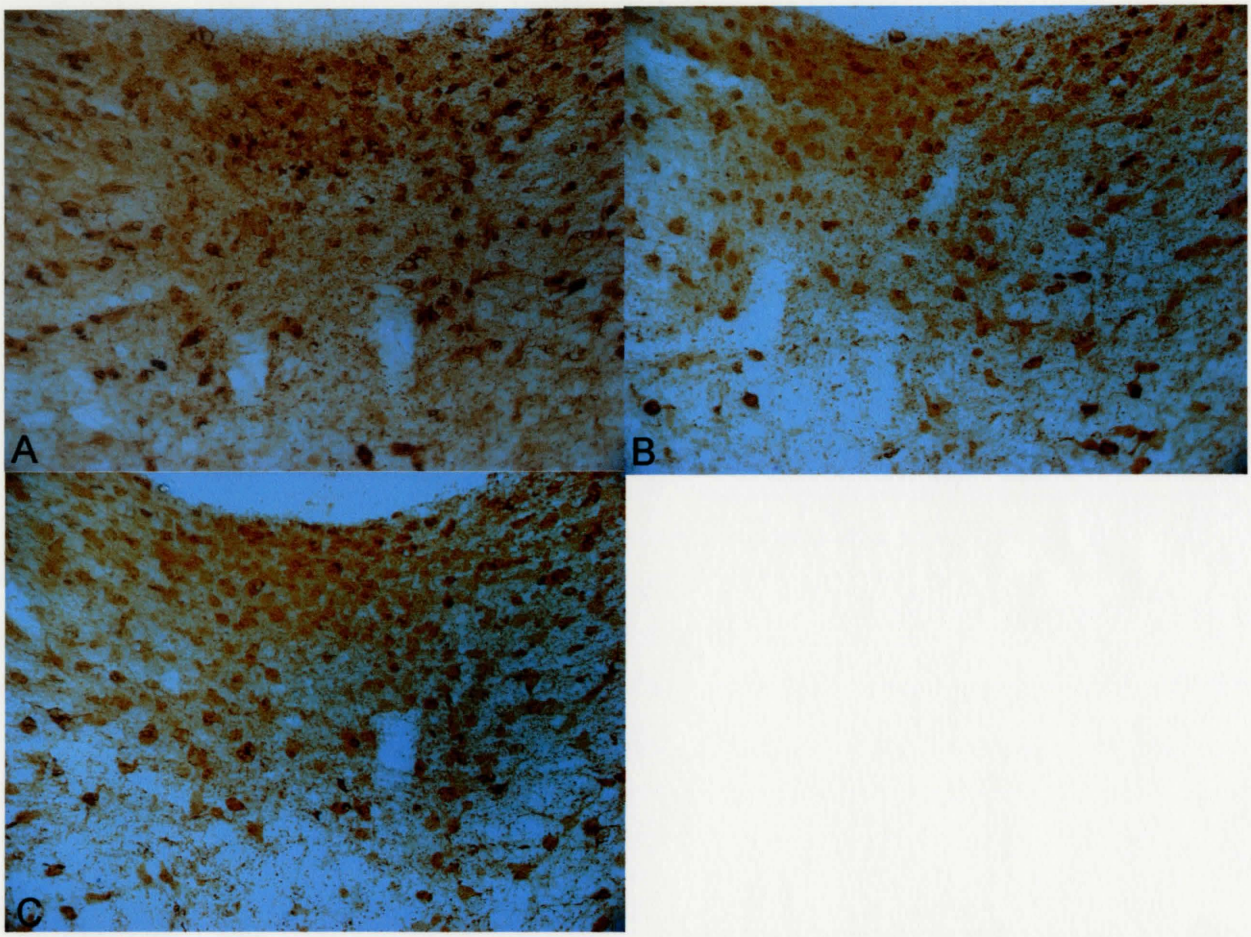

Figure 30 – Photomicrographs (20x magnification) of TH-positive immunoreactivity in the VTA for each group taken at bregma -5.3mm. There was no significant changes in TH-positive cell counts.
A: Control
B: 10 min. HAL
C: Minocycline + 10 min. HAL

TH & OX-42 Double Label

SN

TH counts

Analysis of cell counts revealed that HAL induced significant downregulation of TH-immunoreactivity, $F(2,25) = 19.3$, $p < 0.001$. The 10 minute HAL treatment produced a significant 21% reduction in TH-positive cell counts compared to sham-treated animals ($p < 0.02$). Minocycline-treated animals showed no significant decrease in TH-immunoreactive cell counts compared to sham animals, although a 23% difference was seen between the minocycline-treated animals and the 10 minute HAL treated animals ($p < 0.001$).

Cell counts for Substantia Nigra processed for TH fluorescent immunohistochemistry

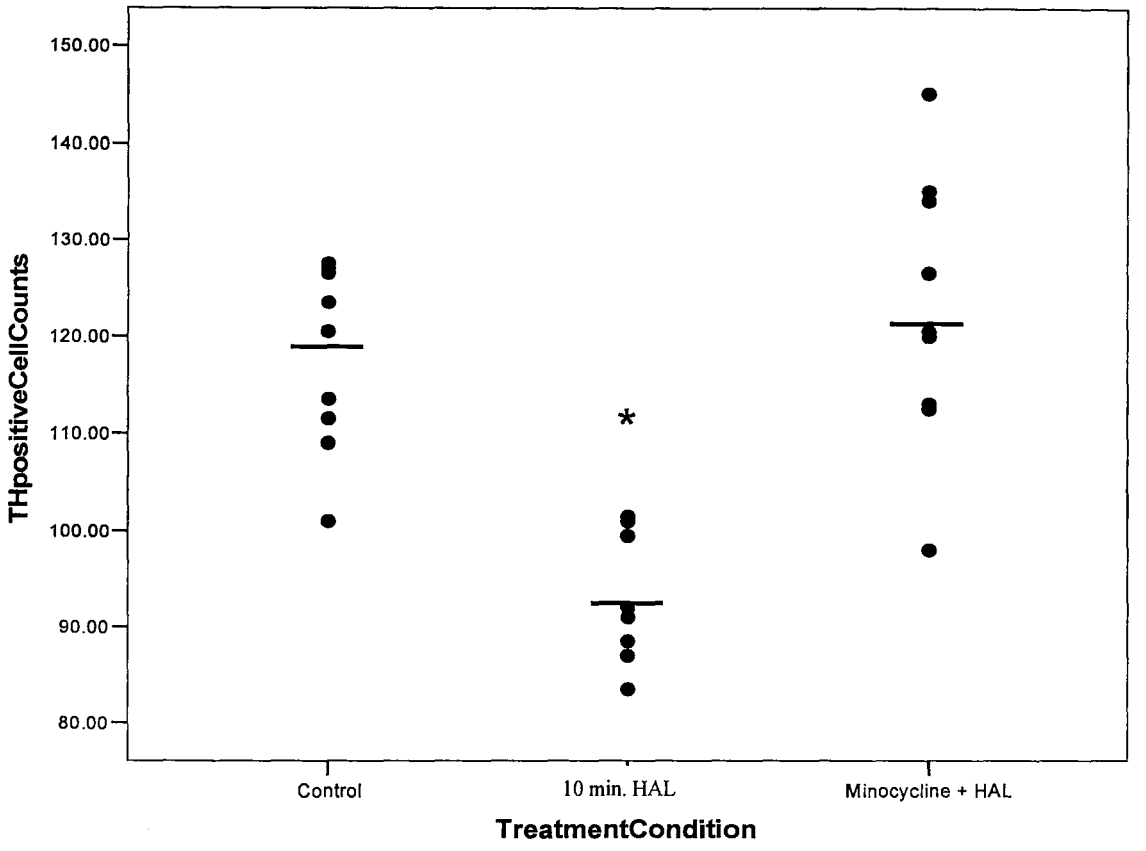

Figure 31 – Scatter plot of TH-positive cells in the substantia nigra per 40 μm hemi section. Each dot represents the mean number of TH-positive cell counts for one animal, with the horizontal line representing the group mean. TH-positive cell counts were significantly decreased in the SN of 10 min. HAL-treated animals by 21% ($p < 0.02$). Treatment with minocycline completely blocked the TH downregulation by HAL.

Treatment Regimen	Control	10 min. HAL	Minocycline + 10 min. HAL
Mean ± S.E.M.	117.8 ± 3.1	93.7 ± 2.3	121.2 ± 4.5

Table 8 – Mean cell counts ± S.E.M. for TH-positive cells in the SN.

Confocal images (20x magnification) of SN processed for TH immunofluorescence

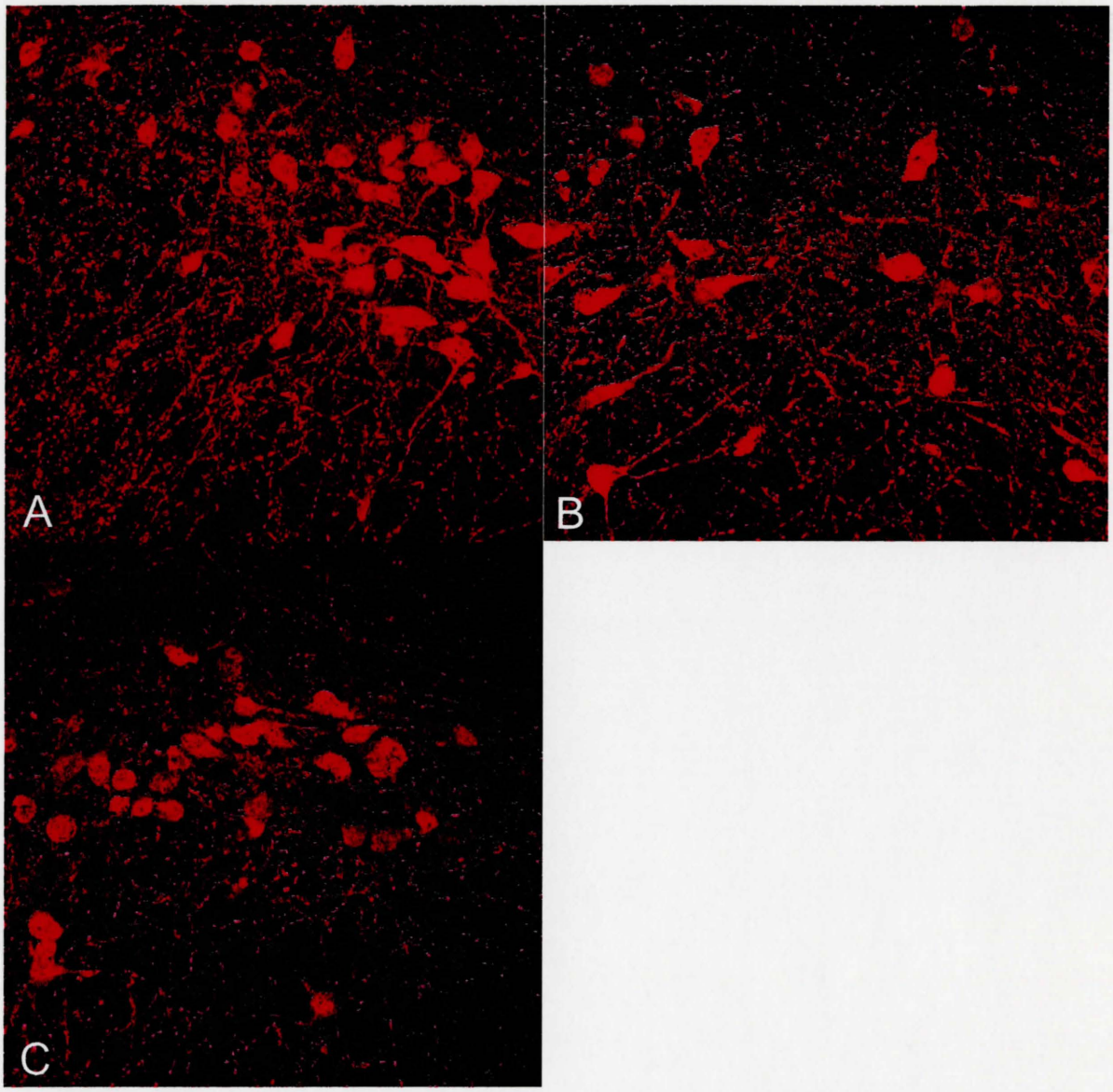

Figure 32 – Fluorescent images of TH-labelled cells of the SN taken per drug treatment group as visualized on the confocal microscope at 20x magnification. A significant decrease was seen in the 10 minute HAL-treated animals.
A: Control
B: 10 min. HAL
C: Minocycline + 10 min. HAL

OX-42 counts

Analysis of cell counts revealed a significant difference in OX-42 immunoreactivity after HAL treatment, $F(2,25) = 39.8$, $p < 0.001$. HAL treatment produced a significant ($p < 0.01$) 33% increase in OX-42 positive cells compared to control animals. A significant 22% decrease in OX-42 immunoreactivity ($p < 0.03$) was seen in animals treated both with 10 minute HAL and minocycline compared to control animals. OX-42 positive cell counts in the 10 minute HAL treatment were also significantly different from minocycline treated rats ($p < 0.001$). A 49% decrease in OX-42 immunoreactive cell counts was seen in the minocycline treated group compared to the 10 minute HAL treatment condition.

Activated microglial cell counts for SN processed for OX-42-immunofluorescence

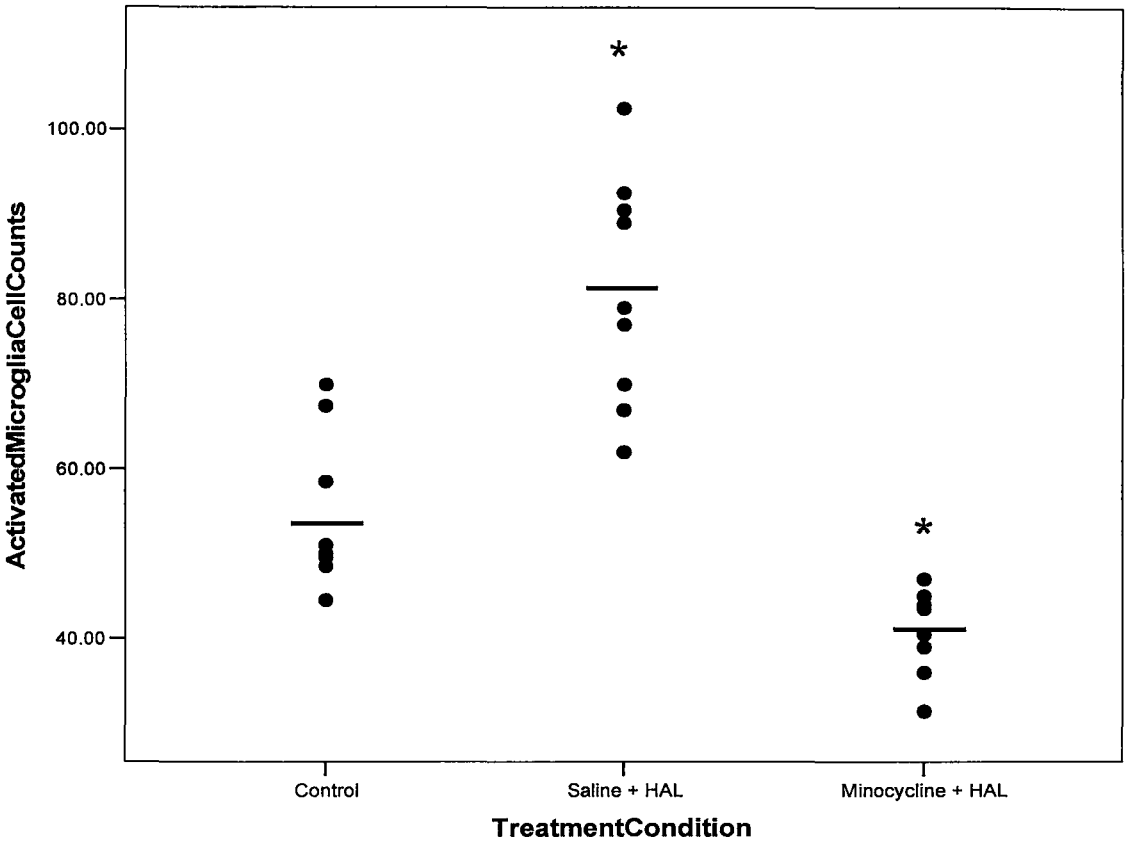

Figure 33 – Scatter plot of OX42-positive cells in the substantia nigra per 40 μm hemi section. Each dot represents the mean number of OX-42-positive cell counts for one animal, with the horizontal line representing the group mean. OX-42-positive cell counts were significantly increased in the SN of HAL-treated animals by 33% ($p < 0.01$). This effect was completely blocked with minocycline.

Treatment Regimen	Control	10 min. HAL	Minocycline + 10 min. HAL
Mean ± S.E.M.	54.3 ± 3.3	81.1 ± 4.5	42.1 ± 1.7

Table 9 – Mean cell counts ± S.E.M. for OX-42-positive cells in the SN.

Confocal images (20x magnification) of SN processed for TH-immunofluorescence

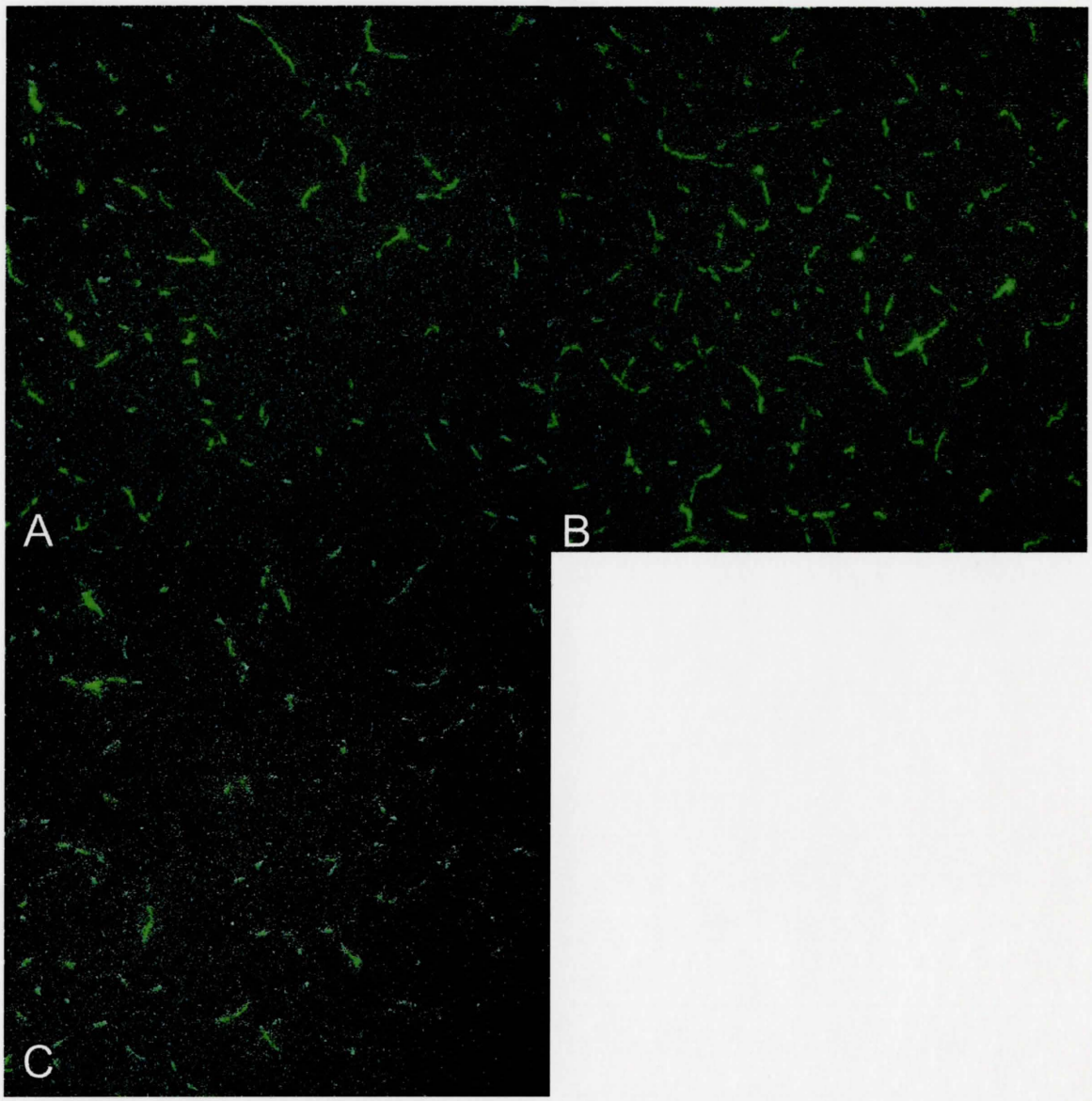

Figure 34 – Fluorescent images of OX-42-labelled cells of the SN taken per drug treatment group as visualized on the confocal microscope at 20x magnification. A significant increase was seen in the 10 min. HAL treated animals. This increase was blocked by treatment with minocycline.
A: Control
B: 10 min. + HAL
C: Minocycline + 10 min. HAL

TH cell diameter

SN

A significant difference was seen between treatment groups, $F(2,25) = 3.71$, $p = 0.039$. 10 minute HAL-treated animals had a significantly higher cell size compared to control animals ($p = 0.037$). Cell sizes in all other groups were not significantly different from each other. See figure 28.

Mean cell diameters in the SN processed for TH-immunohistochemistry

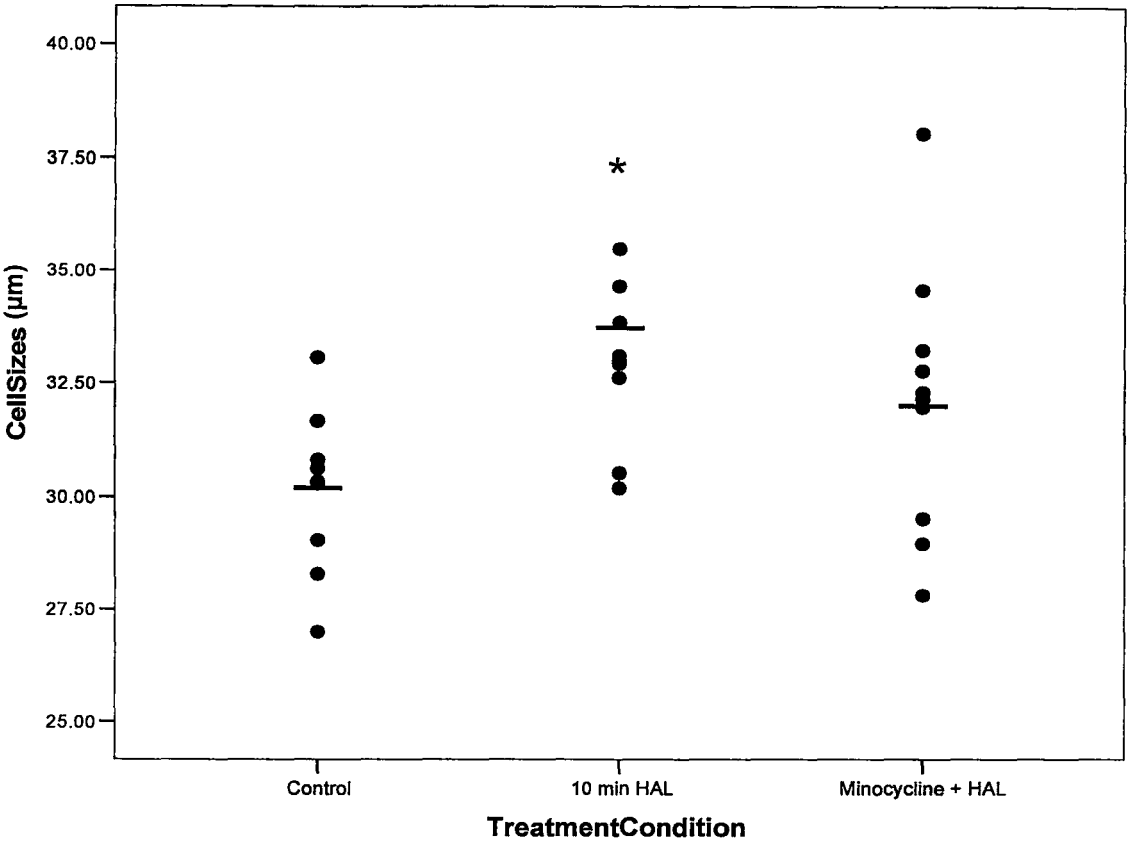

Figure 35 – Mean cell diameter (µm) of TH-positive cells of the substantia nigra per 40 µm hemi section. Each dot represents the mean diameter of 10 TH-positive cells for one animal of, with the horizontal line representing the group mean. There was a significant difference seen between controls and 10 minute HAL-treated animals ($p = 0.037$).

Treatment Regimen	Control	10 min. HAL	Minocycline + 10 min. HAL
Mean ± S.E.M.	30.1 ± 0.60	32.9 ± 0.57	32.1 ± 0.93

Table 10 – Mean cell diameter ± S.E.M. for TH-positive cells in the SN.

DISCUSSION

This study demonstrates that treatment with haloperidol induces downregulation of TH neurons in the substantia nigra and upregulation of activated microglial cells. Treatment with minocycline prevents this change in the microglia and subsequently spares the neural downregulation in the substantia nigra. However, treatment with haloperidol in the ventral tegmental area does not afford the same toxicity to TH-immunoreactive neurons as seen in the substantia nigra.

By blocking the microglial response, TH neurons were spared. Therefore, microglia may mediate the TH-neuron downregulation by haloperidol. The mechanism of this phenomenon has not been clarified, although recent attention has been brought to anti-psychotic medications and their alteration of the immune response. Schizophrenic patients typically have an altered cytokine profile, including increased IL-6 and IL-8 in the serum. There have been reports that typical antipsychotic medications, such as haloperidol, normalize serum IL-1, IL-6 and IL-6R levels in schizophrenic patients (Maes, et al., 1995, 1997). However, treatment with haloperidol has recently been shown to not decrease the levels of either IL-6 or IL-8 upon 12 week treatment (Pollmacher, et al., 1997; Zhang, et al., 2004). Taken together, the increased levels of cytokines could activate microglia in the substantia nigra, causing further cytokine release. Dopamine neurons would be under chronic stress both due to continual dopamine receptor blockade and increased cytokines in their environment. This could potentially induce the loss TH-immunoreactive neurons loss seen in this study.

Gliosis has also been associated with increased concentrations of MAO-B within glial cells (Levitt, et al., 1982; Westlund, et al., 1985). Increased oxidation of dopamine by MAO-B may produce levels of oxygen radicals that are sufficient to trigger oxidative damage of dopaminergic neurons (Cohen, 1990; Gerlach, et al., 1996).

Although cell counts in the SN were significantly decreased with HAL-treatment, the ventral tegmental area cell counts were not. This finding is not surprising once the distribution of microglia in the brain is noted. Microglia, in mouse brain, are densely populated in the hippocampus, olfactory telencephalon, basal ganglia and substantia nigra (Lawson, et al., 1990). Outside of these areas, the microglial populations are less dense. Therefore, activated microglia in densely populated areas would release an abundance of toxic inflammatory mediators creating a toxic environment for neurons to survive in. Another study also noted that microglia also differentially express mRNA of inflammatory mediators. For example, microglia in the hippocampus express significantly higher mRNA levels of TNF-α compared to cerebellum and cortex microglia (Ren, et al., 1999). Therefore, it is possible that the production levels of TNF-α and other cytokines by microglia could vary between the VTA and the substantia nigra. This would induce differing microenvironments for the dopamine neurons, causing specific dopaminergic damage to neurons in the substantia nigra.

Another result of this study was that haloperidol induced an increase in cell size in the substantia nigra. This increase in cell size has been noted in melanin-containing neurons of the substantia nigra of ageing human brain tissue (Cabello, et al., 2002). This result has also been found in a study performed by Cruz-Sanchez, et al. 1997, who performed a detailed Golgi stain and

measured cell size of melanin-producing neurons in the substantia nigra. He too reported a swelling and beading of dendritic branches and distorted cell body shape. The increased cell size has been postulated to be due to an inherent loss of dopaminergic neurons in age. The loss of dopaminergic cells would lead to a decrease in dopamine production. Therefore, the remaining cells might try to compensate for the lack of dopamine and begin overproducing the neurotransmitter, causing the cell to swell. Haloperidol has been known to induce apoptosis in dopaminergic neurons (previous lab. finding). The results of this study suggest that blocking microglial activity partially protects against haloperidol-induced neurotoxicity. Therefore, microglia could be releasing toxic inflammatory mediators, thus causing dysregulated protein synthesis and metabolism in dopamine neurons. This could cause improper dopamine release and metabolism, causing cellular swelling. Vacuoles may also be present in the cytoplasm, since the cells may be undergoing a cell death process, thereby increasing cellular size.

Andersson, et al. 2002 also found that either a 4-month or an 8-month administration HAL increased rat striatal volumes compared to control animals. It is proposed that long term dopamine receptor blockade induces hypertrophy, regeneration, activation and change in the number of striatal synapses (Muller and Seeman, 1977; Benes, et al., 1983; Meshul, et al., 1994; Roberts, et al., 1995). Since striatal synapses originate from cell bodies in the SN, we can propose that there may also be alterations in the dopamine cell bodies. In Benes, et al., 1983, no change in cell size was found in the SN, although animals were treated with chronic HAL. In our study, animals were only treated with HAL for 10 minutes. In a long term treatment, cells could adjust to receptor blockade by altering synapses, for example, as found in the Benes study. In an acute treatment of HAL, few cellular alterations would be completed. Therefore, the cells

may swell upon acute treatment of HAL and adjust to receptor blockade upon chronic administration.

Overall, microglial activation can be blocked by minocycline. The inactivation of microglia has been shown to partially protect against TH-downregulation in the substantia nigra. The use of minocycline may be a potential intervention that can be used to prevent inflammation in Parkinson's disease or be used along with haloperidol to prevent HAL-induced parkinsonism.

3. HALOPERIDOL – INDUCED DOWNREGULATION OF DOPAMINE NEURONS IN THE SUBSTANTIA NIGRA IS ATTENUATED BY CAFFEINE AND NICOTINE

INTRODUCTION

Antipsychotic drugs (APDs) are the mainstay treatment for schizophrenia. These drugs are associated with extrapyramidal side effects, including tardive dyskinesia, akathesisa, dystonia and parkinsonism. The neurobiological basis of these effects is not clearly understood. Previous results from our lab have shown TH downregulation, microglial activation and apoptosis of midbrain dopamine neurons upon treatment with HAL. Epidemiological evidence has shown that nicotine has a protective effect against dopamine neuron loss in Parkinson's disease (Gorell, et al., 1999; Hernan, et al., 2002; Pauly, et al., 2004;). Similar epidemiological evidence has also shown that caffeine has a protective effect against dopamine neuron loss in Parkinson's disease (Ross, et al., 2000; Ascherio, et al., 2001; Hernan, et al., 2002). Taken together, researchers have begun looking at mechanisms of protecting dopamine neurons from the risk of Parkinson's disease.

Adenosine receptors are present on dopaminergic cells of the substantia nigra (Chen, et al., 2001). Caffeine, a non-selective adenosine receptor antagonist, is proposed to directly stimulate dopamine release in the striatum, thereby relieving the side effects induced by APDs (Da Cunha, et al., 2002). Epidemiological evidence also shows that Schizophrenic patients drink more coffee than the general population (Hughes, et al., 1998). The average intake of caffeine per day for the general population is around 210 mg, whereas studies have found Schizophrenic patients

intake approximately 500 mg per day (Hughes, et al., 1998). Taken together, the increased caffeine consumption by these patients could be due to "self-medication" to reduce their EPS.

Microglial cells also have adenosine receptors present on their surface (Hasko, et al., 2005). Specifically, microglia express A_1, A_{2A}, and A_3 receptor subtypes (Hasko, et al., 2005). Each of the subtypes has been noted to have differing functions. Both the A_1 and A_{2A} receptor subtypes promote microglial proliferation, whereas only A_{2A} subtypes promote NGF release and upregulate COX-2 expression (Hasko, et al., 2005). Because many of the different subtypes having varying functions, the action taken by the microglial cells depends on both the receptor subtype and the surrounding environment.

Microglial cells also have nicotinic ACh receptors present on their surface (Shytle, et al., 2004). Nicotine, a nicotinic receptor agonist, has been found to inhibit LPS-induced TNF release in murine microglial cells by activating the α7 receptor subtype and signaling through a MAP kinase intracellular pathway (Shytle, et al., 2004; Suzuki, et al., 2006). Epidemiological evidence has shown that nicotine has been found to be neuroprotective in dopamine neuron loss in both Parkinson's disease and Schizophrenia (Gorell, et al., 1999; Hernan, et al., 2002; Pauly, et al., 2004; Ripoll, et al., 2004; Kuehn, 2006).

Therefore, we investigated the potential for caffeine and nicotine to inhibit microglial activation and show a neuroprotective role for dopaminergic neurons of the substantia nigra.

METHODS

Subjects

Forty-three male Sprague-Dawley rats (Charles River, PQ), weighing 200-225 g, were singly housed with free access to food and water, on a 12 hour:12 hour light:dark cycle. Animals were habituated to their new environment for 7 days prior to treatments. Weights were recorded bi-weekly and adjustments were made to drug dosages. Animal health was monitored throughout the experiment. All efforts were made to follow McMaster University Central Animal Facility Guidelines and Canadian Council on Animal Care.

Drugs

Haloperidol was obtained from Sabex Inc. (QC, Canada). Both caffeine (CO750) and (-) nicotine (N-5260) were purchased from Sigma-Aldrich (MO, USA).

Treatment Regimen

Rats were randomly assigned to one of six different groups. One group of rats (n=9) was pre-treated with caffeine (15 mg/kg/day) in the drinking water 10 days prior to 3 days of intraperitoneal injections with HAL (2 mg/kg/day). A control condition (n=5) for the caffeine was designed as caffeine (15 mg/kg) in the drinking water with 3 days of sham intraperitoneal injections prior to decapitation. Another group of rats (n=10) was pre-treated with 5-daily subcutaneous nicotine injections at 0.6 mg/kg for a total of 3 mg/kg/day for 5 days prior to intraperitoneal injection with HAL (2 mg/kg/day), due to a 2-hour half-life of nicotine. HAL was given for 3 days prior to decapitation. Another group of rats (n=5) received 5-daily subcutaneous nicotine injections (0.5 mg/kg each) with 3 days of intraperitoneal saline (0.9%) injections. Another group (n=9) received sham subcutaneous injections for 3 days prior to the 3

days of HAL (2 mg/kg) injections. The last group (n=5) received sham subcutaneous injections for 3 days prior to 3 days of sham intraperitoneal (i.p.) injections. Injection sites were rotated to avoid the development of adhesions.

Animal Sacrifice Procedure

After the series of injections, animals were anaesthetized with 40 mg of sodium pentobarbital i.p.. Rats were decapitated and brains were immediately removed. Brains were placed in ice cold 4% paraformaldehyde (pH=7.2) and refrigerated for 1 week prior to sectioning.

Tissue Sectioning

Twenty-four hours prior to sectioning, brains were placed in a 15% sucrose solution for cryoprotection. Consecutive coronal sections (40 μm) were taken at -18°C on a cryostat (Leica CM 1900, Heidelberg, Germany) and placed 3 sections per well in 0.1 M phosphate buffered saline (PBS) in a 24-well plate from caudal to rostral.

Immunohistochemistry

Sections of SN were selected for each animal at bregma -5.3 mm to -5.8 mm. Bregma -5.3 mm corresponds to an area with a thick portion of the third cranial nerve, which provides an anatomical landmark and demarcation between the SNc (Substantia nigra, pars compacta) and the ventral tegmental area (VTA). Bregma -5.8 mm corresponds to an area where accessory tracts of the third nerve cross between the SNc and VTA. These landmarks were used to select appropriate tissue for immunohistochemistry.

Sections were then processed for TH immunohistochemistry. Sections were placed in 0.3% hydrogen peroxide in methanol for 30 minutes and then washed in PBS for 10 minutes. Tissues then entered a solution of 5% normal goat serum for 1 hour to prevent non-specific primary antibody binding. Tissues were subsequently incubated in rabbit anti-TH antibody (1:1500; Chemicon, CA, USA) for 2 hours at room temperature and 70 hours at 4°C. Tissues were washed for 10 minutes in PBS, three more times and incubated in biotinylated goat anti-rabbit IgG secondary antibody (1:400; Vector Laboratories, CA, USA). Tissues were washed three more times in PBS for 10 minutes each, and incubated in ABC for 1 hour to form an avidin/biotin complex. All sections were rinsed three more times in PBS for 10 minutes each and placed into the chromagen, 3, 3-diaminobenzidine tetrachloride (D-5637; Sigma, MO, USA). The sections were then mounted onto (3-aminopropyl)triethoxysilane-coated slides and covered slipped with D.P.X., neutral mounting medium (317616; Aldrich, WI, USA).

A second set of sections were also processed for TH and CD11b (OX-42), a microglial marker, fluorescent immunohistochemistry. Sections were placed in 0.3% hydrogen peroxide dissolved in methanol for 30 minutes to destroy endogenous peroxidases present in red blood cells. Tissues were then washed in PBS for 10 minutes. Sections then entered a solution of 10% normal donkey serum for 1 hour to prevent non-specific primary antibody binding. Tissues were then placed in mouse anti-CD11b antibody (1:500; Serotec, NC, USA) for 1 hour at room temperature and 24 hours at 4°C. Tissues were washed for 10 minutes three more times and incubated for 1 hour at room temperature in donkey anti-mouse IgG secondary antibody conjugated to Cy5 (1:800; Chemicon, CA, USA). Sections were kept in the dark for the remaining of the procedure. Tissues were washed three more times for 10 minutes each in PBS

and then re-entered a 1 hour incubation in 10% normal donkey serum. Sections were then placed in rabbit anti-TH antibody (1:500; Chemicon, CA, USA) for 1 hour at room temperature and 24 hours at 4°C. Tissues were rinsed in PBS for three 10 minute PBS washes and subsequently incubated in donkey anti-rabbit IgG, conjugated to Cy3 (1:800; Chemicon, CA, USA) for 1 hour at room temperature. The sections were then rinsed three more times for 10 minutes each and mounted onto (3-aminopropyl)triethoxysilane-coated slides and covered slipped with Vectashield mounting medium for fluorescence (Vector Laboratories, CA, USA).

Quantitative Morphometry

Slides were coded and the treatment regimen was blinded to the person quantifying the section. Tissues were manually counted for TH- and OX-42-immunoreactive cells at 20x magnification for both the left and right hemispheres. Due to the high magnification, the entire SN could not be seen in the field of the microscope. The SN was divided into three areas (lateral, central and medial) for counting. When the cell counting was completed, slides were decoded and arranged due to treatment group. The cell counts were then averaged within groups and a mean ± standard error of the mean (SEM) was calculated. Cell sizes were also quantified for TH-immunoreactive cells by measuring the diameter of the cells in both the x and y directions, with the aid of MetaMorph software.

Statistical Analysis

The cell count data and cell diameter data were analyzed using a one-way analysis of variance (ANOVA), followed by *post-hoc* Tukey test. Significance was determined at the $p < 0.05$ level. All statistics were performed using SPSS version 13.0.

RESULTS

TH counts

SN

Analysis of cell counts produced a highly significant effect for $F(3,36) = 5.4$, $p = 0.004$. HAL produced a highly significant 21% reduction in TH-positive cell counts ($p < 0.002$) compared to controls. Caffeine and nicotine alone had no effect on dopaminergic cell counts compared with sham-pre-treated controls. Therefore, these controls were collapsed into the control and saline injected group. The HAL-treated animals were significantly different from both caffeine and HAL-treated animals ($p = 0.033$) and nicotine and HAL-treated animals ($p = 0.043$). Caffeine and HAL and nicotine and HAL-treated animals were not significantly different from control animals. Therefore, caffeine and nicotine independently blocked TH-downregulation by HAL. Cell counts were adjusted for cell sizes by the Abercrombie formula, as seen in Appendix I.

Cell counts for SN processed for TH-immunohistochemistry

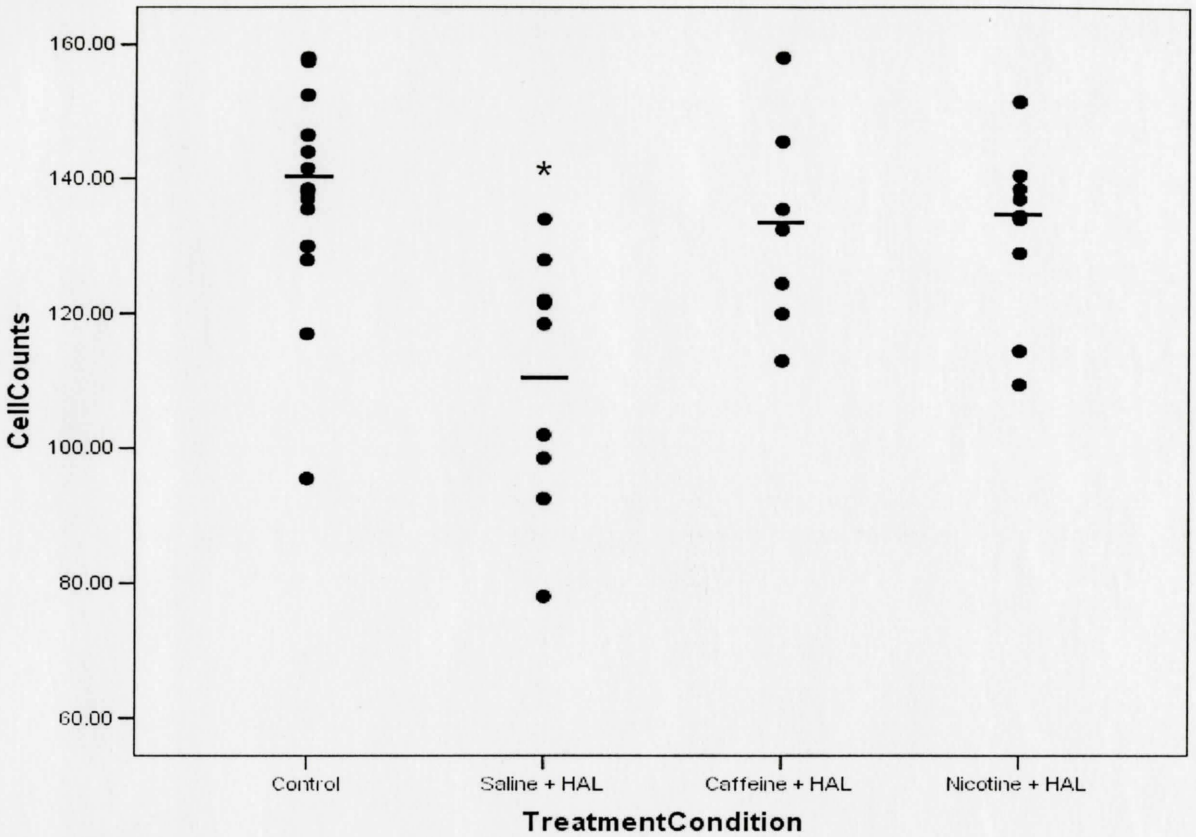

Figure 36 – Scatter plot of TH-positive cells in the substantia nigra per 40 μm hemi section. Each dot represents the mean number of TH-positive cell counts for one animal, with the horizontal line representing the group mean. TH-positive cell counts were significantly decreased in the SN of saline + HAL-treated rats by 21% ($p < 0.002$). This effect was completely blocked with caffeine or nicotine.

Treatment Regimen	Control	Saline + HAL	Caffeine + HAL	Nicotine + HAL
Mean ± S.E.M.	139.8 ± 2.3	110.6 ± 6.2	132.7 ± 5.8	132.1 ± 4.3

Table 11 – Mean cell counts ± S.E.M. for TH-positive cells in the SN.

Photomicrographs (20x magnification) of SN processed for TH-immunohistochemistry

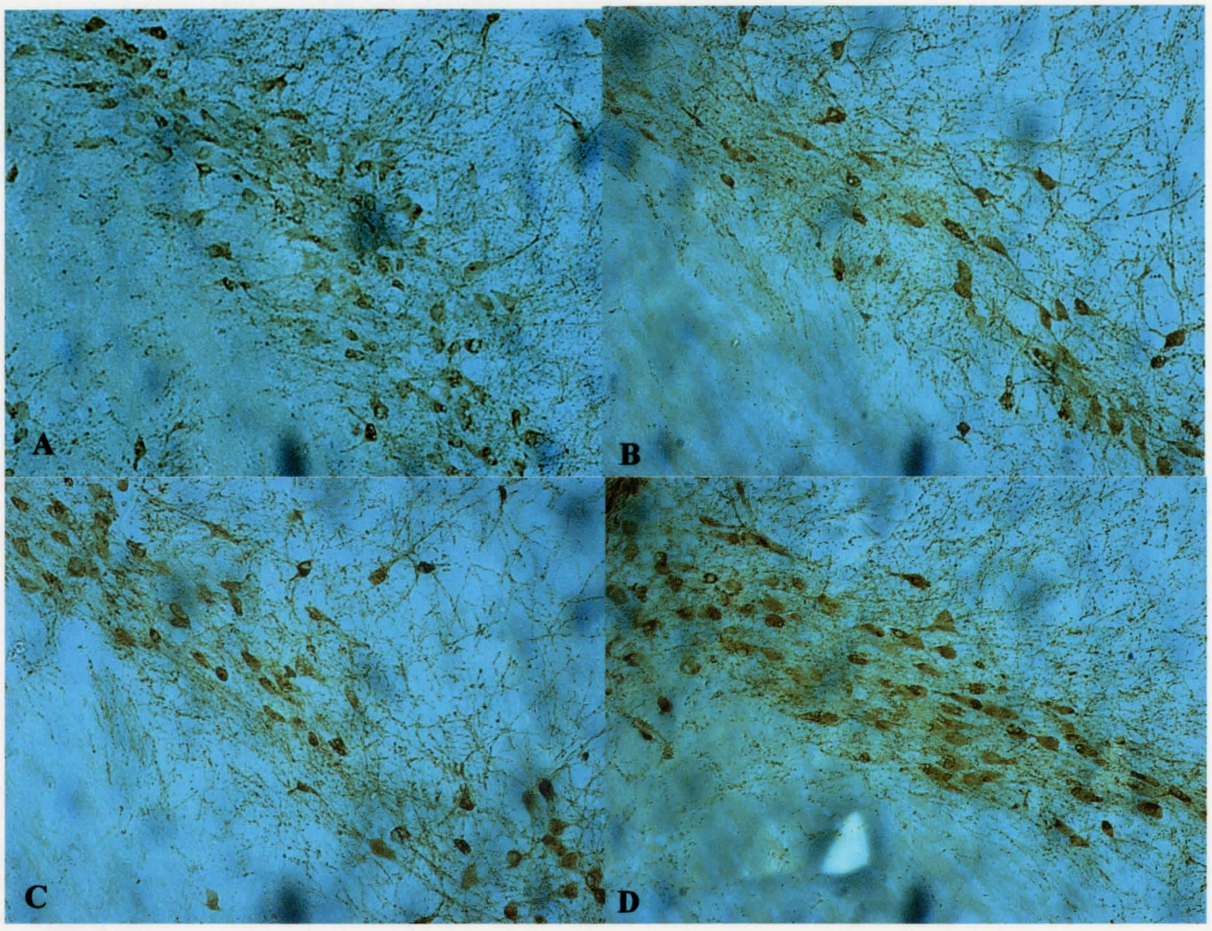

Figure 37 – Photomicrographs (20x magnification) of TH-positive immunoreactivity in the SN for each group taken at bregma -5.3mm. There was a significant decrease in TH-positive cell counts in the saline + HAL treated group.
A: Control
B: Saline + HAL
C: Caffeine + HAL
D: Nicotine + HAL

VTA

Analysis of cell counts revealed that HAL produced no significant effect on TH cells, $F(3,35) = 2.04$, $p = 0.127$. There was no significant reduction in TH-positive cell counts compared to saline-injected animals, although the HAL treated animals were tending towards a decrease. A non-significant 25% reduction in TH-immunoreactive cells compared to saline-injected controls was seen. There was a slight increase seen when the nicotine and HAL treated animals (7%) and caffeine and HAL treated animals (9%) were compared to control animals. These values were not significantly different from control values. Cell counts were adjusted for cell sizes by the Abercrombie formula, as seen in Appendix I.

Cell counts in VTA processed for TH-immunohistochemistry

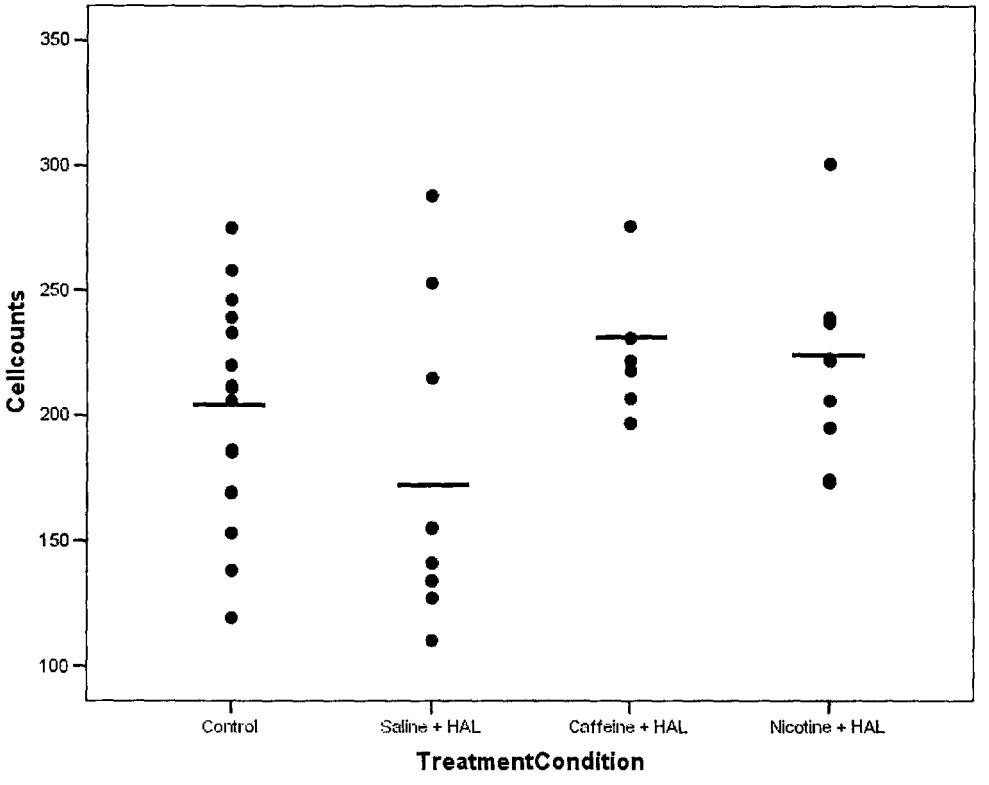

Figure 38 – Number of TH-positive cells in the ventral tegmental area per 40 μm hemi section. Each dot represents the mean number of TH-positive cell counts for one animal, with the horizontal line representing the group mean. TH-positive cell counts were not significantly decreased in the VTA of HAL-treated rats, although the saline + HAL animals tended toward a decrease.

Treatment Regimen	Control	Saline + HAL	Caffeine + HAL	Nicotine + HAL
Mean ± S.E.M.	203.3 ± 11.6	163.0 ± 21.0	225.2 ± 11.3	218.9 ± 13.1

Table 12 – Mean cell counts ± S.E.M. for TH-positive cells in the VTA.

Photomicrographs (20x magnification) of VTA processed for TH-immunohistochemistry

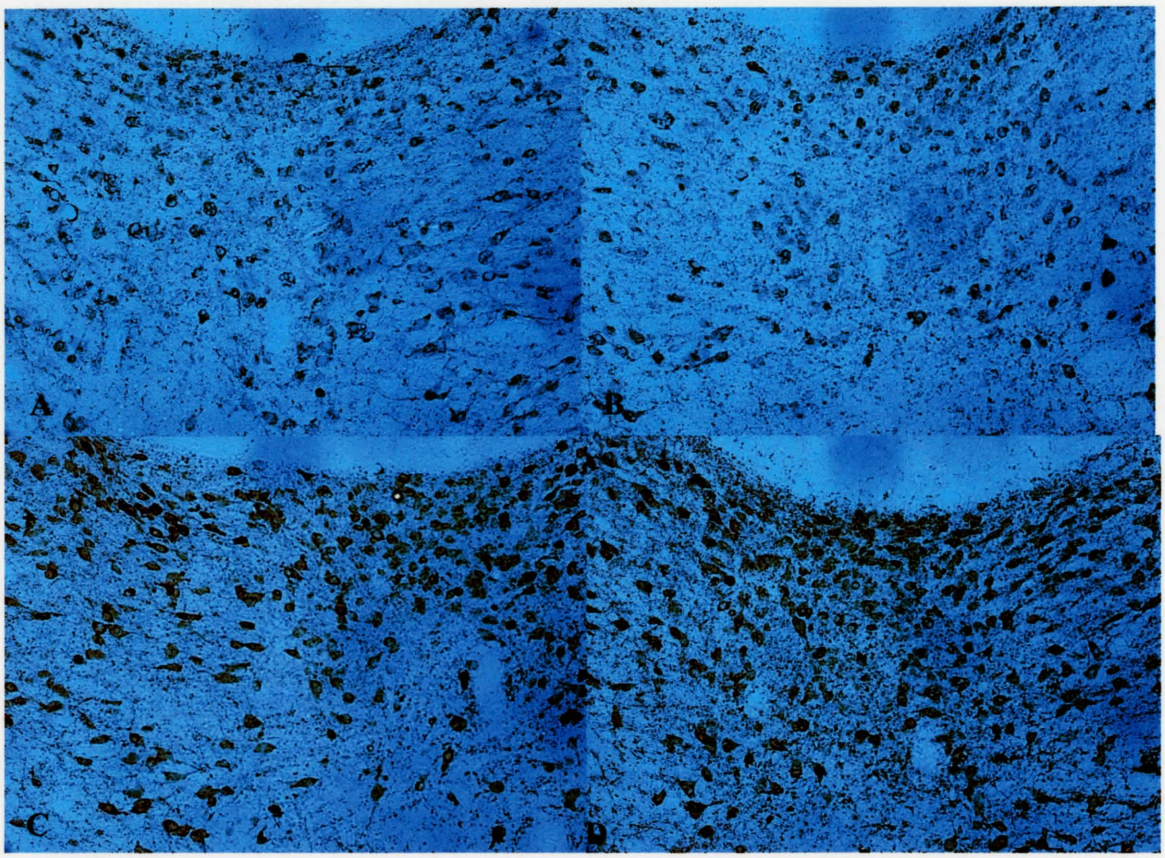

Figure 39 – Photomicrographs (20x magnification) of TH-positive immunoreactivity in the VTA for each group taken at bregma -5.3mm. There was no significant changes in TH-positive cell counts.
A: Control
B: Saline + HAL
C: Caffeine + HAL
D: Nicotine + HAL

TH & OX-42 Double Label

SN

TH counts

Analysis of cell counts revealed a significant HAL-induced effect on TH-immunoreactivity, $F(3,33) = 2.93$, $p = 0.048$. HAL produced a significant 21% reduction in TH-positive cell counts ($p < 0.05$). Caffeine and nicotine alone had no effect on dopaminergic cell counts compared with sham-pre-treated controls. Therefore, these controls were collapsed into the control and saline injected group. There was no significant difference between caffeine-treated animals or nicotine-treated animals compared to controls. Therefore, pre-treatment with either caffeine or nicotine completely blocked HAL-induced TH downregulation.

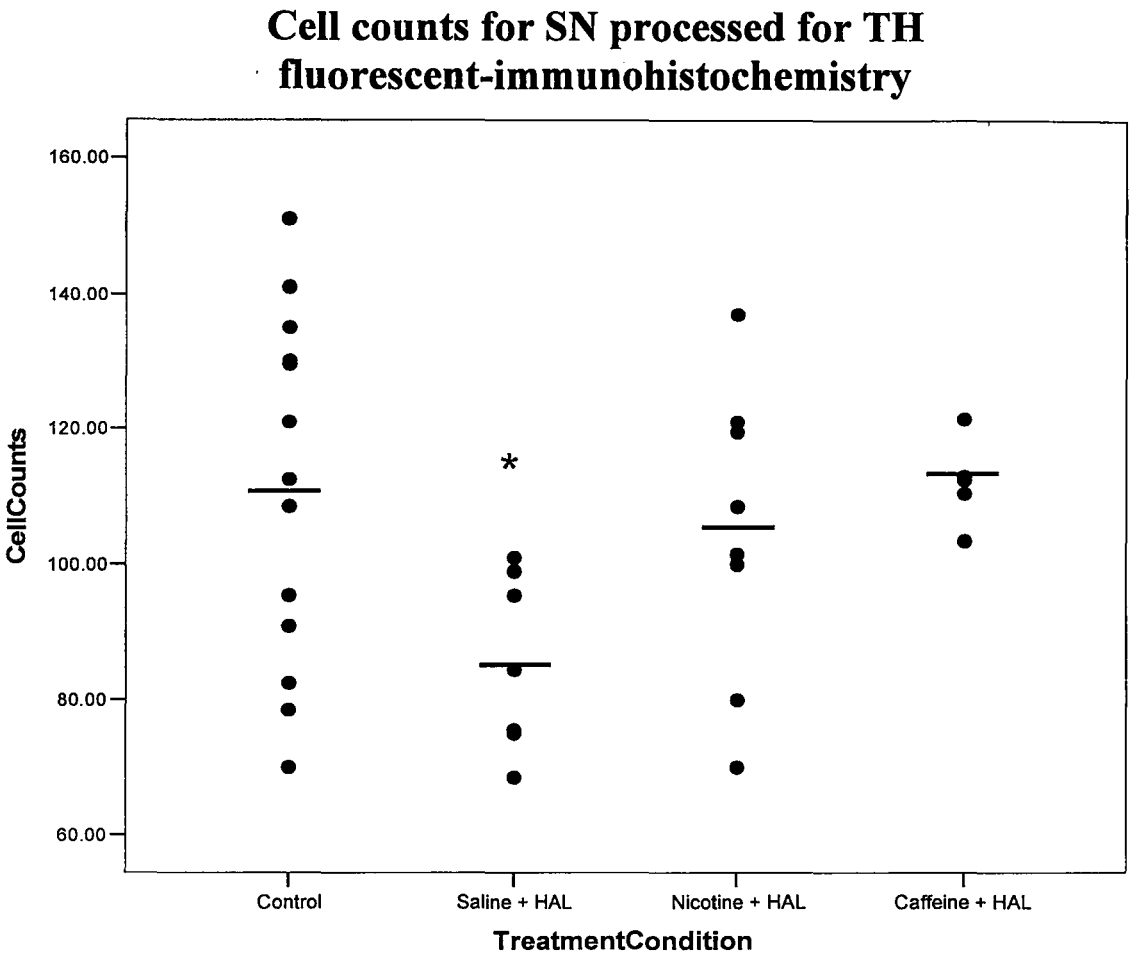

Figure 40 – Scatter plot of TH-positive cells in the substantia nigra per 40 μm hemi section. Each dot represents the mean number of TH-positive cell counts for one animal, with the horizontal line representing the group mean. TH-positive cell counts were significantly decreased in the SN of saline + HAL-treated rats by 21% ($p < 0.05$). This effect was completely blocked with caffeine or nicotine.

Treatment Regimen	Control	Saline + HAL	Nicotine + HAL	Caffeine + HAL
Mean ± S.E.M.	110.0 ± 6.7	86.8 ± 4.5	105.4 ± 5.9	112.2 ± 2.9

Table 13 – Mean cell counts ± S.E.M. for TH-positive cells in the SN.

Confocal images (20x magnification) of SN processed for TH-immunofluorescence

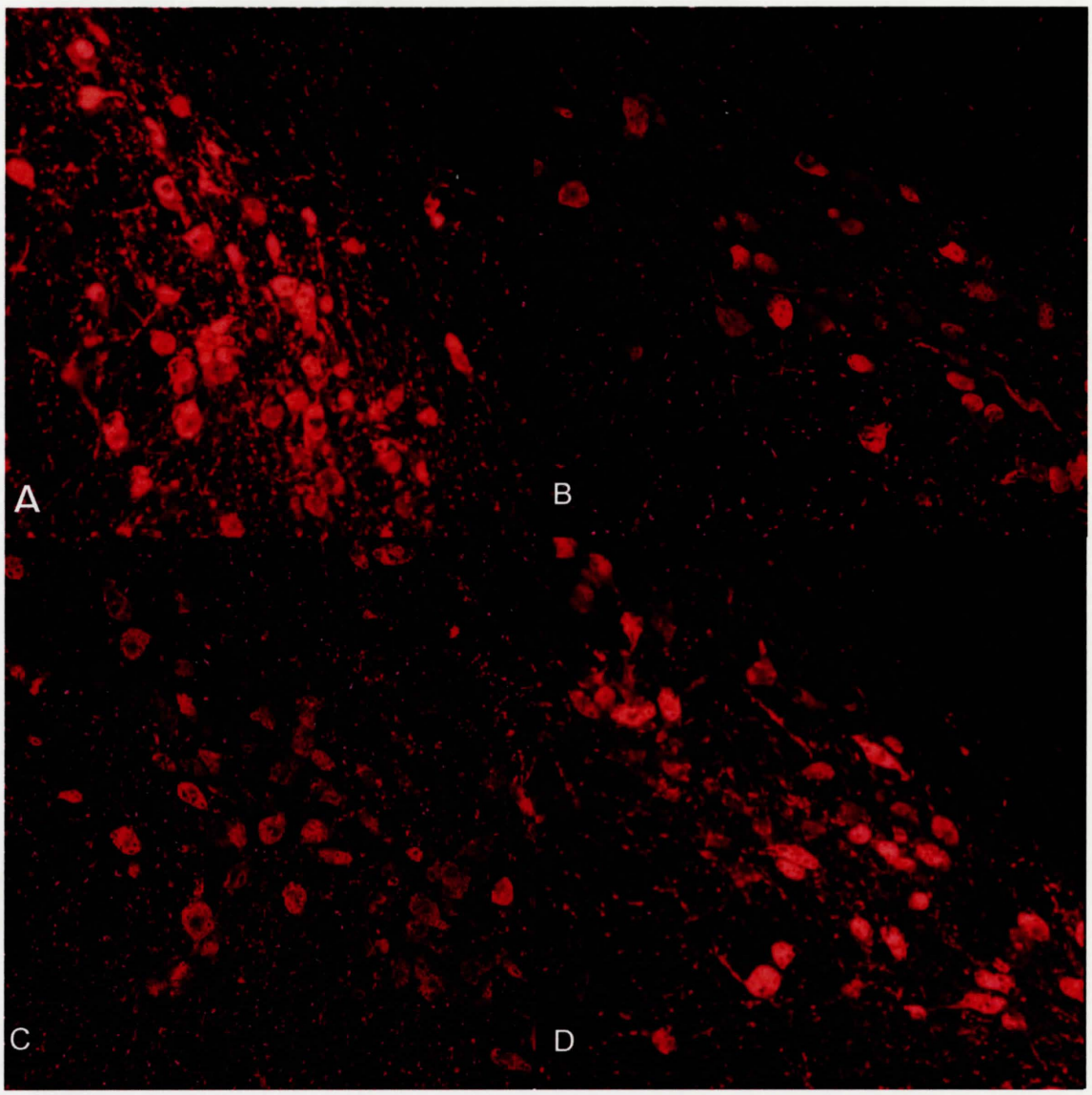

Figure 41 – Fluorescent images of TH-labelled cells of the SN taken per drug treatment group as visualized on the confocal microscope at 20x magnification. A significant decrease was seen in HAL-treated animals.
A: Control
B: Saline + HAL
C: Caffeine + HAL
D: Nicotine + HAL

OX-42 counts

Analysis of cell counts revealed a highly significant HAL-induced effect on OX-42-immunoreactive cells, $F(3,33) = 8.68$, $p < 0.001$. There was no significant difference between the caffeine and nicotine treated controls compared to control animals. A significant 29% increase in OX-42 positive cells was seen in the HAL treated animals compared to the control group ($p = 0.03$). Both the caffeine and HAL treated animals ($p < 0.001$) and the nicotine and HAL-treated animals ($p = 0.004$) were significantly different from the saline and HAL-treated group. Therefore, the increase in OX-42 immunoreactivity was attenuated by independent treatment with caffeine or nicotine.

Cell counts for SN processed for OX-42 fluorescent-immunohistochemistry

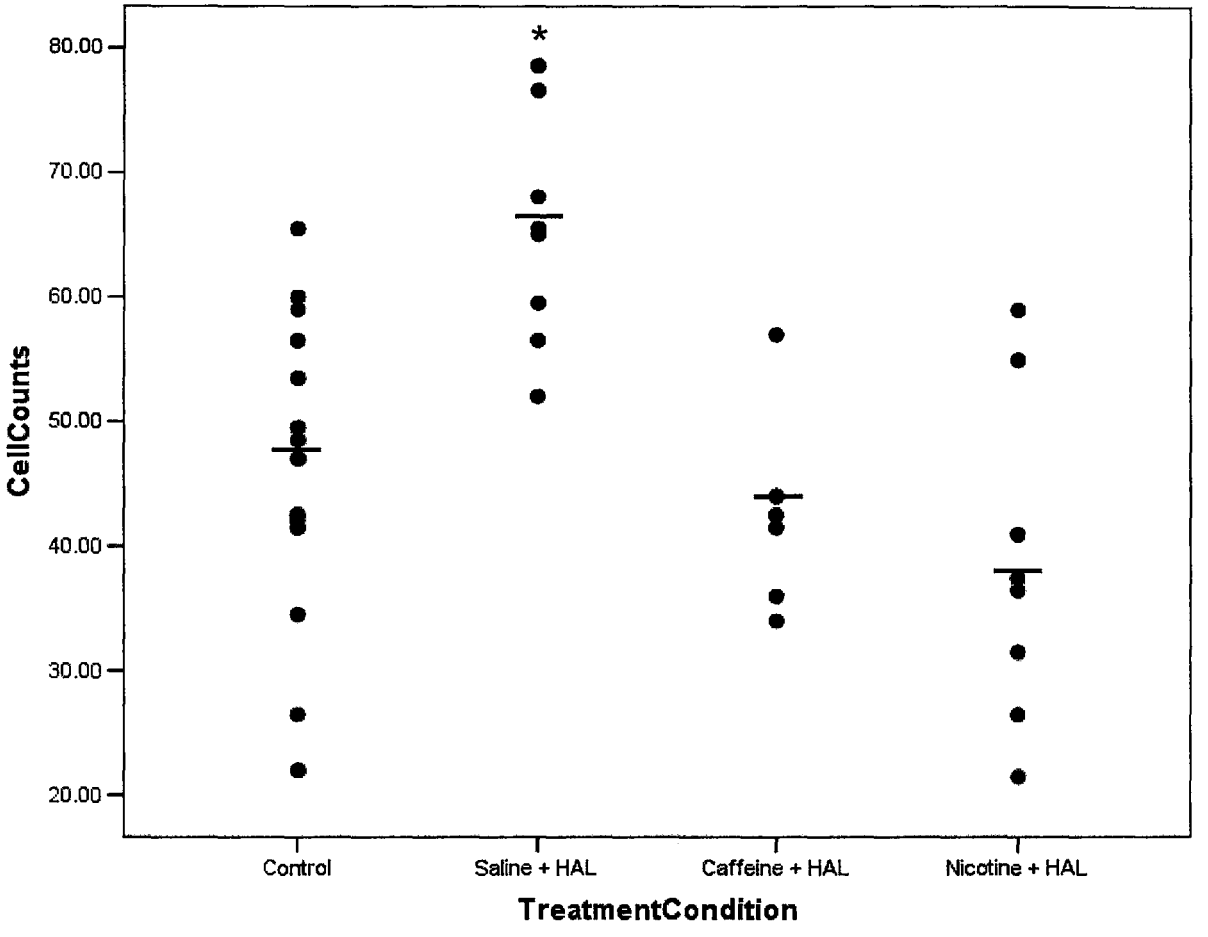

Figure 42 – Scatter plot of OX42-positive cells in the substantia nigra per 40 μm hemi section. Each dot represents the mean number of OX-42-positive cell counts for one animal, with the horizontal line representing the group mean. OX-42-positive cell counts were significantly increased in the SN of saline + HAL-treated rats by 29% ($p = 0.03$). This effect was completely blocked with caffeine or nicotine.

Treatment Regimen	Control	Saline + HAL	Caffeine + HAL	Nicotine + HAL
Mean ± S.E.M.	46.4 ± 3.1	65.2 ± 3.3	42.5 ± 3.3	38.6 ± 4.6

Table 14 – Mean cell counts ± S.E.M. for OX-42-positive cells in the SN.

Confocal images (20x magnification) of SN processed for TH-immunofluorescence

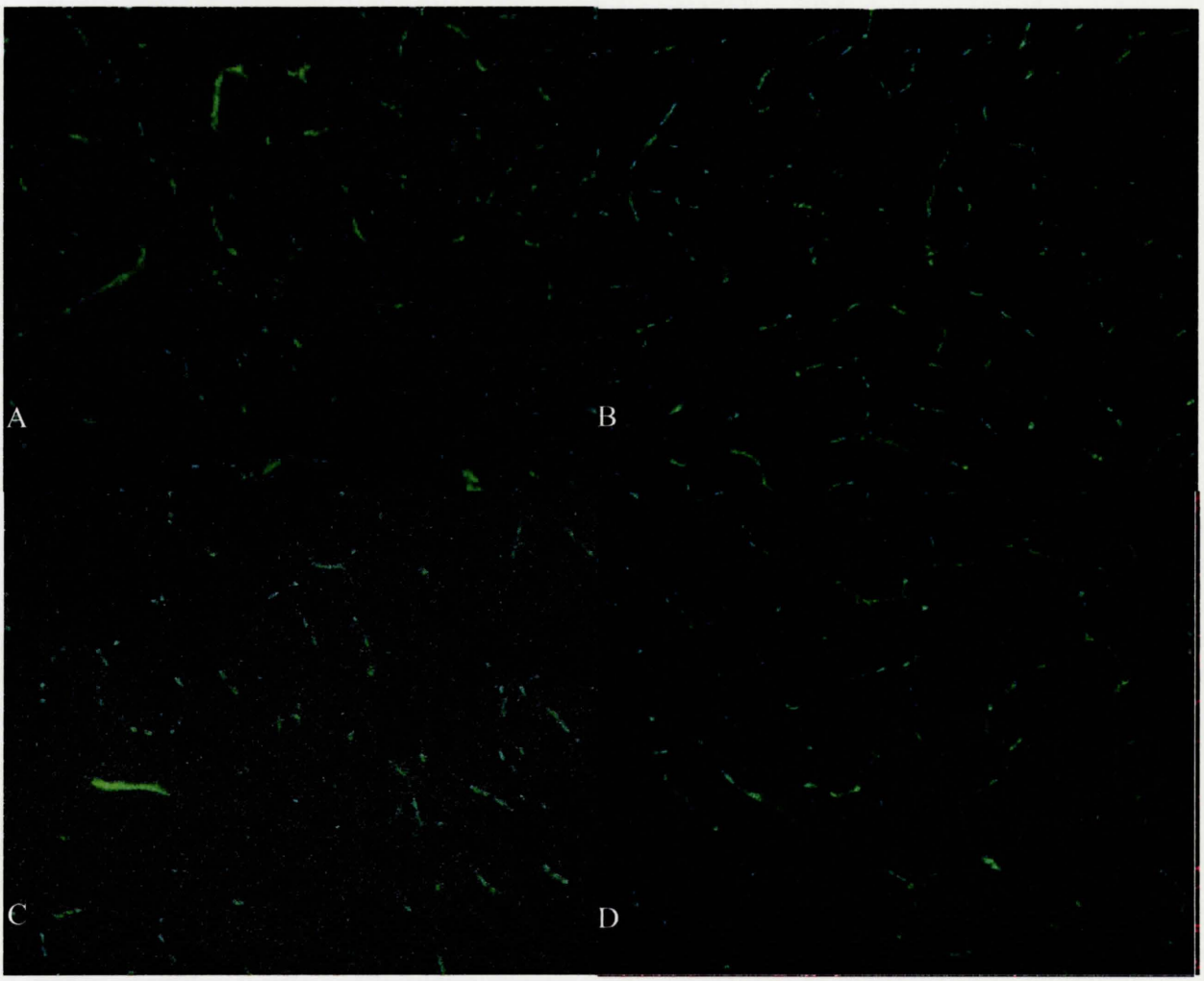

Figure 43 – Fluorescent images of OX-42-labelled cells of the SN taken per drug treatment group as visualized on the confocal microscope at 20x magnification. A significant increase was seen in saline + HAL-treated animals. Treatment with caffeine or nicotine attenuated the increase in OX-42 immunoreactivity seen in the saline + HAL treated groups.

A: Control
B: Saline + HAL
C: Caffeine + HAL
D: Nicotine + HAL

TH cell diameter

SN

There were no significant differences in cell sizes between any groups in the substantia nigra, $F(3,36) = 0.82$, $p = 0.489$. See figure 37.

VTA

There were no significant differences in cell sizes of HAL-treated or saline treated animals, $F(3,36) = 0.59$, $p = 0.627$. See figure 39.

Mean cell diameters in the Substantia Nigra processed for TH-immunohistochemistry

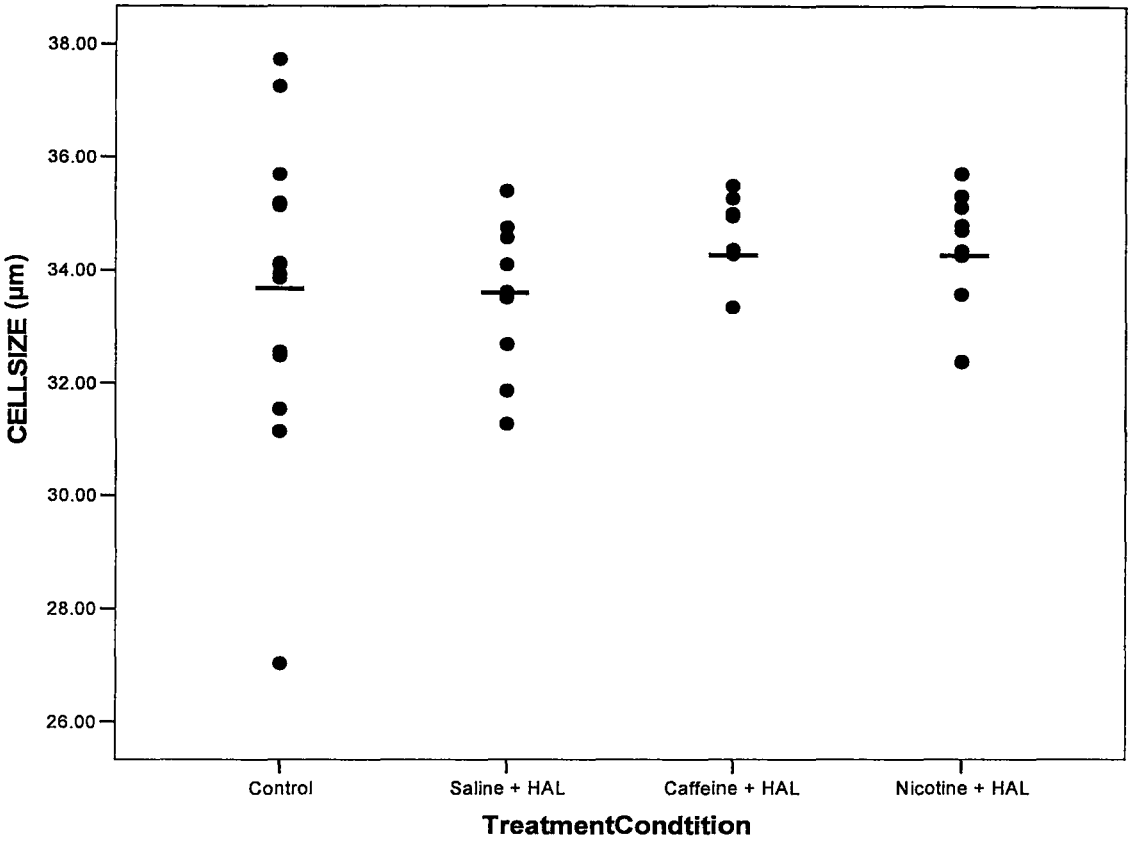

Figure 44 – Mean cell diameter (µm) of TH-positive cells of the substantia nigra per 40 µm hemi section. Each dot represents the mean diameter of 10 TH-positive cells for one animal, with the horizontal line representing the group mean. There was no significant difference seen between any of the groups.

Treatment Regimen	Control	Saline + HAL	Caffeine + HAL	Nicotine + HAL
Mean ± S.E.M.	33.7 ± 0.68	33.5 ± 0.46	34.7 ± 0.28	34.5 ± 0.34

Table 15 – Mean cell diameter ± S.E.M. for TH-positive cells in the SN.

Mean cell diameters in the Ventral Tegmental Area processed for TH-immunohistochemistry

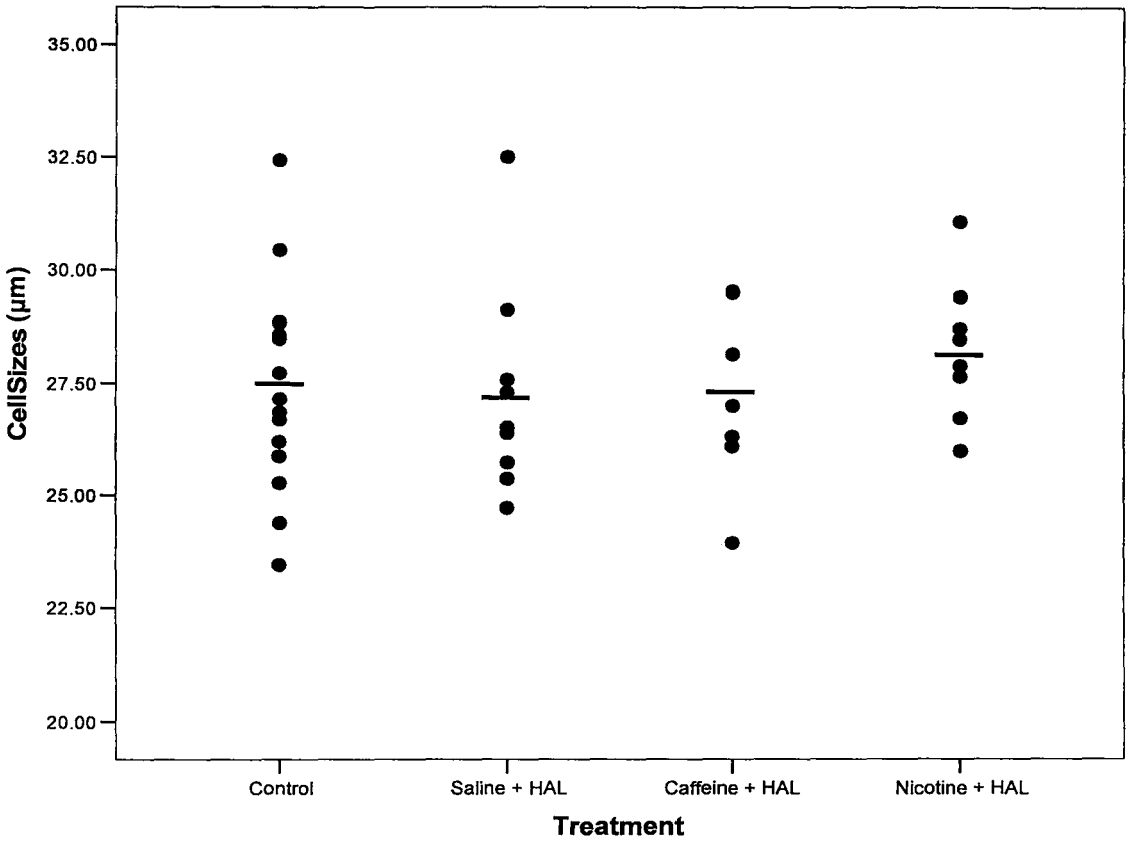

Figure 45 – Mean cell diameter (µm) of TH-positive cells of the ventral tegmental area per 40 µm hemi section. Each dot represents the mean diameter of 10 TH-positive cells for one animal, with the horizontal line representing the group mean. There was no significant difference seen between any of the groups.

Treatment Regimen	Control	Saline + HAL	Caffeine + HAL	Nicotine + HAL
Mean ± S.E.M.	27.4 ± 0.60	27.2 ± 0.79	27.2 ± 0.76	28.4 ± 0.51

Table 16 – Mean cell diameter ± S.E.M. for TH-positive cells in the VTA.

DISCUSSION

This study demonstrates that caffeine and nicotine can protect against downregulation of TH in midbrain dopamine neurons. Parkinson's disease is characterized by selective death of dopaminergic cells of the substantia nigra. Microglia have been increasingly implicated in Parkinson's disease models (Beal, 1998; Vila, et al., 2001; Hirsch, et al., 2003). Epidemiological evidence has shown that caffeine, an adenosine receptor antagonist, affords protection against Parkinson's disease (Hughes, et al., 1998). Adenosine receptors, which are found on microglial cells, have been shown to activate COX-2 and PGE_2 formation in microglia (Fiebich, et al., 1996). Treatment with caffeine, an adenosine receptor antagonist, could prevent COX-2 and PGE_2 formation. COX-2 formation by microglia has been reported to sensitize neurons to excitotoxicty by impairing astrocytes ability to resorb glutamate (Mirjany, et al., 2002). This could create a cytotoxic environment for dopaminergic neurons, initiating cell death processes.

In this study, nicotine has also showed a neuroprotective effect on dopaminergic neurons of the substantia nigra. Microglial activation by HAL has also been inhibited by treatment with nicotine. Although this does not indicate that microglia are inducing TH-downregulation, it does point to a correlative effect. Nicotinic receptors, namely α7 nAChR's, are present on microglial cells. Stimulation of these receptors by nicotine has been reported to prevent massive TNF release induced by LPS (Suzuki, et al., 2006). TNF-α binds to TNF1 receptors and causes receptor aggregation on the neuronal surface. The aggregation of TNF1 receptors subsequently activates caspase-8 and induces apoptosis (Giunta, et al., 2004). Another function of the microglial release of TNF-α is to act in synergy with stromal derived factor-1 (SDF-1) to potentiate glutamate release from neighbouring microglia and astrocytes (Garden, 2002). This

would increase glutamate binding at NMDA receptors on dopaminergic neurons, sensitizing them to excitotoxicity. Therefore, by preventing TNF-α release, nicotine may have protected dopamine neurons from TH-downregulation.

The nicotine-stimulation at nAChR's has also been found to inhibit the activation of JNK and p38 in the post-transcriptional pathway of TNF synthesis (Suzuki, et al., 2006). Therefore, when the HAL-treated animals were also co-administered nicotine, TNF production could have been inhibited. Not only does nicotine prevent the synthesis of TNF, but stimulation of the α7 nAChR attenuates cytokine release intracellularly through negative modulation of p44/42 MAPK phosphorylation (Giunta, et al., 2004). Since nicotine prevents the synthesis and release of TNF, this could be a potential mechanism of neuroprotection. Potentially, caffeine and nicotine can prevent microglial response to APDs, sparing surrounding neurons.

The ventral tegmental area cell counts were not significantly decreased with HAL-treatment compared to controls, unlike in the SN. This finding is not surprising once the distribution of microglia in the brain is noted. Microglia, in mouse brain, are densely populated in the hippocampus, olfactory telencephalon, basal ganglia and substantia nigra (Lawson, et al., 1990). Outside of these areas, the microglial populations are less dense. Therefore, activated microglia in densely populated areas would release an abundance of toxic inflammatory mediators creating a toxic environment for neurons to survive in. Another study reported that microglia also differentially express mRNA of inflammatory mediators. For example, microglia in the hippocampus express significantly higher mRNA levels of TNF-α compared to cerebellum and cortex microglia (Ren, et al., 1999). Therefore, it is possible that microglial production levels of

TNF-α and other cytokines could vary between the VTA and the substantia nigra. This would induce differing microenvironments for the dopamine neurons, causing specific dopaminergic damage to neurons in the substantia nigra.

Overall, caffeine and nicotine have been found to prevent TH-downregulation in dopaminergic neurons of the substantia nigra. This implies that patients who drink coffee or smoke cigarettes should be protected against Parkinson's disease. As well, patients who are medicated with haloperidol in treating Schizophrenic symptoms might be protected against HAL-induced parkinsonism by drinking coffee or smoking cigarettes. The mechanism by which this occurs is postulated through the microglia, which have been shown to be inactivated by both of these compounds.

4. GENERAL DISCUSSION

APDs are the mainstay treatment for Schizophrenia. Specifically, Haloperidol has been used to treat psychotic episodes for decades. Although effective in treating the positive symptoms of this disorder, HAL treatment has been associated with extra pyramidal symptoms. Parkinsonian symptoms are among these side effects and this includes muscular rigidity and a resting tremor. Upon HAL administration, dopamine receptors are immediately blocked, even though parkinsonian symptoms begin 2-3 weeks later. This suggests that receptor blockade is not solely inducing the parkinsonian symptoms. Investigation into this phenomenon has been the subject of this thesis.

Previous investigations in our lab have shown that chronic HAL administration causes downregulation of tyrosine hydroxylase within midbrain dopamine neurons. To further understand the neurobiology of this phenomenon, a timecourse experiment was conducted. In this series of experiments, we found that TH immunoreactivity was significantly decreased at 5 minutes post-HAL administration, with further downregulation seen at 10 minutes. Microglial activation has increasingly been implicated in Parkinson's disease and Parkinson's disease models. Therefore, we have also investigated the ability of the microglia to be potential mediators of the TH downregulation. Microglial activation was found to be significantly different from control animals by 5 minutes post-HAL administration, although they were increased by 22% by 2 minutes. This suggests that microglia could be mediating the HAL toxicity to dopamine neurons.

Minocycline, a semi-synthetic tetracycline, has been recently used as a microglial inhibitor. To further clarify the role of the microglia in mediating HAL toxicity, we co-administered minocycline and HAL to experimental animals. Again, HAL alone induced TH downregulation, but co-treatment with minocycline partially-protected the dopamine neurons. Therefore, this suggests that the microglia are involved in HAL toxicity and able to partially mediate TH downregulation in dopamine neurons.

Another body of literature has examined epidemiological evidence suggesting that caffeine and nicotine are neuroprotective in Parkinson's disease patients. Therefore, we also investigated the potential of caffeine and nicotine to independently protect against TH downregulation, using the HAL model of Parkinson's disease. We found that caffeine and nicotine can independently prevent TH downregulation in dopamine neurons. Keeping with the microglial mechanism, microglia have been found to express both nicotinic acetylcholine receptors and adenosine receptors. Therefore, we postulated that caffeine and nicotine can inhibit microglial activation. After investigating this, we found that caffeine and nicotine can both prevent microglial activation. This finding correlates with sparing of TH immunoreactivity seen in this experiment. Therefore, microglia have a role potentially mediating HAL toxicity to midbrain dopamine neurons.

Microglia are an integral part of the innate immune system. The innate immune system is present in both the peripheral and central nervous systems and functions as a first defense to destroy invading pathogens. It involves cells such as T-cells, dendritic cells, neutrophils, and macrophages. Microglia are specialized macrophages, in that they are only present in the brain.

Microglia are always present in a non-activated state, but can activate once an insult is detected. Microglia also have the ability to produce cytokines and chemokines, which function to attract other microglia and immune cells to the area of insult. In particular, microglia produce TNF-α, a toxic cytokine to many other cells, including dopamine neurons. TNF-α can bind to TNF receptors on microglia, causing the receptors to aggregate. This action causes activation of caspase-8, inducing apoptosis in the cell (Giunta, et al., 2004). This could account for some of the TH downregulation seen in the prior set of experiments. Previous work in our lab has shown apoptotic changes in dopamine neurons treated with HAL.

Microglial cytokines and adenosine have been shown to activate the prostaglandin pathway, upregulating COX-2 expression after exposure to cytokines (Fiebich, et al., 1996; Fiebich, et al., 2000; O'Banion, et al., 1996). This causes increased levels of prostaglandins, which furthers inflammation in the brain. This has been shown to induce apoptosis in neurons and activate resting microglia to produce more prostaglandins (Minghetti, et al., 1997; Takadera, et al., 2004). Subsequently, dopamine neurons would be under increased stress and increase sensitivity to apoptosis. In this case, further experimentation with neurodegeneration and COX-2 inhibitors may be a potential strategy to prevent Parkinson's disease. We have shown here that agents which inhibit microglial activation, including minocycline, nicotine and caffeine, have spared TH-immunoreactivity. The mechanism through which microglia are acting is postulated to be the prostaglandin pathway. Therefore, a COX-2 inhibitor can be used to prevent the synthesis of prostaglandins, reducing the inflammation and further neural damage. Parkinson's disease, and HAL-induced parkinsonism is caused by the depletion of dopamine cells in the substantia nigra.

If microglia are the mediating this loss, then co-administration of HAL and a COX-2 inhibitor, such as aspirin, might prevent further inflammation induced by microglial cytokines.

All together, we have shown that HAL induces changes in both the microglia and dopamine neurons. Microglial inflammation has been shown to partially mediate the TH downregulation seen with HAL administration.

REFERENCES

Andersson, C., Hamer, R.M., Lawler, C.P., Mailman, R.B., Liberman, J.A. 2002. Striatal volume changes in the rat following long-term administration of typical and atypical antipsychotic drugs. Neuropsychopharmacology, 27, 143-151.

Ascherio, A., Zhang, S.M., Hernan, M.A., Kawachi, I., Colditz, G.A., Speizer, F.E., Willett, W.C. 2001. Prospective study of caffeine consumption and risk of Parkinson's disease in men and women. Ann. of Neurol., 50, 56-63.

Axelrod, J., Tomchick, R. 1958. Enzymatic O-methylation of epinephrine and other catechols. J. Biol. Chem., 233, 702-705.

Baron, J.A. 1996. Beneficial effects of nicotine and cigarette smoking: the real, the possible and the spurious. Br. Med. Bull., 52, pp. 58–73.

Beal, M.F. 1998. Excitotoxicity and nitric oxide in Parkinson's disease pathogenesis. Ann. Neurol., 44, S110–4.

Benedetti, M.D., Bower, J.H., Maraganore, D.M., McDonnell, S.K., Peterson, B.J., Ahlskog, J.E., Schaid, D.J., Rocca, W.A. 2000. Smoking, alcohol, and coffee consumption preceding Parkinson's disease: a case-control study. Neurology, 55, 1350–1358.

Benes, F.M., Paskevich, P.A., Domesick, V.B. 1983. Haloperidol-induced plasticity of axon terminals in rat substantia nigra. Science, 221, 969-971.

Benowitz, N.L. 1990. Clinical pharmacology of inhaled drugs of abuse: implications in understanding nicotine dependence. NIDA Res. Monogr., 99, 12–29.

Benowitz, N. L., Jacob, P., III, Mayan, H., Denaro, C. 1995. Sympathomimetic effects of paraxanthine and caffeine in humans. Clin. Pharmacol. Ther., 58, 684– 691.

Benowitz, N.L. 1996. Pharmacology of nicotine: addiction and therapeutics. Annu. Rev. Pharmacol. Toxicol., 36, 597–613.

Brandange, S., Lindblom, L. 1979. The enzyme "aldehyde oxidase" is an iminium oxidase. Reaction with nicotine delta 1′(5′) iminium ion. Biochem. Biophys. Res. Commun., 91, 991–996.

Broch, O.J., Fonnum, F. The regional and subcellular distribution of catechol-O-methyl transferase in the rat brain. 1972. J. Neurochem., 19, 2049-2055.

Cabello, C.R., Thune, J.J., Pakkenberg, H., Pakkenberg, B. 2002. Ageing of substantia nigra in humans: cell loss may be compensated for by hypertrophy. Neuropathol appl. Neurobiol., 28, 283-291.

Capuano, B, Crosby, I.T., Lloyd, E.J. 2002. Schizophrenia: Genesis, Receptorology and Current Therapeutics. Curr. Med. Chem., 9, 521-548.

Cadet, J.L., Jayanthi, S., Deng, X. 2003. Speed kills: cellular and molecular bases of methamphetamine-induced nerve terminal degeneration and neuronal apoptosis. FASEB, 17, 1775-1788.

Caulfield, M.P. 1993. Muscarinic receptors—characterization, coupling and function. Pharmacol. Ther., 58, 319-379.

Chen, J.F., Xu, K., Petzer, J.P., Staal, R., Xu,Y.H., Beilstein, M., Sonsalla, P.K., Castagnoli, K., Castagnoli, N. Jr., Schwarzschild, M.A. 2001. Neuroprotection by caffeine and A(2A) adenosine receptor inactivation in a model of Parkinson's disease. J. Neurosci., 21, RC143.

Cohen, G. 1990. Monoamine oxidase and oxidative stress at dopaminergic synapses. J. Neural Transm., 32, (Suppl.) 229–238.

Cruz-Sanchez, F.F., Cardoza, A., Castejon, C., Tolosa, E., Rossi, M.L. 1997. Aging and the nigro-striatal pathway. J. Neural. Trasm., 51, 9-25.

Czlonkowska, A., Kohutnicka, M., Kurkowska-Jastrzebska, I., Czlonkowski, A. 1996. Microglial reaction in MPTP (1-methyl-4-phenyl-1,2,3,6-tetrahydropyridine) induced Parkinson's diseasemice model. Neurodegeneration, 5, 137–143.

Da Cunha, C., Angelucci, M.E.M., Canteras, N.S., Wonnacott, S., Takahashi, R.N. 2002. The lesion of the rat substantia nigra pars compacta dopaminergic neurons as a model for Parkinson's disease memory disabilities. Cell. Mol. Neurobiol., 22, 227-237.

Dixon, A.K., Gubitz, A.K., Sirinathsinghji, D.J., Richardson, P.J., Freeman, T.C., 1996. Tissue distribution of adenosine receptor mRNAs in the rat. Br. J. Pharmacol. 118, 1461–1468.

Du, Y., Ma, Z., Lin, S., Dodel, R.C., Gao, F., Bales, K.R., Triärhou, L.C., Chernet, E., Perry, K.W., Nelson, D.L., Luecke, S., Phebus, L.A., Bymaster, F.P., Paul, S.M. 2001. Minocycline prevents nigrostriatal dopaminergic neurodegeneration in the MPTP model of Parkinson's disease. Proc. Natl Acad. Sci. USA, 98, 14669–14674.

Fall, P.A., Fredrikson, M., Axelson, O., Granerus, A.K. 1999. Nutritional and occupational factors influencing the risk of Parkinson's disease: a case-control study in southeastern Sweden. Mov. Disord., 14, 28–37.

Fiebich, B.L., Biber, K., Lieb, K., van Calker, D., Berger, M., Bauer, J., Gebicke-Haerter, P.J. 1996. Cyclooxygenase-2 expression in rat microglia is induced by adenosine A2a-receptors. Glia, 18, 152–160.

Fiebich, B.L., Mueksch, B., Boehringer, M., Hull, M. 2000. Interleukin-1beta induces cyclooxygenase-2 and prostaglandin E2 synthesis in human neuroblastoma cells: involvement of

p38 mitogen-activated protein kinase and nuclear factor-kappaB. J. Neurochem., 75, 2020–2028.

Fields, R.D., Burnstock, G. 2006. Purinergic signalling in neuron–glia interactions. Nat. Rev. Neurosci., 7, 423-436.

Francis, J.W., Von Visger, J., Markelonis, G.J., Oh, T.H. 1995. Neuroglial responses to the dopaminergic neurotoxicant 1-methyl-4-phenyl-1,2,3,6-tetrahydropyridine in mouse striatum. Neurotoxicol. Teratol., 17, 7–12.

Fredholm, B.B., Ijzerman, A.P., Jacobson, K.A., Klotz, K.-N., Linden, J. 2001. International Union of Pharmacology. XXV. Nomenclature and classification of adenosine receptors. Pharmacol. Rev. 53, 527–552.

Garden, G.A. 2002. Microglia in human immunodeficiency virus-associated neurodegeneration. Glia, 40, 240–251.

Gerlach, M., Riederer, P., Youdim, M.B.H. 1996. Molecular mechanisms for neurodegeneration: synergism between reactive oxygen species, calcium and excitotoxic amino acids. Adv. Neurol., 69, 177–194.

Gorell, J.M., Rybicki, B.A., Johnson, C.C., Peterson, E.L. 1999. Smoking and Parkinson's disease: a dose-response relationship. Neurology, 52, 115–119.

Gorrod, J.W., Hibberd, A.R. 1982. The metabolism of nicotine-delta 1α(5α)-iminium ion, in vivo and in vitro. Eur. J. Drug Metab. Pharmacokinet., 7, 293–298.

Gotti, C., Clementi, F. 2004. Neuronal nictotinic receptors: from structure to function. Progress in Neurobiol., 74, 363-396.

Grandinetti, A., Morens, D.M., Reed, D., MacEachern, D. 1994. Prospective study of cigarette smoking and the risk of developing idiopathic Parkinson's disease. Am. J. Epidemiol., 139, 1129–1138.

Giunta, B., Ehrhart, J., Townsend, K., Sun, N., Vendrame, M., Shytle, D., Tan, J., Fernandez, F. 2004. Galantamine and nicotine have a synergistic effect on inhibition of microglial activation induced by HIV-1 gp120. Brain Res. Bull., 64, 165-70.

Hasko, G., Pacher, P., Vizi, E.S., Illes, P. 2005. Adenosine receptor signalling in the brain immune system. Trends in Pharmacol. Sci., 26, 511-516.

He, Y., Appel, S., Le, W. 2001. Minocycline inhibits microglial activation and protects nigral cells after 6-hydroxydopamine injection into mouse striatum. Brain Res., 909, 187–193.

Hellenbrand, W., Seidler, A., Boeing, H., Robra, B.P., Vieregge, P., Nischan, P., Joerg, J., Oertel, W.H., Schneider, E., Ulm, G. 1996. Diet and Parkinson's disease: I. A possible role for

the past intake of specific foods and food groups. Results from a self-administered food-frequency questionnaire in a case-control study. Neurology, 47, 636–643.

Hernan, M.A., Takkouche, B., Caamano-Isorna, F., Gestal-Otero, J.J. 2002. A meta-analysis of coffee drinking, cigarette smoking, and the risk of Parkinson's disease. Annals of Neurol., 52, 276-284.

Hiroi, N., Martín, A.B., Grande, C., Alberti, I., Rivera, A., Moratalla, R. 2002. Molecular dissection of dopamine receptor signalling. Journal of Chemical Neuroanat., 23, 237-242.

Hirsch, E.C., Breidert, T., Rousselet, E., Hunot, S., Hartmann, A., Michel, P.P. 2003. The role of glial reaction and inflammation in Parkinson's disease. Ann N.Y. Acad. Sci., 991, 214–28.

Hughes, J.R., McHugh, P., Holtzman, S. 1998. Alcohol & Drug Abuse: Caffeine and Schizophrenia. Psychiatr. Serv., 49, 1415-1417.

Hukkanen, J., Peyton, J. III, Benowitz, N.L. 2005. Metabolism and disposition kinetics of nicotine. Pharmacol. Rev., 57, 79-115.

Jimenez-Jimenez, F.J., Mateo, D., Gimenez-Roldan, S. 1992. Premorbid smoking, alcohol consumption, and coffee drinking habits in Parkinson's disease: a case-control study. Mov. Disord., 7, 339–344

Jones, H. Royden. 2005. Netter's Neurology. Icon Learning Systems. pp. 372-374.

Kandel, E.R., Schwartz, J.H., Jessell, T.M. 2000. Principles of Neural Science. New York: McGraw-Hill.

Kapur, S., Mamo,. D. 2003. Half a century of antipsychotics and still a central role for dopamine D2 receptors. Progress in Neuro-Psychopharmacol. & Biol. Psych., 27, 1081-1090.

Karlin A. 2002. Emerging structure of the nicotinic acetylcholine receptors. Nat. Rev. Neurosci., 3, 102-114.

Kemp, P.M., Sneed, G.S., George, C.E., Distefano, R.F. 1997. Postmortem distribution of nicotine and cotinine from a case involving the simultaneous administration of multiple nicotine transdermal systems. J. Anal. Toxicol., 21, 310–313.

Kim, S.U., de Vellis, J. 2005. Microglia in health and disease. J. of Neurosci. Res., 81, 302-313.

Kriz, J., Nguyen, M.D., Julien, J.P. 2002. Minocycline slows disease progression in a mouse model of amyotrophic lateral sclerosis. Neurobiol. Dis., 10, 268–278.

Kuehn, B.M. 2006. Link between smoking and mental illness may lead to treatments. JAMA, 295, 483-484.

Kumer, S.C., Vrana, K.E. 1996. Intricate regulation of tyrosine hydroxylase activity and gene expression. J. of Neurochem., 67, 443-463.

Langston, J.W., Forno, L.S., Tetrud, J., Reeves, A.G., Kaplan, J.A., Karluk, D. 1999. Evidence of active nerve cell degeneration in the substantia nigra of humans years after 1-methyl-4-phenyl-1,2,3,6-tetrahydropyridine exposure. Ann. Neurol., 46, 598–605.

LaVoie, M.J., Card, J.P., Hastings, T.G. 2004. Microglial activation precedes dopamine terminal pathology in methamphetamine-induced neurotoxicity. Exp. Neurol., 187, 47-57.

Lawson, L.J., Perry, V.H., Dri, P., Gordon, S. 1990. Heterogeneity in the distribution and morphology of microglia in the normal adult mouse brain. Neuroscience, 39, 151–170.

Levinson, A.J., Garside, S., Rosebush, P.I., Mazurek, M.F. 1998. Haloperidol induces persistent down-regulation of tyrosine hydroxylase immunoreactivity in substantia nigra but not ventral tegmental area in the rat. Neuroscience, 84, 201-211.

Levitt, P., Pintar, J.E., Breakefield, X.O. 1982. Immunocytochemical demonstration of monoamine oxidase B in brain astrocytes and serotonergic neurons. Proc. Natl. Acad. Sci. USA, 79, 6385–6389.

Linden, J. 2001. Molecular approach to adenosine receptors: receptor-mediated mechanisms of tissue protection. Annu. Rev. Pharmacol. Toxicol., 41, 775–787.

Liu, B, Hong, J.S. 2003. Role of microglia in inflammation-mediated neurodegenerative diseases: mechanisms and strategies for therapeutic intervention.
J. Pharmacol. Exp. Ther., 304, 1-7.

Lotharius, J., Brundin, P. 2002. Pathogenesis of Parkinson's disease: dopamine, vesicles and α-synuclein. Nat. Rev. Neurosci., 3, 932-942.

Maes, M., Bosmans, E., Calabrese, J., Smith, R., Meltzer, H.Y. 1995. Interleukin-2 and interleukin-6 in schizophrenia and mania: effects of neuroleptics and mood stabilizers. J. Psychiatr. Res., 29, 141-52.

Maes, M., Bosmans, E., Kenis, G., De Jong, R., Smith, R.S., Meltzer, H.Y. 1997. In vivo immunomodulatory effects of clozapine in schizophrenia. Schizophr Res., 26, 221-5.

Mandel, H.G. 2002. Update on caffeine consumption, disposition, and action. Food and Chem. Toxicol., 40, 1231-1234.

Meshul, C.K., Stallbaumer, R.K., Taylor, B., Janowsky, A. 1994. Haloperidol-induced morphological changes in striatum are associated with glutamate synapses. Brain Res., 648, 181-185.

Minghetti, L., Polazzi, E., Nicolini, A., Creminon, C., Levi, G. 1997. Up-regulation of cyclooxygenase-2 expression in cultured microglia by prostaglandin E2, cyclic AMP and non-steroidal anti-inflammatory drugs. Eur. J. Neurosci., 9, 934–940.

Mirjany, M., Ho, L., Pasinetti, G.M. 2002. Role of cyclooxygenase-2 in neuronal cell cycle activity and glutamate-mediated excitotoxicity. J. Pharmacol. Exp. Ther., 301, 494–500.

Missale, C., Nash, S.R., Robinson, S.W., Jaber, M., Caron, M.G. 1998. Dopamine receptors: from structure to function. Physiol. Rev., 78, 189-225.

Morano, A., Jimenez-Jimenez, F.J, Molina, J.A., Antolin, M.A. 1994. Risk-factors for Parkinson's disease: case-control study in the province of Caceres, Spain. Acta. Neurol. Scand., 89, 164–170.

Morens, D.M. Grandinetti, A., Reed, D., White, L.R., Ross, G.W. 1995. Cigarette smoking and protection from Parkinson's disease: false association or etiologic clue?. Neurology, 45, 1041–1051.

Muller, P., Seeman, P. 1977. Brain neurotransmitter receptors after long-term haloperidol: dopamine, acetylcholine, serotonin, alpha-noradrenergic and naloxone receptors. Life Sci., 21, 1751-1758.

Nawrot, P., Jordan, S., Eastwood, J., Rotstein, J., Hugenholtz, A., Feeley, M. 2003. Effects of caffeine on human health. Food Additives and Contaminants, 20, 1-30.

O'Banion, M.K., Miller, J.C., Chang, J.W., Kaplan, M.D., Coleman, P.D. 1996. Interleukin-1b induces prostaglandin G/H synthase-2 (cyclooxygenase-2) in primary murine astrocyte cultures. J. Neurochem., 66, 2532–2540.

Orr, C.F., Rowe, D.B., Halliday, G.M. 2002. An inflammatory review of Parkinson's disease. Prog. in Neurobiol., 68, 325-340.

Pankow, J.F., Tavakoli, A.D., Luo, W., Isabelle, L.M. 2003. Percent free base nicotine in the tobacco smoke particulate matter of selected commercial and reference cigarettes. Chem. Res. Toxicol., 16,1014–1018.

Pauly, J.R., Charriez, C.M., Guseva, M.V., Scheff, S.W. 2004. Nicotinic receptor modulation for neuroprotection and enhancement of functional recovery following brain injury. Annals of N.Y. Acad. Sci., 1035, 316-334.

Pollmacher, T., Hinze-Selch, D., Fenzel, T., Kraus, T., Schuld, A., Mullington, J. 1997. Plasma Levels of Cytokines and Soluble Cytokine Receptors During Treatment With Haloperidol. Am. J. Psychiatry, 154, 1763-1765.

Quik, M. 2004. Smoking, nicotine and Parkinson's disease. Trends in Neurosci., 27, 561-568.

Ren, L., Lubrich, B., Biber, K., Gebicke-Haerter, P.J. 1999. Differential expression of inflammatory mediators in rat microglia cultured from different brain regions. Brain Res. Mol. Brain Res., 65, 198–205.

Ribeiro, J.A., Sebastião, A.M., de Mendonça, A. 2003. Adenosine receptors in the nervous system: pathophysiological implications. Prog. in Neurobiol., 68, 377-392.

Ripoll, N., Bronnec, M., Bourin, M. 2004. Nicotinic receptors and schizophrenia. Curr. Med. Res. Opin., 20, 1057-1074.

Roberts, R.C., Gaither, L.A., Gao, X.M., Kashyap, S.M., Taminga, C.A. 1995. Ultrastructural correlates on haloperidol-induced oral dyskinesias in rat striatum. Synpase, 20, 234-243.

Robinson, S.W., Jarvie, K.R., Caron, M.G. 1994. High affinity agonist binding to the dopamine D3 receptor: chimeric receptors delineate a role for intracellular domains. Mol. Pharmacol, 46, 352-356.

Ross, G.W., Abbott, R.D., Petrovich, H., Morens, D.M., Grandinetti, A., Tung, K.H., Tanner, C.M., Masaki, K.H., Blanchette, P.L., Curb, J.D., Popper, J.S., White, L.R. 2000. Association of coffee and caffeine intake with the risk of Parkinson's diease. J.A.M.A., 283, 2674-2679.

Rümenapp, U., Asmus M., Schablowski H., Woznicki M., Han L., Jakobs K.H., Fahimi-Vahid M., Michalek C., Wieland T., Schmidt M. 2001. The M_3 muscarinic acetylcholine receptor expressed in HEK-293 cells signals to phospholipase D via G_{12} but not G_q-type G proteins. Regulators of G proteins as tools to dissect pertussis toxin-resistant G proteins in receptor-effector coupling. J. Biol. Chem., 276, 2474-2479.

Ryu, J.K., Franciosi, S., Sattayaprasert, P., Kim, S.U., McLarnon, J.G. 2004. Minocycline inhibits neuronal death and glial activation induced by beta-amyloid peptide in rat hippocampus. Glia, 48, 85–90.

Saura, J., Angulo, E., Ejarque, A., Casado, V., Tusell, J.M., Moratalla, R., Chen, J.-F., Schwarzschild, M.A., Lluis, C., Franco, R., Serratosa, J. 2005. Adenosine A2A receptor stimulation potentiates nitric oxide release by activated microglia. J. of Neurochem., 95, 919–929.

Schneider, N.G., Olmstead, R.E., Franzon, M.A., Lunell, E. 2001. The nicotine inhaler: clinical pharmacokinetics and comparison with other nicotine treatments. Clin. Pharmacokinet., 40, 661–684.

Seaton, M.J., Vesell, E.S., Luo, H., Hawes, E.M. 1993. Identification of radiolabeled metabolites of nicotine in rat bile. Synthesis of S-(-)-nicotine N-glucuronide and direct separation of nicotine-derived conjugates using high-performance liquid chromatography. J. Chromatogr., 621, 49–53.

Shen, W.W. 1999. A history of antipsychotic drug development. Comp. Psych., 40, 407-414.

Shytle, R.D., Mori, T., Townsend, K., Vendrame, M., Sun, N., Zeng, J., Ehrhart, J., Silver, A.A., Sanberg, P.R., Tan, J. 2004. Cholinergic modulation of microglial activation by α7 nicotinic receptors. J. of Neurochem., 89, 337–343.

Smythies, J. 2005. Section II: The dopamine system. Int. Rev. Neurobiol., 64, 123-172.

Sriram, K., Miller, D.B., O'Callaghan, J.P. 2006. Minocycline attenuates microglial activation but fails to mitigate striatal dopaminergic neurotoxicity: role of tumor necrosis-α. J. Neurochem., 96, 706-718.

Stirling, D.P., Khodarahmi, K., Liu, J., McPhail, L.T., McBride, C.B., Steeves, J.D., Ramer, M.S., Tetzlaff, W. 2004. Minocycline treatment reduces delayed oligodendrocyte death, attenuates axonal dieback, and improves functional outcome after spinal cord injury. J. Neurosci., 24, 2182–2190.

Streit, W.J. 2002. Microglia as neuroprotective, immunocompetant cells of the CNS. Glia, 40, 133-139.

Suzuki, T., Hide, I., Matsubara, A., Hama, C., Harada, K., Miyano, K., Andrä, M., Matsubayashi, H., Sakai, N., Kohsaka, S., Inoue, K., Nakata, Y. 2006. Microglial α7 nicotinic acetylcholine receptors drive a phospholipase C/IP3 pathway and modulate the cell activation toward a neuroprotective role. J. Neurosci. Res., 83, 1461-1470.

Takadera, T., Shiraishi, Y., Ohyashiki, T. 2004. Prostaglandin E2 induced caspase-dependent apoptosis possibly through activation of EP2 receptors in cultured hippocampal neurons. Neurochem. Int., 45, 713–719.

Tanner, C.M., Goldman, S.M., Aston, D.A., Ottman, R., Ellenberg, J., Mayeux, R., Langston, J.W. 2002. Smoking and Parkinson's disease in twins. Neurology, 58, 581–588.

Teismann, P., Schulz, J.B. 2004. Cellular pathology of Parkinson's disease: astrocytes, microglia and inflammation. Cell Tissue Res., 318, 149-161.

Tikka, T.M., Fiebich, B.L., Goldsteins, G., Keinanen, R., Koistinaho, J. 2001. Minocycline, a tetracycline derivative, is neuroprotective against excitotoxicity by inhibiting activation and proliferation of microglia. J. Neurosci., 21, 2580–2588.

Tikka, T.M., Koistinaho, J.E. 2001. Minocycline provides neuroprotection against N-methyl-D-aspartate neurotoxicity by inhibiting microglia. J. Immunol., 166, 7527–7533.

Van Den Bosch, L., Tilkin, P., Lemmens, G., Robberecht, W. 2002. Minocycline delays disease onset and mortality in a transgenic model of ALS. Neuroreport, 13, 1067–1070.

van Koppen, C.J., Kaiser, B. 2003. Regulation of muscarinic acetylcholine receptor signaling. Pharmacol. and Ther., 98, 197-220.

Vijitruth, R., Liu, M., Choi, D.-Y., Nguyen, X.V., Hunter, R.L., Bing, G. 2006. Cyclooxygenase-2 mediates microglial activation and secondary dopaminergic cell death in the mouse MPTP model of Parkinson's disease. J. Neuroinflammation, 3, 3-6.

Vila, M., Jackson-Lewis, V., Guegan, C., Wu, D.C., Teismann, P., Choi, D.K., Tieu, K., Przedborski, S. 2001. The role of glial cells in Parkinson's disease. Curr. Opin. Neurol., 14, 483–9.

Westlund, K.N., Denney, R.M., Kochersperger, L.M., Rose, R.M., Abell, C.W. 1985. Distinct monoamine oxidase A and B populations in primate brain. Science, 230, 181–183.

Wu, D.C., Jackson-Lewis, V., Vila, M., Tieu, K., Teismann, P., Vadseth, C., Choi, D.K., Ischiropoulos, H., Przedborski, S. 2002. Blockade of microglial activation is neuroprotective in the 1-methyl-4-phenyl-1,2,3,6-tetrahydropyridine mouse model of Parkinson disease. J. Neurosci., 22, 1763–1771.

Xu, K., Bastia, E., Schwarzschild, M. 2005. Therapeutic potential of adenosine A2A receptor antagonists in Parkinson's disease. Pharmacol. & Ther., 105, 267-310.

Yrjanheikki, J., Keinanen, R., Pellikka, M., Hokfelt, T., Koistinaho, J. 1998. Tetracyclines inhibit microglial activation and are neuroprotective in global brain ischemia. Proc. Natl Acad. Sci. USA, 95, 15769–15774.

Yrjanheikki, J., Tikka, T., Keinanen, R., Goldsteins, G., Chan, P.H., Koistinaho, J. 1999. A tetracycline derivative, minocycline, reduces inflammation and protects against focal cerebral ischemia with a wide therapeutic window. Proc. Natl Acad. Sci. USA, 96, 13496–13500.

Youdim, M.B.H., Edmondson, D., Tipton, K.F. 2006. The therapeutic potential of monoamine oxidase inhibitors. Nat. Rev. Neurosci., 7, 295-309.

Youdim, M.B.H., Riederer, P.F. 2004. A review of the mechanisms and role of monoamine oxidase inhibitors in Parkinson's disease. Neurology, 63, S32-S35.

Zhang, X.Y., Zhou, D.F., Cao, L.Y., Zhang, P.Y., Wu, G.Y., Shen, Y.C. 2004. Changes in serum interleukin-2, -6, and -8 levels before and during treatment with risperidone and haloperidol: relationship to outcome in schizophrenia. J Clin. Psychiatry, 65, 940-7.

Zimmermann, H., Braun, N. 1999. Ecto-nucleotidases – molecular structures, catalytic properties, and functional roles in the nervous system. Prog. Brain Res., 120, 371-385.

APPENDIX I

Abercrombie Formula

$$P = A \frac{M}{L + M},$$

Where P is the corrected number of cell counts per section
A is the crude number of cell counts per section
M is the section thickness (μm)
L is the average diameter of the cell (μm)

Treatment condition	Section thickness (μm)	Diameter of cell (μm)	Crude cell counts	Corrected cell counts
Control	40	30.1	139.6	79.7
1 min.	40	30.8	140.2	79.2
2 min.	40	32.6	155.5	85.7
5 min.	40	31.5	120.9	67.6
10 min.	40	32.9	101.2	55.5

Table 17 – Abercrombie corrected cell counts in the substantia nigra for timecourse experiment.

Treatment condition	Section thickness (μm)	Diameter of cell (μm)	Crude cell counts	Corrected cell counts
Control	40	30.1	139.6	79.7
10 min. HAL	40	32.9	101.2	55.5
Minocycline + HAL	40	30.1	124.7	71.2

Table 18 – Abercrombie corrected cell counts in the substantia nigra for minocycline experiment.

Treatment condition	Section thickness (μm)	Diameter of cell (μm)	Crude cell counts	Corrected cell counts
Control	40	27.4	139.8	83.0
HAL	40	27.3	110.6	65.7
Caffeine + HAL	40	27.2	132.7	79.0
Nicotine + HAL	40	28.4	132.1	77.3

Table 19 – Abercrombie corrected cell counts in the ventral tegmental area for caffeine & nicotine experiment.

Treatment condition	Section thickness (μm)	Diameter of cell (μm)	Crude cell counts	Corrected cell counts
Control	40	33.6	203.2	110.4
HAL	40	34.3	163.0	87.8
Caffeine + HAL	40	34.7	225.2	120.6
Nicotine + HAL	40	34.5	218.9	117.5

Table 20 – Abercrombie corrected cell counts in the substantia nigra for caffeine & nicotine experiment.